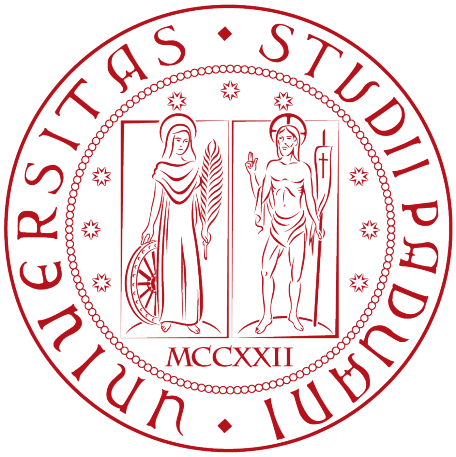

UNIVERSITÀ DEGLI STUDI DI PADOVA
DIPARTIMENTO DI FISICA E ASTRONOMIA "GALILEO GALILEI"

CORSO DI LAUREA MAGISTRALE IN
FISICA

APPLICATION OF THE EXCURSION SET THEORY TO MODIFIED GRAVITY

Relatore: Prof. Sabino Matarrese

Correlatore: Dr. Philippe Brax

Laureando
Nicola Bellomo 1081548

Anno Accademico 2014-2015

Abstract

Gravity could be modified compared to General Relativity on very large scales, as suggested by the discovery of the accelerated expansion of the Universe. One possible explanation would be the existence, on cosmological scales, of scalar fields, which have hidden their presence until now thanks to particular screening mechanisms and which would influence the growth of large scale structures by their coupling to Cold Dark Matter.
Since a complete analysis of the structure formation problem would require complete N-body simulations, which are really complex from a computational point of view, the goal of this thesis is to find a set of semi-analytical approximations that allows to obtain reliable results.
First of all we will investigate the spherical collapse of such structures, in order to understand how this new scale-dependent fifth force, mediated by the scalar field, changes the critical initial overdensity necessary to collapse and also how different models modify this value.
In a second step, we will use the excursion set theory to relate the statistics of the density field at early times to the number of virialized, gravitationally bound structures. Since the fifth force is stronger for smaller objects, a smaller initial overdensity is required to collapse and we expect to find a larger number of haloes with respect to General Relativity.

Contents

Chapter 1

Introduction

At the end of the past century two different projects, the High-Z Supernova Search Team [21] and the Supernova Cosmology Project [19], detected a remarkable inconsistency between what we thought to be our Universe and what it really is: observing high redshift Type Ia supernovae they found an evidence that we are in an epoch where the Universe is not only expanding, but it is also accelerating! This discovery, which over the years has been supported also by other evidences, was so significant that it opened a new era in cosmology and even in particle physics: supposing that our Universe is filled with a single fluid with equation of state $p = w\rho$, we can easily see from the first Friedman equation

$$\frac{\ddot{a}}{a} = -\frac{\rho + 3p}{6M_p^2} \tag{1.1}$$

that, in order to obtain a positive acceleration $\ddot{a} > 0$, we need $w < -\frac{1}{3}$, i.e. our fluid, which will be called dark energy, is not composed by regular matter, since GR tells us that for this kind of material $0 \leq w \leq \frac{1}{3}$. The two groups noticed that this dark energy component could be given by a cosmological constant term and suddendly such term, introduced by Einstein nearly a century ago to obtain a static Universe, became the most puzzling component of our Universe.

1.1 Observational Evidence

Before going on and discuss what could be the problems related to the cosmological constant, let's briefly review the first observational evidence that we need a dark energy component and how this new component solved an existing problem about the age of Universe.
Type Ia supernovae [27] occur when a white dwarf star in a binary system accretes enough material from its partner that its mass becomes closer to the Chandrasekhar limit, where electron degeneracy cannot compensate anymore gravitational forces. The star becomes unstable and, due to the increased temperature and density, carbon and oxygen conversion into nichel triggers an explosion: since the mass is nearly the same when this happens, it is believed that the absolute luminosity of such explosion doesn not vary, therefore they can be used as standard candles. In principle, the nature of the explosion isn't affected by the nature of the partner or by the starting mass of the white dwarf, but it might depend from the metallicity, which, in some measure, depends from the epoch. This variation of the absolute luminosity is related to the rising and declining time of the light curve and it has been calibrated

through observations of similar supernovae in galaxies at known distance. The measured apparent magnitude m, proportional to the logarithm of the energy flux $\mathcal{F}$ we receive from the supernova, is related to the absolute magnitude M, connected to the logarithm of the absolute luminosity L, by the following relation

$$m - M = 5 \log_{10} \left(\frac{d_L}{Mpc} \right) + 25, \tag{1.2}$$

where d_L is the luminosity distance, defined by $d_L^2 = \frac{L}{4\pi\mathcal{F}}$ in order to preserve the inverse-square law for the diminuition of the light. Since the Hubble rate can be written as

$$H^2 = H_0^2 \left[\sum_i \Omega_{i0} (1+z)^{3(1+w_i)} \right], \tag{1.3}$$

where the sum runs over every component of Universe, it can be shown [12] that

$$d_L(z) = \frac{1+z}{H_0} \int_0^z \frac{dz'}{\sqrt{\sum_i \Omega_{i0} (1+z')^{3(1+w_i)}}}. \tag{1.4}$$

At low redshifts, this quantity reduces to $d_L(z) \simeq z H_0^{-1}$, therefore we can use low redshift supernovae to determine the absolute magnitude M; then we can use 1.2 to establish d_L for high redshift supernovae and we can compare this value to the theoretical one given by 1.4. The two groups we have mentioned found that observations were consistent for a flat Universe where $\Omega_{m0} \sim 0.3$ and $\Omega_{de0} \sim 0.7$, i.e. our Universe is dominated by a dark energy contribution, responsible of an acceleration started at

$$z_{acc} = \sqrt[3]{\frac{2\Omega_{de0}}{\Omega_{m0}}} - 1 \sim 0.67. \tag{1.5}$$

This result allowed to solve another issue related to the Universe age t_0. For consistency, this quantity has to be bigger than the age of the oldest stars, which was measured to be at least $11 - 12$ Gyr. From [12] we find that

$$t_0 = \int_0^\infty \frac{dz}{(1+z)H(z)}, \tag{1.6}$$

where $H(z)$ is given by 1.3. Neglecting the radiation component, since the radiation era didn't last for so a long time, and the curvature component, because observations constrain our Universe to be almost flat, for a matter dominated Universe, where $\Omega_m = 1$, we would have

$$t_0 = \frac{2}{3H_0} \sim 9 - 10 \text{ Gyr}, \tag{1.7}$$

while including also a dark-energy contribution we find

$$t_0 = \frac{2}{3H_0\sqrt{\Omega_{\Lambda 0}}} \log \left[\frac{1+\sqrt{\Omega_{\Lambda 0}}}{\sqrt{\Omega_{m0}}} \right] \sim 14 \text{ Gyr}, \tag{1.8}$$

value which solves the age problem.
Over the years this evidence about the existence of such new dark energy component has been confirmed either by new supernovae that has been discovered and by other experiments which has analyzed the CMB temperature anisotropies and the large scale structure formation.

1.2 Cosmological Constant Problem

Even if observations indicate the presence of a cosmological constant (CC) type term, from a particle physics point of view such term brings a fine-tuning problem. As for the quantity that Einstein studied, the CC is characterized by a constant energy density

$$\rho_\Lambda = M_p^2 \Lambda = -p_\Lambda \tag{1.9}$$

and generates the accelerated expansion through its negative pressure. Observationally we have found that

$$\Lambda_{obs} \simeq H_0^2 \sim 10^{-84}\ \text{GeV}^2 \Longrightarrow \rho_\Lambda \simeq H_0^2 M_p^2 \sim 10^{-48}\ \text{GeV}^4. \tag{1.10}$$

Theoretically such term arises as an energy density of the vacuum, in fact the vacuum stress-energy tensor, because of Lorentz invariance of the vacuum state and invoking the general covariance principle, reads as $T_{\mu\nu} = \rho_{vac} g_{\mu\nu}$, where in general the zero point energy of a quantum field with mass m is given by

$$\rho_{vac} = \frac{1}{2} \int \frac{d^3k}{(2\pi)^3} \sqrt{k^2 + m^2} \tag{1.11}$$

and presents an ultraviolet divergence. Assuming that the quantum theory is reliable until the Planck mass M_p, we can put a cut-off to the previous integral which will read as

$$\rho_{vac} \sim M_p^4 \sim 10^{72}\ \text{GeV}^4, \tag{1.12}$$

120 orders of magnitude bigger than the observed value. Even with a more conservative choice, for example choosing the cut-off at approximately 1 TeV because under such scale the Standard Model has been carefully investigated, we end up with a value

$$\rho_{vac} \sim 10^{12}\ \text{GeV}^4, \tag{1.13}$$

with a difference of 60 orders of magnitude with respect to the observed value. This contribution is due to the ordering ambiguity of the fields, but since the procedure to "rescale"the zero point energy is *ad hoc* and experiments showed that indeed the energy of the vacuum can produce macroscopic effects, such as on the Casimir force experiment, one can try to properly cancel it through counter terms, even if the degree of fine-tuning required is absurdly high.
If we lived in a Universe with an unbroken supersimmetry, then ρ_{vac} would be exactly zero because the zero-point energy of every bosonic particle would be canceled by its fermionic counter part; unfortunately, even if such theory is valid, the SUSY is broken in our world and since the breaking happens at least around 1 TeV, we are far from having explained the smallness of the cosmological constant.
It is worthy to mention that it exists some sort of anthropic principle, even if physicists don't like such kind of motivation. The presence itself of observers means that the dark energy component became significative only at late times, allowing the structure formation, in particular the galaxy formation, because starting from matter-dark enrgy equivalence structures stop growing. This fact puts a strict bound [26] on

$$\rho_\Lambda \leq 500 \rho_{m0} \sim 10^{-46}\ \text{GeV}^4, \tag{1.14}$$

even if this principle doesn't explain the underlying physics.

1.3 Dynamical Dark Energy

Since the cosmological constant problem has not been resolved yet, different authors tried other approaches, in particular it is possible to assume that, for some unknown reason, the cosmological constant is exactly zero and the accelerated expansion is due to some form of dynamical dark energy. Since it is thought that the Universe has already experienced an accelerated expansion phase known as inflation, it was quite natural to think that also in the present epoch the accelerated expansion could be driven by a scalar field; moreover, in theories that extends the Standard Model, such as Supersymmetry or String Theory, we can find different candidates for such a field. We won't go through all the different theories that have been proposed during these years but the interested reader can find an extended review in [12]. As an example of such models, let's briefy introduce Quintessence theories: here the field is characterized by the action

$$S = \int d^4x\sqrt{-g}\left[\frac{1}{2}\partial^\mu\phi\partial_\mu\phi - V(\phi)\right] \tag{1.15}$$

the equation of state

$$w_\phi = \frac{p_\phi}{\rho_\phi} = \frac{\dot{\phi}^2 - 2V(\phi)}{\dot{\phi}^2 + 2V(\phi)}, \tag{1.16}$$

therefore it can mimic the cosmological constant behaviour and produce the Universe expansion under the slow-roll condition $\dot{\phi}^2 \ll V(\phi)$. This does not resolve the problems, in fact in addition to the "old"fine-tuning problem, a coupling between scalar field and matter arises due to quantum correction, even if at classical level there isn't. This coupling will produce, since the mass of the field has to be small in these thoeries, long range forces and a possible time dependance of constants of nature, which has to be constrained. Unless there is an underlying symmetry that suppresses these couplings, we have to required that these values must be small, which is indeed another fine-tuning requirement.
In order to avoid any additional fine tuning request, we will investigate the behaviour of a class of models in which there is, also at classical level, a non-zero coupling to matter and where there are screening mechanisms that allow the new force to be undetected until now. Precisely because of this the new force, which will act as an additional gravitational contribution, these models are called "Modified Gravity"(MG) models.

The thesis is organized as follows. In Chapter 2 we introduce such models, which are cast as scalar-tensor theories coupled with matter; then we present some generic feature and we analyze in detail the three typical class of models we will investigate. In Chapter 3 we discuss cosmological implications of such scalar field and we introduce an intuitive parametrization of such theories that will allow us to describe the linear and non-linear anomalous matter growth during structure formation. In Chapter 4 we will analyze in detail the gravitational collapse in MG through analytical and numerical methods, showing how the fifth force mediated by the scalar field affects the dynamics of the collapse. In Chapter 5 we will introduce the excursion set theory, a framework that will allow us to link the results we found in the previous chapter to the statistics of virialized structures, obtaining, in the end, how their number changes in a MG scenario. Finally, in Chapter 6, we will briefly discuss possible extensions of this work.

All through this thesis we will adopt the following conventions. We will use natural units, so $c = \hbar = 1$, and the reduced Plank mass will be given by $M_p^2 =$

$(8\pi G)^{-1}$. We choose to work with the mostly minus Minkowski flat metric $\eta_{\mu\nu} = \text{diag}(+1, -1, -1, -1)$. We will indicate the covariant derivative and the covariant Dalembertian respectivey as D_μ and $\Box_g = g^{\mu\nu} D_\mu D_\nu$.

Chapter 2

Modified Gravity Models

In this chapter we will show how Einstein gravity can be consistently modified in order to explain the expansion of the Universe, without considering a cosmological constant; we will do so introducing a new scalar degree of freedom that will mediate a new fifth force because of its coupling to matter. Since GR has been well tested in our solar system, there must be some mechanism that explains why the force has not been detected: this screening property, i.e. this suppression of the fifth force with respect to the Newtonian one, is due to nonlinearities developed by the field. In principle, in a generic lagrangian we can include terms that involve the field, its first and second derivatives, but not higher order derivatives since we want to obtain second order equations of motion: each one of this kind of terms, in particular regions, can dominate over the others, generating those nonlinearities; moreover we can classify such mechanisms according to particular screening criterions. We will mainly focus on the first type of screening mechanism and just in the last section we will quickly review the basic features of the second and the third kind, where derivatives of the field become relevant.

2.1 Screening by Deep Potentials

In this first class of models screening occurs in regions where the Newtonian potential reaches and exceeds some large critical value. In the Einstein Frame (EF), i.e. the frame where gravity has the form of GR, the action has general form given by

$$S = \int d^4x\sqrt{-g}\left[-\frac{M_p^2}{2}R + \frac{1}{2}\partial^\mu\phi\partial_\mu\phi - V(\phi)\right] + S_{matter}\left[A^2(\phi)g_{\mu\nu}, \psi^{(i)}\right], \quad (2.1)$$

where R is the Ricci scalar and the field behaviour will be characterized by its potential $V(\phi)$ and its coupling function $A(\phi)$ to different matter fields $\psi^{(i)}$, labelled by i. In principle, differents A_i are allowed, but since this would imply a violation of the Equivalence Principle because different kinds of matter will couple to gravity with different strenghts, we choose to study just the case in which $A_i = A,\ \forall i$.
Notice that the matter action is a functional of the Jordan Frame (JF) metric $\tilde{g}_{\mu\nu} = A^2(\phi)g_{\mu\nu}$, i.e.

$$S_{matter}\left[\tilde{g}_{\mu\nu}, \psi^{(i)}\right] = \int d^4x\sqrt{-\tilde{g}}\mathcal{L}_m\left[\tilde{g}_{\mu\nu}, \psi^{(i)}\right]: \quad (2.2)$$

this is the frame in which matter minimally couples to gravity and from now on we will indicate every quantity calculated in the JF with a $\tilde{}$, while quantities without it are calculated in the EF.

The equation of motion (EOM) for ϕ is obtained through a variational principle from 2.1; in particular, introducing the JF stress-energy tensor (SET)

$$\tilde{T}_m^{\mu\nu} = -\frac{2}{\sqrt{-\tilde{g}}}\frac{\delta S_m}{\delta \tilde{g}_{\mu\nu}} \tag{2.3}$$

and, in a second step, its trace $\tilde{T}_m = \tilde{T}_m^{\mu\nu}\tilde{g}_{\mu\nu}$, we have that

$$\begin{aligned}\delta S_{matter} &= \int d^4x \frac{\delta(\sqrt{-\tilde{g}}\mathcal{L})}{\delta \tilde{g}_{\mu\nu}}\frac{\delta \tilde{g}_{\mu\nu}}{\delta\phi}\delta\phi = \\ &= -\int d^4x \frac{\sqrt{-g}A^4}{2}\tilde{T}_m^{\mu\nu}\tilde{g}_{\mu\nu}\frac{2}{A}\frac{\partial A}{\partial\phi}\delta\phi,\end{aligned} \tag{2.4}$$

therefore the EOM reads as

$$\Box_g\phi = -\frac{\partial V}{\partial\phi} - \tilde{T}_m A^3\frac{\partial A}{\partial\phi}. \tag{2.5}$$

Because of the minimal coupling, this matter stress-energy tensor is covariantly conserved, i.e. $\tilde{D}_\mu\tilde{T}_m^{\mu\nu} = 0$, while in the EF the conserved quantity is the global stress-energy tensor $T_m^{\mu\nu} + T_\phi^{\mu\nu}$: these two matter SET are connected through the appropriate power of A, in particular

$$\tilde{T}_m = \tilde{g}_{\mu\nu}\tilde{T}_m^{\mu\nu} = A^2 g_{\mu\nu}\left(-\frac{2}{A^4\sqrt{-g}}\frac{\delta S_m}{\delta g_{\mu\nu}}\frac{\delta g_{\mu\nu}}{\delta\tilde{g}_{\mu\nu}}\right) = A^{-4}g_{\mu\nu}T_m^{\mu\nu} = A^{-4}T_m, \tag{2.6}$$

so that we can rewrite equation 2.5 as

$$\Box_g\phi = -\frac{\partial V_{eff}}{\partial\phi} = -\frac{\partial V}{\partial\phi} - \frac{T_m}{M_p}\beta(\phi) \tag{2.7}$$

where $V_{eff} = V + \rho_m \log A$ and we have introduced the coupling to matter function

$$\beta(\phi) = \frac{M_p}{A}\frac{\partial A}{\partial\phi}. \tag{2.8}$$

In this kind of scalar-tensor theories, masses of fundamental fermion particles are given by $m_p = A(\phi)m_{bare}$, where m_{bare} is their mass appearing in the matter lagrangian. This means that the mass evolves according to the cosmological evolution of the scalar field and that their variation is given by

$$\frac{\Delta m_p}{m_p} = \frac{\beta(\phi)}{M_p}\Delta\phi. \tag{2.9}$$

Since this variation is tightly bounded by Big Bang Nucleosynthesis, we have to avoid large excursions of the field in order to preserve the formation of elements: this can be achieved requiring that the field has to sit on its potential energy minimum, which has to be stable, before BBN and has to follow it along the evolution of the Universe; moreover this minimum position should not vary too much. In other words, the conformal factor $A(\phi)$ should read as 1 + small corrections dependent from ϕ.

2.2 Appearance of a Fifth Force

This new scalar field, which will drive the Universe expansion, mediates also a new fifth force. We are interested in what happens in the EF, where we can distinguish

effects due to the usual Einstein gravity from those due to the scalar field, but let's start from the JF instead: here, by definition, matter fields will couple minimally to gravity, therefore the acceleration of a test particle in free fall will reads as $\ddot{\mathbf{x}} = -\nabla\tilde{\Psi}_N$, where $\tilde{\Psi}_N$ is this frame Newtonian potential. This relation appears taking the "classical limit"of the geodesic equation

$$\frac{d^2x^\mu}{d\lambda^2} + \tilde{\Gamma}^\mu_{\alpha\beta}u^\alpha u^\beta = 0, \tag{2.10}$$

where $x^\mu(\lambda)$ is the test particle world-line and $u^\alpha = \frac{dx^\alpha}{d\lambda}$ is its 4-velocity, normalized in such a way that $u^\mu u_\mu = 1$. We can explicitly rewrite 2.10 in the EF, obtaining

$$\frac{d^2x^\mu}{d\lambda^2} + \left[\Gamma^\mu_{\alpha\beta} + \frac{\partial \log A}{\partial\phi}\left(\delta^\mu{}_\alpha\partial_\beta\phi + \delta^\mu{}_\beta\partial_\alpha\phi - g_{\alpha\beta}\partial^\mu\phi\right)\right]u^\alpha u^\beta = 0. \tag{2.11}$$

Now the classical limit is obtained considering a weak and static gravitational field, i.e.

$$g_{\mu\nu} = \eta_{\mu\nu} + h_{\mu\nu}, \quad |h_{\mu\nu}| \ll 1; \quad \partial_0 g_{\mu\nu} = 0 \tag{2.12}$$

and assuming that particles velocities are small, i.e. $v \ll 1$. From this last assumption it follows that each component $v^i = \frac{dx^i}{dx^0} = \frac{u^i}{u^0}$ has to be small, therefore $u^i \ll u^0$. Under this approximation, equation 2.11 reads at first order as

$$\begin{aligned} 0 &= \frac{d^2x^\mu}{d\lambda^2} + \left[\Gamma^\mu_{00} + \frac{\partial \log A}{\partial\phi}\left(\delta^\mu{}_0\partial_0\phi + \delta^\mu{}_0\partial_0\phi - g_{00}\partial^\mu\phi\right)\right](u^0)^2 = \\ &= \frac{d^2x^\mu}{d\lambda^2} + \left[-\partial^\mu\left(\frac{h_{00}}{2} + \log A\right) + 2\delta^\mu{}_0\partial_0\log A)\right](u^0)^2. \end{aligned} \tag{2.13}$$

Choosing $x^0(\lambda) = t$, the 0-th component of the previous equation reas as

$$\frac{d^2t}{d\lambda^2} + (u^0)^2\partial_0\log A = 0, \tag{2.14}$$

while the i-th component, recalling that $h_{00} = 2\Psi_N$, where Ψ_N is the usual Newtonian potential because in the EF the Einstein-Hilbert action is the same that in GR, is given by

$$\begin{aligned} 0 &= \frac{d^2x^i}{d\lambda^2} - \partial^i\left(\Psi_N + \log A\right)(u^0)^2 = \\ &= \frac{d^2x^i}{dt^2}(u^0)^2 + v^i\frac{d^2t}{d\lambda^2} - (u^0)^2\partial^i(\Psi_N + \log A). \end{aligned} \tag{2.15}$$

Considering equation 2.14, the second term is negligible due to the v^i prefactor, therefore we have proved the the test particle acceleration is given by

$$\ddot{\mathbf{x}} = -\nabla\left[\Psi_N + \log A\right], \tag{2.16}$$

where the second term will produce a fifth force, dependent from the choice of the potential $V(\phi)$ and coupling function $A(\phi)$.

2.3 Models

We will now introduce the three principal kind of models: the chameleon ([17],[5]), the symmetron ([14],[15]) and the dilaton ([7],[8]). We will present the features of these models and how they hide their presence, i.e. their screening mechanism.

2.3.1 Chameleon

Despite we will not study this kind of field in the following part of the thesis, we will explain it in detail because its screening criterion can be generalized to the other models we will use.
The chameleon field, as the name itself suggests, mimics the environment where it lives and achieves a large (small) mass in high (low) density regions. This model is characterized by a runaway potential and a mostly constant coupling to matter; so, since the effective mass will receive contributions from both terms, in particular

$$m_{eff}^2 = \frac{d^2V_{eff}}{d\phi^2} = \frac{d^2V}{d\phi^2} + \rho\frac{d^2A}{d\phi^2}, \tag{2.17}$$

we can assume without any loss of generality that $V(\phi)$ and $A(\phi)$ are respectively a monotonically decreasing and increasing functions of ϕ, in order to obtain a sort of balance between them. This balance will in the end produce a density dependent minimum position. On the base of what we explained before, we can take

$$A(\phi) \simeq 1 + \beta\frac{\phi}{M_p}, \tag{2.18}$$

while for $V(\phi)$ we have to require also that $\partial_\phi^2 V > 0$ and $\partial_\phi^3 V < 0$: the first condition is given by the fact that the major contribution to the effective mass comes from the potential and we want to guarantee stability, the second one ensures that the effective mass is an increasing function of the density. An example of such potential is given by the Ratra-Peebles potential

$$V(\phi) = \frac{M^{n+4}}{\phi^n}, \quad n > 0. \tag{2.19}$$

Let's now analyze how the field behaves: we consider a spherically simmetric body with constant mass M, radius R and density ρ_o, living in a static, homogeneous and isotropic background with density ρ_b. Under these hypothesis, the field will try to reach its environment-dependent effective potential energy minimum, which we will indicate respectively as ϕ_o and ϕ_b; moreover the KG equation reduces to

$$\nabla^2\phi = \frac{1}{r^2}\frac{d}{dr}\left[r^2\frac{d\phi}{dr}\right] = \frac{dV}{d\phi} + \beta\frac{\rho}{M_p} \tag{2.20}$$

where, as explained,

$$\rho(r) = \begin{cases} \rho_o & r \leq R \\ \rho_b & r > R \end{cases}. \tag{2.21}$$

This equation has to be solved imposing that the solution is non-singular at the origin and that the field recovers its background value far away from the object, i.e.

$$\left.\frac{d\phi}{dr}\right|_{r\to 0} \to 0; \quad \phi(r \to \infty) \to \phi_b. \tag{2.22}$$

Instead of numerically solve equation 2.20, let's derive the qualitative behaviour of the solution.
Outside the object, but still within the Compton wavelength m_b^{-1}, where $m_b = m_{eff}(\phi_b)$, the field can reach its minimum, therefore 2.20 approximately reads as $\nabla^2\phi = 0$, which has solution

$$\phi(r) \simeq \phi_b - \frac{Ce^{-m_b(r-R)}}{r}, \quad R \leq r \leq m_b^{-1}, \tag{2.23}$$

where C is a constant and we have introduced by hand the Yukawa suppression because our field is massive, even if in this region the mass is tiny. From this profile we can see that further than m_b^{-1}, the exponential factor flattens the field on its background value, resulting in an absence of any fifth force.
The field profile inside the body depends on the object properties, in particular we can identify two different regimes, called thin-shell (t-s) and thick-shell (T-s) regime. In the first one the object is big enough that the field can reach its minimum, i.e. $\phi(r=0) - \phi_o = \phi_i - \phi_o \ll \phi_o$: because of this fact, in this regime the field has to satisfy $\nabla^2\phi = 0$ until some radius R_S close to R, where the field starts feeling the sudden change in the environment density, therefore in the effective potential, and begins to increase. As soon as it is displaced significantly from its equilibrium position, we will not have anymore any compensation in the RHS of 2.20, which will read in this shell $[R_S, R]$ as

$$\frac{d^2\phi}{dr^2} + \frac{2}{r}\frac{d\phi}{dr} \simeq \frac{\beta\rho_o}{M_p} \tag{2.24}$$

and has solution

$$\phi(r) = \frac{\beta\rho_o}{6M_p}r^2 + \frac{A}{r} + B. \tag{2.25}$$

Imposing continuity of ϕ and $\frac{d\phi}{dr}$ at $r = R_S$ we find that

$$A = \frac{\beta\rho_o}{3M_p}R_S^3, \quad B = \phi_o - \frac{\beta\rho_o}{2M_p}R_S^2; \tag{2.26}$$

requiring same conditions at $r = R$ and using $m_b R \ll 1$, $|R_S - R| \ll R$, we find that

$$C = \frac{\beta M}{4\pi M_p}\frac{3\Delta R_S}{R_S} \tag{2.27}$$

$$\frac{\Delta R_S}{R_S} = \frac{R - R_S}{R_S} = \frac{\phi_b - \phi_o}{6\beta M_p|\Psi_N|} \tag{2.28}$$

where Ψ_N is the Newtonian potential. Equation 2.28 is the all-important thin-shell condition. In the T-s regime, the object is not able to perturb too much the environment, thus the field profile. In this case the field do not sit on its minimum inside the object, but it assumes a value $\phi_i \geq \phi_o$; so that we have to solve equation 2.24 for $r \in [0, R]$ and to impose the non singularity condition, which gives

$$\phi(r) = \frac{\beta\rho_o}{6M_p}r^2 + \phi_i. \tag{2.29}$$

Requiring continuity at $r = R$, this time we find that

$$C = \frac{\beta M}{4\pi M_p}, \quad \phi_i = \phi_b - 3\beta M_p\Psi_N. \tag{2.30}$$

We can estimate the value of the thin shell condition in this regime, finding

$$\frac{\Delta R}{R} \geq \frac{\phi_b - \phi_i}{6\beta M_p\Psi_N} \simeq \mathcal{O}(1), \tag{2.31}$$

thus we can separate the two regimes according to the value assumed by this condition. Let's notice that this second regime interior solution could be obtained from the first one taking the limit $R_S \to 0$ and substituting $\phi_o \to \phi_i$.
As we can see from the complete profile, in the t-s regime just a thin shell below the surface of the object contributes to the fifth force and the force exerted on a test

particle is suppressed by the t-s factor, making the body screened; on the contrary, in the T-s regime the coupling is not suppressed and the objects will be unscreened. This screening/unscreening criterion tells us how big the deviation from GR will be, so let's now suppose to deal with screened objects, since until now we have not observed any significative deviation from Newtonian gravity. Under this assumption, we notice that this fifth force will be scale(mass)-dependent, in fact once that the environment ($\rho_o,\ \rho_b$) is fixed, we would have $|\Psi_N| \sim M^{\frac{2}{3}} \sim R^2$, therefore, for a given value of β, bigger (or heavier) objects will be more screened with respect to smaller (or lighter) objects.
Finally, let's write down the effective gravitational potential outside the body but still at short distances compared to m_b^{-1}, given by

$$\Psi = \Psi_N + \log A \simeq \Psi_N + \frac{\beta}{M_p}\phi(r) \simeq \frac{\beta\phi_b}{M_p} - \frac{GM}{r}\left[1 + 2\beta^2\left(\frac{3\Delta R_S}{R_S}\right)\right], \tag{2.32}$$

where we can notice that for objects in the T-s regime, the effect of MG is to rescale the Newton constant by a factor $(1 + 2\beta^2)$.

2.3.2 Symmetron

In these kind of models we have a symmetry breaking potential (hence the name of the model) that allows the field to develop a non-zero (zero) coupling to matter in low (high) density regions. The easiest example of such potential is given by the mexican hat

$$V(\phi) = V_0 - \frac{1}{2}\mu^2\phi^2 + \frac{\lambda}{4}\phi^4, \tag{2.33}$$

even if other shapes are possible, as we will see in the next chapter. In these models the coupling function is given by

$$A(\phi) = 1 + \frac{A_2}{2}\phi^2, \tag{2.34}$$

where, as explained, we suppose that the quadratic correction is small. In the end, the effective potential reads as

$$V_{eff} \simeq V_0 + \frac{1}{2}\left[A_2\rho_m - \mu^2\right]\phi^2 + \frac{\lambda}{4}\phi^4. \tag{2.35}$$

In dense regions, where matter density is higher than the critical value $\rho_c = \frac{\mu^2}{A_2}$, the mass term in square brackets will be positive, therefore the potential will have only one global minimum in $\bar{\phi} = 0$; on the other hand, when the environment density is low, two global minima appear at $\bar{\phi} = \pm\sqrt{\frac{A_2(\rho_c - \rho_m)}{\lambda}}$. The mass of the field, evaluated at its proper minimum, reads as

$$m_{eff}^2 = A_2(\rho_m - \rho_c) + 3\lambda\phi^2 \simeq \begin{cases} A_2\rho_m & \rho_m \gg \rho_c \\ 2A_2\rho_c & \rho_m \ll \rho_c \end{cases} \tag{2.36}$$

and we will assume that this phase transition happens in the recent past, so that the mass of the symmetron in the cosmological background is approximately given by $m_0^2 \sim \mu^2 \sim A_2\rho_{0m}$.
The effective coupling to matter $\beta \simeq M_p A_2\phi$ depends from the VEV of the field, therefore in dense regions we will not have any modification to gravity.
Let's suppose to have the same environmental setup we described in the chameleon case. If the body density is high enough compared to the critical one, then, inside the

object, the field sits on the $\phi = 0$ minimum. Expanding the field as $\phi = \phi_{min} + \delta\phi = \delta\phi$, the effective potential is approximately given by $V_{eff} \simeq \frac{A_2\rho_m}{2}\delta\phi^2 = \frac{1}{2}m_o^2\delta\phi^2$, so that we have to solve $\nabla^2\delta\phi = m_o^2\delta\phi$; imposing the same boundary conditions given in 2.22, the field profile reads as

$$\phi(r) = A\frac{\sinh(m_o r)}{m_o r}, \quad r \leq R \tag{2.37}$$

Outside the body but at short distances with respect to m_b^{-1}, assuming that density vanishes at infinity, the field will sit at $\phi_\star = \bar{\phi}(\rho_m = 0)$. As before we can expand around $\phi_\star$, thus in this case the effective potential will be approximately $V_{eff} \simeq \mu^2\delta\phi^2 = \frac{m_b^2}{2}\delta\phi^2$ and we have to solve $\nabla^2\delta\phi = m_b^2\delta\phi$, obtaining is this way

$$\phi(r) = \phi_\star + \frac{B}{r}e^{-m_b(r-R)}. \tag{2.38}$$

Asking for continuity at $r = R$ we can determine the two constants A and B, finding the complete profile

$$\phi(r) = \begin{cases} \frac{\phi_\star}{\cosh(m_o R)}\frac{\sinh(m_o r)}{m_o r} & r \leq R \\ \phi_\star - \phi_\star\left[1 - \frac{\tanh(m_o R)}{m_o R}\right]\frac{R}{r}e^{-m_b(r-R)} & R < r < m_b^{-1} \end{cases}, \tag{2.39}$$

where for dense enough bodies we have $m_o R \gg 1$. The coupling to matter outside the object reads as $\beta_\star \simeq M_p A_2 \phi_\star$ so we can see that a test particle, outside the object but at distances much smaller than m_b^{-1} will feel the effective gravitational potential

$$\begin{aligned} \Psi = \Psi_N + \log A \simeq \Psi_N + \frac{A_2\phi_\star^2}{2}\left[1 - \frac{R}{r}\right]^2 \simeq \\ \simeq \frac{A_2\phi_\star^2}{2} - \frac{GM}{r}\left[1 + \frac{2\beta_\star^2}{2A_2M_p^2|\Psi_N|}\right] + \mathcal{O}\left(\frac{R^2}{r^2}\right), \end{aligned} \tag{2.40}$$

therefore the fifth force will be heavily suppressed if

$$1 \ll 2A_2M_p^2|\Psi_N| = \frac{2\beta_\star M_p|\Psi_N|}{\phi_\star}, \tag{2.41}$$

i.e. we find the same thin-shell condition

$$\frac{\phi_\star - \phi_o}{2\beta_\star M_p\Psi_N} \ll 1, \tag{2.42}$$

where now $\phi_o \simeq 0$, we had already found for the chameleon field. Conclusions which had followed from this result are still valid.

2.3.3 Dilaton

The third model we are going to introduce is the environment-dependent dilaton. In this model we have a quadratic coupling function $A(\phi) = 1 + \frac{A_2}{2}(\phi - \phi_\star)^2$, characterized by the presence of a miminum and where the quadratic correction is still small, and a slowly varying runaway potential, for example $V(\phi) = V_0 e^{-\frac{\phi}{M_p}}$, such that $\partial_\phi^2 V(\phi_\star) \sim H_0^2$. In this kind of model the field will not couple to matter inside a dense body, while in rarefied environments it will mediate a fifth force: when density is large, the effective potential

$$V_{eff} = V(\phi) + \frac{\rho_m A_2}{2}(\phi - \phi_\star)^2 \tag{2.43}$$

will be dominated by the second term and its minimum ϕ_o will be close to $\phi_\star$ for large enough A_2, therefore $\beta(\phi_o) \simeq M_p A_2(\phi_o - \phi_\star) \simeq 0$. On the other hand, in low density regions, $\beta(\phi_b) \neq \beta(\phi_\star) = 0$ and the field can have a non-zero coupling to matter. The density dependent minimum of V_{eff} is given by

$$\phi_{min}(\rho) = \phi_\star - \frac{\partial_\phi V(\phi_{min})}{A_2\rho} \simeq \phi_\star - \frac{\partial_\phi V(\phi_\star)}{A_2\rho} \tag{2.44}$$

and the mass of the field reads as $m^2 = \partial^2_\phi V + A_2\rho_m$. Today, in the cosmological background, the mass of the dilaton will reads as $m_0^2 \simeq 3A_2 M_p^2 \Omega_{0m} H_0^2$.
Inside a dense body, the minimum of the field will be very close to $\phi_\star$, therefore, expanding

$$\nabla^2\phi = \partial_\phi V + A_2\rho_o(\phi - \phi_\star) \tag{2.45}$$

around $\phi = \phi_o + \delta\phi$, we find that the fluctuation has to satisfy $\nabla^2\delta\phi = m_o^2\delta\phi$ and the complete interior profile will read as

$$\phi(r) = \phi_o + A\frac{\sinh(m_o r)}{r}. \tag{2.46}$$

Outside we will expand

$$\nabla^2\phi = \partial_\phi V + A_2\rho_b(\phi - \phi_\star) \tag{2.47}$$

around $\phi = \phi_b + \delta\phi$ and using 2.44 we find that

$$\phi(r) = \phi_b - B\frac{e^{-m_b(r-R)}}{r}. \tag{2.48}$$

Imposing continuity between inside and outside we obtain

$$\phi(r) = \begin{cases} \phi_o + \frac{\phi_b - \phi_o}{\cosh(m_o R)}\frac{\sinh(m_o r)}{m_o r} & r \leq R \\ \phi_b - (\phi_b - \phi_o)\left[1 - \frac{\tanh(m_o R)}{m_o R}\right]\frac{R}{r}e^{-m_b(r-R)} & R < r < m_b^{-1} \end{cases}, \tag{2.49}$$

where

$$\phi_b - \phi_o = \frac{\beta_b}{A_2 M_p}\left(1 - \frac{\beta_o}{\beta_b}\right) = \frac{\beta_b}{A_2 M_p}\left(1 - \frac{\rho_b}{\rho_o}\right). \tag{2.50}$$

Finally, the interesting part of the effective gravitational potential will read as

$$\Psi \simeq -\frac{GM}{r}\left[1 + \frac{2\beta_b^2}{2A_2 M_p^2|\Psi_N|}\left(1 - \frac{\rho_b}{\rho_o}\right)\right] + \mathcal{O}\left(\frac{R^2}{r^2}\right) \tag{2.51}$$

and the body will be screened if

$$\frac{1 - \frac{\rho_b}{\rho_o}}{2A_2 M_p^2|\Psi_N|} \ll 1 \Longrightarrow \phi_b - \phi_o \ll 2\beta_b M_p|\Psi_N|, \tag{2.52}$$

as in the chameleon and symmetron case.

2.3.4 $f(R)$ Theories

Another well known family of theories that can reproduce the expansion of the Universe is given by $f(R)$ theories: first of all we will show how they can be cast as scalar-tensor theories, then, in a second moment, we will display how some of them

present a chameleon type of screening. In this case the Einstein-Hilbert action reads as

$$S_{EH} = -\frac{M_p^2}{2}\int d^4x\sqrt{-g}\,[R + f(R)] = -\frac{M_p^2}{2}\int d^4x\sqrt{-g}\left[R + f(\Phi) + \frac{df}{d\Phi}(R-\Phi)\right], \tag{2.53}$$

where we have introduce the auxiliary field Φ. The equivalence between the second and third member is proved finding the EOM for Φ which gives, assuming that $\frac{d^2f}{d\Phi^2} \neq 0$, the non-dynamical constrain $\Phi = R$. Under the conformal rescaling of the metric $g_{\mu\nu} = \Omega^2\bar{g}_{\mu\nu}$, where

$$\Omega^{-2} = 1 + \frac{df}{d\Phi} = e^{-\sqrt{\frac{2}{3}}\frac{\phi}{M_p}} \tag{2.54}$$

and ϕ is a new field defined by the above relation, we have that $\sqrt{-g} = \Omega^4\sqrt{-\bar{g}}$ and the Ricci scalar reads as

$$R = \Omega^{-2}\left[\bar{R} - 6\bar{\Box}_g \log\Omega - 6\bar{g}^{\mu\nu}\partial_\mu \log\Omega\partial_\nu \log\Omega\right]. \tag{2.55}$$

Since the term proportional to

$$\int d^4x\sqrt{-\bar{g}}\bar{\Box}_g \log\Omega = \int d^4x\sqrt{-\bar{g}}\frac{1}{\sqrt{-\bar{g}}}\partial_\mu\left(\sqrt{-\bar{g}}\bar{g}^{\mu\nu}\partial_\nu \log\Omega\right) \tag{2.56}$$

gives a surface contribution, we will neglect it. In the end we have that 2.53 has become

$$\int d^4x\sqrt{-\bar{g}}\left[-\frac{M_p^2}{2}\bar{R} + \frac{1}{2}\bar{g}^{\mu\nu}\partial_\mu\phi\partial_\nu\phi - V(\phi)\right], \tag{2.57}$$

where we have defined

$$V(\phi) = \frac{M_p^2}{2}\frac{f(R) - R\frac{df}{dR}}{\left(1+\frac{df}{dR}\right)^2}. \tag{2.58}$$

In the meantime, the matter action $S_{matter}\left[g_{\mu\nu}, \psi^{(i)}\right]$ has become $S_m\left[e^{\sqrt{\frac{2}{3}}\frac{\phi}{M_p}}\bar{g}_{\mu\nu}, \psi^{(i)}\right]$, gaining the conformal factor. From its form we can deduce immediately that $\beta = \frac{M_p}{A}\frac{dA}{d\phi} = \frac{1}{\sqrt{6}}$ is constant, as in the chameleon case.
Viceversa, we can reconstruct the value of R and $f(R)$: the first one reads as

$$R(\phi) = \frac{\sqrt{6}}{M_p}e^{\sqrt{\frac{2}{3}}\frac{\phi}{M_p}}\frac{d}{d\phi}\left[e^{-2\sqrt{\frac{2}{3}}\frac{\phi}{M_p}}V(\phi)\right] \tag{2.59}$$

and is obtained deriving 2.58 with respect to the scalar field and using 2.54; the second one is obtained through a direct substitution of 2.59 into 2.58. The complete expression will read as

$$R + f(R) = -\frac{2}{M_p^2}e^{-2\sqrt{\frac{2}{3}}\frac{\phi}{M_p}}V(\phi) + \frac{\sqrt{6}}{M_p}e^{-2\sqrt{\frac{2}{3}}\frac{\phi}{M_p}}\frac{dV}{d\phi}. \tag{2.60}$$

Conditions on the potential $V(\phi)$ become condition on $f(R)$ and its derivatives (see [6]) and it can easily shown that, for example, theories with $f(R) \sim R^{p+1}$, $-1 < p < 0$ have the corresponding potential that goes as $V(\phi) \sim \phi^{-n}$, where $n = -\frac{1+p}{p} > 0$, as in the Ratra-Peebles potential. We will return on this fact in the next chapter.

2.3.5 Universality of Thin Shell Condition

We have seen that, despite being so different, all models has the same thin-shell condition that allows us to understand if a given object is screened or not. Moreover, this condition does not depend from specific details of the models but just from the density-dependent field value which minimises the effective potential inside and outside the body. This particular features was noticed for the first time in [9], where it was argued why this universal condition occurs: it was found that every model shares some common property with the others, such as a field mass which increases with the environment density, and indeed we have seen a recurrent but quite model indipendent pattern, which enforces the general form of the solution, during our calculation of the field profile.
Furthermore this screening condition can be related to local experimental constrains on modified gravity effects. For example, the fact that we do not observe deviations from Einstein gravity in the Milky Way, i.e. that the Milky Way is screened, allow us to put bounds on the mass of the scalar field in vacuum: in general it has been found that $\frac{m_0}{H_0} \geq 10^3$, which means that the range of the fifth force is approximately given by $m_0^{-1} \leq 10^{-3} H_0^{-1} \sim Mpc$ (see e.g. Figure 1 in [2] for chameleon and $f(R)$ theories). Under this constrain, we find that the A_2 parameter in the symmetron and dilaton case has to satisfy $A_2 \geq 10^6 M_p^{-2}$.

2.4 Other Screening Mechanisms

In this section we will briefly expose the two other types of screening, where nonlinearities come from higher-derivative interactions.
The first one is called kinetic screening and here the fifth force is suppressed when the gravitational acceleration is higher than some critical value. Defining the Lorentz invariant quantity $X = \frac{1}{2}\partial^\mu\phi\partial_\mu\phi$, the generic lagrangian in this kind of models called "$P(X)$ models"will read as

$$\mathcal{L} = \sum_{j=1}^{n} c_j \frac{X^j}{\Lambda^{4(j-1)}} - \frac{gT}{M}\phi = P(X) - \frac{gT}{M}\phi \tag{2.61}$$

where Λ is some characteristic mass scale and we have introduced a coupling between the field and the matter, with relative strenght g, that allows the creation of nonlinearities. There are two regions: close and far from the matter source, i.e. below or above some critical radius $r_\star$, defined as the distance where $\frac{X}{M^4} \simeq 1$ and all terms of the lagrangian becomes significatives. At distances bigger than this radius, nonlinearities are negligible and the field will mediate a gravitational strenght fifth force, while close to the source the force will be suppressed and we have the screening effect.
The second screening mechanism is given by the Vainshtein effect: here the lagrangian will contain also second derivatives of the field and the additional force is shut down in regions where the local curvature exceeds a given critical threshold. This mechanism is based on the interplay between classical nonlinearities and quantum corrections and we can distinguish three regions: below some radius r_Q, too much close to the mass source, both classical and quantum corrections are important and this effective field theory is not reliable; above r_Q but below the Vainshtein radius r_V only classical nonlinearities are important and they suppress the fifth force. Finally, at distances bigger than r_V both classical and quantum corrections are negligible and there is a fifth force comparable to the Newtonian one.

Chapter 3

Cosmological Scalar Field Dynamics

In this chapter we will describe how different aspects of cosmology are modified when we consider this new scalar field instead of the usual cosmological constant. First of all we will present the evolution of the field along the history of the Universe, in order to better understand why we must require that the field has to closely follow its effective potential energy minimum, in order to avoid any alteration on the formations of elements. This requirement allows us to introduce a new way to parametrize our field, which we will use all through this and the next chapter because of its simplicity. Then we will explicitly show that such a field can drive the accelerated expansion of the Universe and also how it modifies the growth of structure, motivating why we will study it in the next chapter.

3.1 Cosmological History

Through the different epochs, there are two characteristic time scales we have to consider: the first one is given by H^{-1} and it represents the typical time scale in which we observe significant changes in the energy density field for species that populate our Universe, therefore it will be also the time scale in which the density-dependent minimum position will change; the second one is the field response time, given by m_ϕ^{-1}. The requirement of a faithful tracking of the minimum is fulfilled if we ask that $m_\phi^{-1} \ll H^{-1}$: this means that if the field starts at or close to the minimum, it will be able to quickly adjust its dynamics in order to reach and follow the minimum position along its evolution, in other words the minimum solution is stable. This condition can be proved as valid from the Big Bang up to now in the specific models we have described earlier (see e.g. [5] for the chameleon case).
During the inflationary era, where H is nearly constant, the only source that will contribute to the SET trace is the inflaton. Since its energy density is almost constant, the minimum position ϕ_{inf} (in symmetron and dilaton cases it is indipendent from the self-interaction potential $V(\phi)$ that will be relevant only at lower energy scales), as well as the scalar field mass, will be fixed during this period and the field will quickly sit on it, in fact, considering the fluctuation $\delta\phi = \phi - \phi_{min}$, from the perturbed KG equation we have that

$$\delta\ddot{\phi} + 3H\delta\dot{\phi} + m_\phi^2\delta\phi = 0, \tag{3.1}$$

so, under our minimum stability assumption,

$$\delta\phi \simeq e^{-\frac{3Ht}{2}}\left(c_1 e^{im_\phi t} + c_2 e^{-im_\phi t}\right). \tag{3.2}$$

If we average over oscillations, we find that the fluctuations amplitude $\left\langle(\delta\phi)^2\right\rangle \sim a^{-3}$ rapidly decreases in time therefore, by the end of the inflation, the field will certainly be at its minimum.
In the chameleon case [5], considering as istantaneous the reheating phase, when both relativistic and non-relativistic species were created, the scalar field enters in the radiation era, where $3M_p^2H^2(a) \simeq \rho_r(a)$, at $\phi_i = \phi_{inf} \ll \phi_{min}(t_i)$, where the minimum position is determined just by the non-relativistic matter density, since relativistic species have a negligible SET trace. Here, because of the displacement of the field with respect to the minimum and the minimum stability requirement,

$$m^2(\phi_i) \simeq \partial_\phi^2 V \gg m^2(\phi_{min}(t_i)) \gg H_i^2, \tag{3.3}$$

therefore the driving force $-\partial_\phi V$ will dominate over the friction term $3H\dot{\phi}$ and the field will be underdamped. According to the EOM, the field starts rolling down on its potential following $\ddot{\phi} \simeq -\partial_\phi V$ and acquires a kinetic energy $\frac{1}{2}\dot{\phi} = V(t_i) - V(t)$ that soon becomes dominant since the potential is a decreasing function of the field, i.e.

$$\frac{\frac{\dot{\phi}^2}{2}}{V} = \frac{V(t_i)}{V(t)} - 1 \gg 1 \Longrightarrow w_\phi \simeq 1, \tag{3.4}$$

thus the scalar field energy density will scale as $\rho_\phi = \rho_{\phi i} a_i^6 a^{-6}$ and the kinetic energy as $\dot{\phi} = \sqrt{2\rho_{\phi i}} a_i^3 a^{-3}$. Once that it has reached the minimum, it overshoots and finally stop at some value ϕ_f, when the friction term in KG equation becomes relevant. We can estimate ϕ_f starting from the kinetic energy expression, finding

$$\frac{d\phi}{da} = \sqrt{6\Omega_{\phi i}} M_p \frac{a_i}{a^2} \Longrightarrow \phi(a) - \phi_i = \sqrt{6\Omega_{\phi i}} M_p \left(1 - \frac{a_i}{a}\right), \tag{3.5}$$

and noticing that we have $\dot{\phi} \simeq 0$ for $a \gg a_i$, therefore $\phi_f = \phi_i + \sqrt{6\Omega_{\phi i}} M_p$.
Now the field is in the opposite situation, where $\phi_f \gg \phi_{min}(t_f)$: here the friction term will dominate over the driving force $-\partial_\phi V$ and also over the $-\frac{\rho_m \beta}{M_p}$ term, thus the chameleon will be overdamped and essentially frozen at this value until matter-radiation equality, where the Hubble friction term will have the same order of the coupling-to-matter term, allowing the field to start rolling towards the minimum and resulting in a great variation of fermion masses between BBN and now. On the other hand we have to consider that, during the radiation era, every time that a massive species j becomes non-relativistic at $T \sim m_j$, the field receives a kick that pushes it towards its minimum. This is due to the fact that the SET trace for such species becomes non-zero for about one e-fold of expansion, therefore the behaviour of the field in this epoch is well approximated by KG equation

$$\ddot{\phi} + 3H\phi = -\sum_j \beta_j H_j k_j M_p \delta(t - t_j), \tag{3.6}$$

where $k_j = \frac{g_j}{g_\star(m_j)}$ is the ratio between the number of degrees of freedom g_j of the j-th species and the usual function $g_\star(m_j)$ that evaluates at a given temperature the effective number of dof. Every kick displaces the field by

$$\Delta\phi_j = -\beta_j H_j k_j M_p \tag{3.7}$$

and if one of these kick succeeds in bringing the field close to the minimum, then the field settles on it and successive kicks will just produce oscillations around the minimum; otherwise, as we have told, the field have to wait until matter-radiation equality to move towards its minimum. The last kick received would be given by

electrons at $z \sim 10^9$, so, in order to do not have significant changes in the masses of fundamental fermion particles during BBN ($z_{BBN} \sim 10^9 - 10^8$), the field has to sit on its minimum well before this moment.
The symmetron [15] and the dilaton [13] cases have a similar behaviour, since their minimum position did not displace at the end of the inflationary phase, because at early times just the coupling-to-matter term is relevant and we can neglect the potential. The field enters the radiation era at some ϕ_i and will essentially remain frozen at this value due to the Hubble friction term until when $H^2 \sim A_2\rho_m$, at some redshift $z \geq 10^6 z_{eq}$; then it will undergo damped oscillation around its minimum and kicks will not perturbe its dynamics. In [15] it has been analyzed the fact that the field could be considerably displaced from its minimum if during the reheating the tipycal decay time of the inflaton is bigger than its characteristic response time. Since we want to avoid higher orders corrections in the coupling function, in order to keep it quadratic all along the field evolution in time, bounds on these inflaton parameters has been introduced.

3.2 Equation of State

In an Universe filled just with non-relativistic matter and the scalar field, as could be considered our Universe after matter-radiation equality at $z_{eq} = \frac{\Omega_{m0}}{\Omega_{r0}} - 1$, the first Friedmann equation

$$\frac{\ddot{a}}{a} = -\frac{\rho_m + (1+3w_\phi)\rho_\phi}{6M_p^2} \tag{3.8}$$

tells us that we will have an accelerated expansion just if $w_\phi < -\frac{1}{3}\left[1 + \frac{\Omega_m}{\Omega_\phi}\right]$. The aim of this section is to prove that in late times the scalar field we introduced can satisfy this relation, driving in this way the expansion.
As we have seen in the previous section, we have to require a small excursion of the scalar field in order to have a small change in fermion masses and, when $m^2 \gg H^2$, this can be achieved in a large class of models, where the potential energy minimum is stable. In a spatially uniform matter background $\bar{\rho}_m$, the background field $\phi_{min}(t)$, defined by the minimum equation

$$\left[\frac{dV}{d\phi} + \frac{\bar{\rho}_m}{M_p}\beta\right]_{\phi_{min}} = 0 \tag{3.9}$$

evolves in time according to the minimum equation $\Box_g\phi = -\frac{dV_{eff}}{d\phi} = 0$. Deriving with respect to the time equation 3.9, we can also analyze the changing in time of the minimum position obtaining, since $\dot{\rho}_m = -3H\rho_m$ and

$$m^2 = \frac{d^2V_{eff}}{d\phi^2} = \frac{d^2V}{d\phi^2} + \frac{\rho_m}{M_p}\frac{d\beta}{d\phi}, \tag{3.10}$$

the explicit minimum equation

$$\frac{d\phi_{min}}{dt} = \frac{3H\bar{\rho}_m\beta(\phi_{min})}{M_p m^2(\phi_{min})}. \tag{3.11}$$

In order to avoid such heavy notation, from now on we will not indicate anymore that we are considering the field at its minimum at the background level. The general form of the scalar field SET reads as

$$T^{\mu\nu}_\phi = \partial^\mu\phi\partial^\nu\phi - g^{\mu\nu}\left[\frac{1}{2}\partial^\rho\phi\partial_\rho\phi - V(\phi)\right], \tag{3.12}$$

so that we can easily calculate its 00 and ij components, i.e. its energy density and its pression, at the background level, finding

$$T^0_{\ 0} = \rho_\phi = \frac{1}{2}\left(\frac{d\phi}{dt}\right)^2 + V(\phi), \tag{3.13}$$

$$T^i_{\ j} = -p_\phi \delta^i_{\ j} = -\left[\frac{1}{2}\left(\frac{d\phi}{dt}\right)^2 - V(\phi)\right]\delta^i_{\ j}. \tag{3.14}$$

In this kind of scalar theories coupled to matter, it is more convenient to define the scalar field energy density in another way: let's suppose that in our Universe we have only the scalar field and a CDM fluid, characterized by its SET given, in the EF, by

$$T^{\mu\nu}_m = \rho_E u^\mu u^\nu, \tag{3.15}$$

where u^μ is normalized in such a way that $u^\mu u_\mu = 1$. Here the second Friedman equation reads as

$$H^2 = \frac{\rho_E + \rho_\phi}{3M_p^2}, \tag{3.16}$$

where ρ_E is not conserved in the usual way, in fact, as we have pointed out in the previous chapter, the conserved SET in this frame is given by $T^{\mu\nu}_m + T^{\mu\nu}_\phi$. From the scalar field KG equation and since $[D_\mu, D_\nu]\phi = 0$, it follows immediately that

$$D_\mu T^{\mu\nu}_m = -D_\mu T^{\mu\nu}_\phi = \rho_E \partial^\nu \log A, \tag{3.17}$$

where its LHS reads as

$$(D_\mu \rho_E)u^\mu u^\nu + \rho_E (D_\mu u^\mu)u^\nu + \rho_E u^\mu (D_\mu u^\nu). \tag{3.18}$$

If now we contract 3.17 with u_ν and use

$$u^\nu D_\mu u_\nu = \frac{1}{2} D_\mu (u^\nu u_\nu) = 0, \tag{3.19}$$

we are able to find the final form of the energy density conservation equation for ρ_E, which reads as

$$\dot{\rho}_E + 3H\rho_E = \rho_E \frac{\dot{A}}{A}, \tag{3.20}$$

where we have introduced the Hubble rate $D_\mu u^\mu = 3H$ and the shortened notation $\dot{\rho}_E = u^\mu D_\mu \rho_E$. We can therefore define the new matter energy density as $\rho_m = A^{-1}\rho_E$, so that the conservation equation for ρ_m has the more familiar expression

$$\dot{\rho}_m + 3H\rho_m = 0; \tag{3.21}$$

at the same time, this choice induces a new definition of the energy density of the scalar field, which now reads as

$$\rho_\phi = \frac{1}{2}\left(\frac{d\phi}{dt}\right)^2 + V(\phi) + (A-1)\rho_m \simeq \frac{1}{2}\left(\frac{d\phi}{dt}\right)^2 + V_{eff}(\phi), \tag{3.22}$$

in order to preserve the Friedman equation 3.16, now given by

$$H^2 = \frac{\rho_m + \rho_\phi}{3M_p^2}. \tag{3.23}$$

In the end, we are ready to evaluate the equation of state

$$w_\phi + 1 = \frac{p_\phi}{\rho_\phi} + 1 = \frac{\left(\frac{d\phi}{dt}\right)^2}{\rho_\phi} + (A-1)\frac{\rho_m}{\rho_\phi} : \tag{3.24}$$

the first term, using equation 3.11, reads as

$$27\beta^2\Omega_m \left(\frac{H}{m}\right)^4 \frac{\Omega_m}{\Omega_\phi}, \tag{3.25}$$

while for the second one we have to use a first order expansion of A and a second order expansion of V close to the minimum of the field, which give

$$A(\phi) - 1 \simeq \frac{\partial A}{\partial \phi}\Delta\phi \simeq \frac{\beta}{M_p}\Delta\phi, \tag{3.26}$$

$$0 \simeq \Delta V \simeq (\partial_\phi V)\Delta\phi + (\partial^2_\phi V)(\Delta\phi)^2 \Longrightarrow \Delta\phi \simeq -\frac{\partial_\phi V}{\partial^2_\phi V}. \tag{3.27}$$

Combining these two quantities and using equations 3.9 and 3.10, we obtain that the second term goes as

$$(A-1)\frac{\rho_m}{\rho_\phi} \simeq \frac{\beta^2\rho_m}{m^2 M_p^2}\frac{\Omega_m}{\Omega_\phi} = 3\beta^2\Omega_m\left(\frac{H}{m}\right)^2\frac{\Omega_m}{\Omega_\phi}. \tag{3.28}$$

We can conclude that, as long as Ω_m and Ω_ϕ are of the same order of magnitude and their ratio does not compensate the significant $\frac{H^2}{m^2}$ suppression, i.e. in the late times Universe, $w_\phi + 1 \simeq 0$, therefore the background scalar field behaves as a cosmological constant.

3.3 Reconstruction of the Dynamics

In the previous chapter we have seen how, starting from the lagrangian and in particular from explicit forms of the potential $V(\phi)$ and the coupling function $A(\phi)$, we can construct different models with peculiar behaviours of the scalar field. This is a good approach but, since we would like to parametrize our models in a cheap way and we would like to create also new models more intuitively, probably it is not the best one to study the cosmological dynamics of the field. Considering what we have said earlier, the evolution of ϕ through epochs is quite constrained by theoretical reasons and is determined by the minimum equations 3.9 and 3.11: from these two expressions we can see that, if we known the time evolution of the mass and the coupling to matter, i.e. if we know $m(a)$ and $\beta(a)$, we are able to completely reconstruct from 3.11 the background value of the scalar field

$$\phi(a) - \phi_i = \int_{a_i}^{a} d\bar{a}\frac{3\beta(\bar{a})\bar{\rho}_m(\bar{a})}{\bar{a}m^2(\bar{a})M_p} \tag{3.29}$$

and, from 3.9, using 3.11, the parametric form of the potential

$$V(a) - V_i = -\int_{a_i}^{a} d\bar{a}\frac{3\beta^2(\bar{a})\bar{\rho}^2_m(\bar{a})}{\bar{a}m^2(\bar{a})M_p^2}, \tag{3.30}$$

where we have assumed that the field have been sat on its minimum since $a_i < a_{BBN}$. This parametrical representation of the field, since we know how $\rho_m(a)$ changes in

time, allows us to reconstruct these quantities for every matter density of interests, from the cosmological background density ($\rho_0 \sim 10^{-29}$ g/cm^3) to the Earth one (up to $\rho_{core} \sim 10$ g/cm^3), just choosing the right scale factor: this density range forces us to choose at least $z_i = 10^{10}$. Moreover, even in this parametrization, we can evaluate the all-important thin shell condition

$$\frac{\phi(a_b) - \phi(a_o)}{\beta(a_b) M_p |\Psi_N|} = \frac{1}{\beta(a_b) M_p |\Psi_N|} \int_{a_o}^{a_b} d\bar{a} \frac{3\beta(\bar{a})\rho_m(\bar{a})}{\bar{a} m^2(\bar{a}) M_p}. \tag{3.31}$$

In other words, the full nonlinear dynamics of the theory since before BBN can be recovered just from the knowledge of time evolution of the mass and the coupling to matter. Let's now show how this is done in those models we have introduced in the previous chapter.

3.3.1 Chameleon and $f(R)$

In these models ([2],[9]) the coupling to matter β is constant and the mass increases with the density, therefore a reasonable parametrization is given by

$$m(a) = m_0 a^{-r}. \tag{3.32}$$

For $r \neq \frac{3}{2}$, equation 3.29 reads as

$$\begin{aligned} \frac{\phi(a) - \phi_i}{M_p} &= \frac{9\beta\Omega_{m0}H_0^2}{(2r-3)m_0^2} \left[a^{2r-3} - a_i^{2r-3}\right] \simeq \\ &\simeq \frac{9\beta\Omega_{m0}H_0^2}{(2r-3)m_0^2} a^{2r-3} \end{aligned} \tag{3.33}$$

when $r > \frac{3}{2}$ (notice that we have to require this condition in order to don't have a large excursion in time of the background level field). At the same time equation 3.30 reads as

$$V(a) - V_i = -\frac{27\beta^2\Omega_{m0}H_0^4 M_p^2}{2(r-3)m_0^2} \left[a^{2(r-3)} - a_i^{2(r-3)}\right] \tag{3.34}$$

so, using the parametrical reconstruction of the field in 3.33,

$$V(\phi) = V_0 - C\left(\frac{\phi - \phi_i}{M_p}\right)^{\frac{2(r-3)}{2r-3}}, \tag{3.35}$$

where both V_0 and C are numerical constants. For $\frac{3}{2} < r < 3$, $V(\phi) \sim \phi^{-n}$ behaves as chameleon theories with Ratra-Peebles exponent $n = \frac{2(3-r)}{2r-3}$. When $\beta = \frac{1}{\sqrt{6}}$, from equation 2.59, we can find the relation between ϕ and R, that is given by

$$\begin{aligned} R(\phi) &\simeq -\frac{2\sqrt{6}(r-3)C}{(2r-3)M_p^2}\left(\frac{\phi - \phi_i}{M_p}\right)^{-\frac{3}{2r-3}} - \frac{4V_0}{M_p^2} + \frac{4C}{M_p^2}\left(\frac{\phi - \phi_i}{M_p}\right)^{\frac{2(r-3)}{2r-3}} \simeq \\ &\simeq -\frac{2\sqrt{6}(r-3)C}{(2r-3)M_p^2}\left(\frac{\phi - \phi_i}{M_p}\right)^{-\frac{3}{2r-3}} - \frac{4V_0}{M_p^2}, \end{aligned} \tag{3.36}$$

where the first term dominates over the third one when the field excursion is small. Finally, we can end the reconstruction obtaining

$$f(R) = \frac{2}{M_p^2} V(\phi(R)) = \frac{2}{M_p^2}\left[V_0 - C\left(\frac{R + \frac{4V_0}{M_p^2}}{R_\star}\right)^{-\frac{2}{3}(r-3)}\right], \tag{3.37}$$

where for $r > 3$, we have the so called large curvature $f(R)$ models.

3.3.2 Symmetron

In the symmetron model ([9],[10]), the field develops a (non-)zero coupling to matter in (low) high density regions or, alternatively, at redshifts ($z \leq z_\star$) $z > z_\star$. Here $z_\star$ is the redshift associated to the critical density $\rho_c = \rho_m(a_\star) = \rho_\star$ mentioned in the previous chapter. This behaviour can be reproduced by

$$\beta(a) = \begin{cases} 0 & z > z_\star \\ \beta_\star \sqrt{1 - \left(\frac{a_\star}{a}\right)^3} & z \leq z_\star \end{cases} \tag{3.38}$$

and since for $\rho_m < \rho_c$ we have

$$m^2 = 2A_2\rho_c \left(1 - \frac{\rho_m}{\rho_c}\right) = 2A_2\rho_c \left(1 - \frac{a_\star^3}{a^3}\right), \tag{3.39}$$

we can consistently define for $z \leq z_\star$

$$m(a) = m_\star \sqrt{1 - \left(\frac{a_\star}{a}\right)^3}. \tag{3.40}$$

From 3.29, given that $\phi_i = 0$, we find

$$\phi(a) = \begin{cases} 0 & z > z_\star \\ \phi_\star \sqrt{1 - \left(\frac{a_\star}{a}\right)^3} & z \leq z_\star \end{cases}, \tag{3.41}$$

where $\phi_\star = \frac{2\beta_\star \rho_\star}{m_\star^2 M_p}$, while from 3.30 we find

$$V(a) - V_i = \begin{cases} 0 & z > z_\star \\ \frac{\beta_\star^2 \rho_\star^2}{2m_\star^2 M_p^2} \left[\left(\frac{a_\star}{a}\right)^6 - 1\right] & z \leq z_\star \end{cases}. \tag{3.42}$$

Using the parametrical reconstruction of the field we can show that

$$V(\phi) - V_i = \frac{\beta_\star^2 \rho_\star^2}{2m_\star^2 M_p^2} \left[\left(1 - \frac{\phi^2}{\phi_\star^2}\right)^2 - 1\right] = -\frac{1}{2}\mu^2\phi^2 + \frac{1}{4}\lambda\phi^4, \tag{3.43}$$

where $\mu^2 = \frac{m_\star^2}{2}$, $\lambda = \frac{m_\star^2}{2\phi_\star^2}$, and that

$$\beta(\phi) = \beta_\star \frac{\phi}{\phi_\star}, \tag{3.44}$$

as in the symmetron model.
Now, starting from 3.38 and 3.40, we can slightly modify the mass and coupling to matter functions in order to create new generalized symmetron models: as shown in the previously cited papers, picking up for $z \leq z_\star$

$$\beta(a) = \beta_\star \left[1 - \left(\frac{a_\star}{a}\right)^3\right]^{1/q} \tag{3.45}$$

$$m(a) = m_\star \left[1 - \left(\frac{a_\star}{a}\right)^3\right]^{1/p}, \tag{3.46}$$

we can create models where the potential and the coupling to matter are given by

$$V(\phi) - V_i = -c_1\phi^n + c_2\phi^m \tag{3.47}$$

$$\beta(\phi) = \beta_\star \left(\frac{\phi}{\phi_\star}\right)^{n-1}, \tag{3.48}$$

where $m,\ n$ are function of $q,\ p$, as well as the two positive (for $m > n$) constants $c_1,\ c_2$. In order to keep the potential symmetric around $\phi = 0$, m and n should be taken even integers. Moreover, in [9], using the standard environmental setup introduced in the previous chapter, it has been explicitly shown that these models have the same screening property of the regular symmetron.

3.3.3 Dilaton

Sometimes, as in the dilaton case ([10],[2]), it's more convenient to express the coupling to matter function as a function of the field, instead of the scale factor. It is possible to rewrite equation 3.11 as

$$\int_{\phi_i}^{\phi} \frac{d\phi}{\beta(\phi)} = \int_{a_i}^{a} d\bar{a} \frac{3\bar{\rho}_m(\bar{a})}{\bar{a}m^2(\bar{a})M_p} \tag{3.49}$$

and since in our case we will study the dynamics around the minimum $\phi_\star$, where $\beta(\phi) = M_p A_2(\phi - \phi_\star)$, we can easily reconstruct

$$\log\left|\frac{\phi - \phi_\star}{\phi_i - \phi_\star}\right| = 3A_2\bar{\rho}_{0m}\int_{a_i}^{a} d\bar{a}\frac{1}{\bar{a}^4 m^2(\bar{a})} \tag{3.50}$$

or, equivalently,

$$|\beta(\phi)| = |\beta(\phi_i)| \exp\left[3A_2\rho_{0m}\int_{a_i}^{a} d\bar{a}\frac{1}{\bar{a}^4 m^2(\bar{a})}\right]. \tag{3.51}$$

The coupling at initial time or, alternatively, in dense environments is linked to the coupling in the cosmological background by

$$|\beta(\phi_0)| = |\beta(\phi_i)| \exp\left[3A_2\rho_{0m}\int_{a_i}^{1} d\bar{a}\frac{1}{\bar{a}^4 m^2(\bar{a})}\right], \tag{3.52}$$

so, as long as $A_2 > 0$ (i.e. the minimum of the coupling function is stable) and mass does not compensate the divergence in the integral, we can obtain in dense regions a small coupling value $\beta(\phi_i) \ll 1$. After that, we can use this last equations to express the coupling to matter as

$$\beta(\phi) = \beta(\phi_0) \exp\left[3A_2\rho_{0m}\int_{1}^{a} d\bar{a}\frac{1}{\bar{a}^4 m^2(\bar{a})}\right]. \tag{3.53}$$

In general, we have seen that

$$m^2(a) \simeq A_2\rho \simeq 3A_2 M_p^2 H^2(a) : \tag{3.54}$$

between our initial time and the matter-radiation equality $\rho \simeq \rho_r = \rho_{0r}a^{-4}$, so

$$\beta(a) = \beta(a_i)e^{3\frac{\Omega_{m0}}{\Omega_{r0}}(a-a_i)} \tag{3.55}$$

and because of the compensation the coupling to matter variation is not so big, while in the matter-dominated era $\rho \simeq \rho_{0m}a^{-3}$ and

$$\beta(a) = \beta(a_{eq})\left(\frac{a}{a_{eq}}\right)^3. \tag{3.56}$$

To generalize the dilaton, let's consider a class of models with a quadratic coupling function where, around its minimum $\phi_\star$, the coupling to matter reads as $\beta(\phi) =$

$M_p A_2(\phi-\phi_\star)$. It sounds reasonable parametrize the dilaton mass as $m(a) = m_0 a^{-r}$, so that

$$\beta(a) = \beta(a_0)\exp\left[s\int_1^a d\bar{a}\bar{a}^{2r-4}\right] = \begin{cases}\beta_0 a^s & r = \frac{3}{2}\\ \beta_0 e^{\frac{s}{2r-3}(a^{2r-3}-1)} & r \neq \frac{3}{2}\end{cases}, \tag{3.57}$$

where $s = 9A_2 M_p^2 \Omega_{m0}\frac{H_0^2}{m_0^2}$ and β is a decreasing function of the scale factor for every value of r. From 3.57 it follows that

$$a = \left[1 + \frac{2r-3}{s}\log\frac{\beta}{\beta_0}\right]^{-\frac{1}{2r-3}}, \tag{3.58}$$

so, when we calculate the first derivative of the potential, we find

$$\frac{dV}{d\phi} = \frac{\frac{dV}{da}}{\frac{d\phi}{da}} = -\frac{\beta(a)\bar{\rho_m}}{M_p} = -\frac{\beta(\phi)\bar{\rho}_{0m}}{M_p}\left[1 + \frac{2r-3}{s}\log\frac{\beta}{\beta_0}\right]^{-\frac{3}{2r-3}}, \tag{3.59}$$

where $\log\frac{\beta}{\beta_0} < 0$. This last equation shows why, in order to have a well defined first derivative, we have to impose that $r < \frac{3}{2}$.

3.4 Growth of Structures

As we have seen, at the background level, our scalar field models are indistinguishable from the Λ-CDM one. This is not true at perturbative level where, inside the field Compton wavelength, the density constrat grows in a different way with respect to the cosmological standard model. In this section we will show how the anomalous growth can be descibed only via the $\beta(a) - m(a)$ parametrization, giving us another proof of the usefulness of this formalism.
We will consider perturbations in the Newtonian conformal gauge where, in absence of any anisotropic stress and defining $v^i = \frac{dx^i}{d\tau}$,

$$\begin{aligned} ds^2 &= a^2\left[(1+2\Psi_N)d\tau^2 - (1-2\Psi_N)d\mathbf{x}\cdot d\mathbf{x}\right] = \\ &= a^2 d\tau^2\left[1 + 2\Psi_N - (1-2\Psi_N)v^i v_i\right]. \end{aligned}, \tag{3.60}$$

In our investigation on large-scale structures (LSS) we will consider non-relativistic particles and weak Newtonian potentials, therefore both $v^2 = v^i v_i$ and Ψ_N will be small with respect to unity, as well as their time derivative, since these kind of structures evolves on Hubble time scales; on the other hand, we will keep their spatial gradients because LSS are much smaller than the horizon. The perturbed quantities we will consider are

$$\rho_m(t,\mathbf{x}) = \bar{\rho}_m(t)\left[1 + \delta(t,\mathbf{x})\right] \tag{3.61}$$

$$\phi(t,\mathbf{x}) = \phi_{min}(t) + \delta\phi(t,\mathbf{x}) \tag{3.62}$$

$$v^i(t,\mathbf{x}) = 0 + \delta v^i(t,\mathbf{x}). \tag{3.63}$$

Expanding the KG equation 2.7 around background values, such that $\Box_g\phi_{min} = -\partial_\phi V_{eff}(\phi_{min}) = 0$, we find that at first order in perturbation theory the fluctuation of the field evolves according to

$$\ddot{\delta\phi} + 3H\dot{\delta\phi} - \nabla^2\delta\phi = -\frac{\beta\bar{\rho}_m}{M_p}\delta - m^2\delta\phi. \tag{3.64}$$

Switching from cosmic time to conformal time variable, we have that $\dot{\phi} = \frac{d\tau}{dt}\delta\phi' \simeq \frac{\delta\phi'}{a}$ and $\mathcal{H} = \frac{a'}{a}$, where $' = \partial_\tau$; going in the Fourier space (without adding any particular sign to indicate it), where k is the comoving wavenumber, equation 3.64 becomes

$$\delta\phi'' + 2\mathcal{H}\delta\phi' + (k^2 + a^2m^2)\delta\phi = -\frac{\beta\bar{\rho}_m a^2}{M_p}\delta. \tag{3.65}$$

In the sub-horizon regime $k^2 \gg (aH)^2 = \mathcal{H}^2$, so the solution follows

$$\delta\phi \simeq -\frac{\beta}{k^2 + a^2m^2}\frac{\bar{\rho}_m a^2}{M_p}\delta \tag{3.66}$$

and rapidly oscillates around this analytic solution, as numerical proved in [9].
The CDM particles 4-velocity, at the leading order in this gauge, reads as

$$u^\mu = \frac{dx^\mu}{ds} = \frac{d\tau}{ds}\frac{dx^\mu}{d\tau} \simeq a^{-1}\left(1 - \Psi_N + \frac{v^2}{2}, v^i\right), \tag{3.67}$$

so that the different terms in the energy density conservation equation 3.21 are given by

$$\dot{\rho}_m = u^0\partial_\tau\rho_m + u^i\partial_i\rho_m \simeq a^{-1}\left(\rho_m' + v^i\partial_i\rho_m\right) \tag{3.68}$$

$$\begin{aligned} D_\mu u^\mu = \partial_\mu u^\mu + \Gamma^\mu_{\mu\alpha}u^\alpha = \partial_\mu u^\mu + \frac{u^\alpha}{\sqrt{-g}}\partial_\alpha\sqrt{-g} \simeq \\ \simeq \left(\frac{1}{a}\right)' + \frac{1}{a}\partial_i v^i + \frac{1}{a^5}(a^4)' = a^{-1}\left(3\mathcal{H} + \partial_i v^i\right). \end{aligned} \tag{3.69}$$

Gathering all the terms, the complete equation reads as

$$\rho_m' + v^i\partial_i\rho_m + \left(3\mathcal{H} + \partial_i v^i\right)\rho_m = 0, \tag{3.70}$$

so at the background level it reads as

$$\bar{\rho}_m' + 3\mathcal{H}\bar{\rho}_m = 0 \tag{3.71}$$

while at the first order, using this last equation, as

$$\delta' + \partial_i\delta v^i = 0 \Longrightarrow \delta'' + \partial_i(\delta v^i)' = 0. \tag{3.72}$$

Then we need to find the generalized geodesic equation: starting from equation 3.17 and using equation 3.20 we obtain

$$u^\mu D_\mu u^\nu = \partial^\nu \log A - \frac{\dot{A}}{A}u^\nu, \tag{3.73}$$

where we are interested just in the $\nu = i$ component, in order to study CDM particles velocities. Under the weak field assumption, the inverse of the metric reads as

$$g^{\mu\nu} = \begin{pmatrix} a^{-2}(1 - 2\Psi_N) & \mathbf{0}_3 \\ \mathbf{0}_3 & -a^{-2}(1 + 2\Psi_N)\mathbf{1}_3 \end{pmatrix}, \tag{3.74}$$

so we are able to calculate the components of the affine connection

$$\Gamma^\mu_{\alpha\beta} = \frac{1}{2}g^{\mu\nu}\left[\partial_\alpha g_{\nu\beta} + \partial_\beta g_{\nu\alpha} - \partial_\nu g_{\alpha\beta}\right], \tag{3.75}$$

in particular

$$\Gamma^i_{00} = (1+2\Psi_N)\delta^{ij}\partial_j\Psi_N \tag{3.76}$$

$$\Gamma^i_{0j} = (1-4\Psi_N^2)\mathcal{H}\delta^i_j = \Gamma^i_{j0} \tag{3.77}$$

$$\Gamma^i_{jk} = (1+2\Psi_N)\left[\delta^i_k\partial_j\Psi_N + \delta^i_j\partial_k\Psi_N - \delta_{jk}\delta^{il}\partial_l\Psi_N\right]. \tag{3.78}$$

In this way, at the first order,

$$\begin{aligned} u^\mu D_\mu u^i &= u^\mu\partial_\mu u^i + \Gamma^i_{\mu\nu}u^\mu u^\nu = \\ &= u^0\partial_0 u^i + u^j\partial_j u^i + \Gamma^i_{00}u^0u^0 + 2\Gamma^i_{0j}u^0u^j + \Gamma^i_{jk}u^ju^k \simeq \\ &\simeq \frac{1}{a^2}\left[(\delta v^i)' + \mathcal{H}v^i + \delta^{ij}\partial_j\Psi_N\right]. \end{aligned} \tag{3.79}$$

At perturbative level, the i-th component of the RHS of 3.73 reads as

$$-\frac{1}{a^2}\left[\delta^{ij}\partial_j\log A + \frac{\beta\phi'_{min}}{M_p}\delta v^i\right], \tag{3.80}$$

therefore we finally obtain

$$(\delta v^i)' + \left[\mathcal{H} + \beta\frac{\phi'_{min}}{M_p}\right]\delta v^i + \frac{\beta}{M_p}\delta^{ij}\partial_j\delta\phi = -\delta^{ij}\partial_j\Psi_N. \tag{3.81}$$

Using the minimum equation 3.11, we find that

$$\frac{\phi'_{min}}{M_p} = 9\Omega_m\beta\mathcal{H}\left(\frac{\mathcal{H}^2}{a^2m^2}\right) \ll \mathcal{H} \tag{3.82}$$

due to the suppression factor, therefore we can neglect the second term in square brackets. Taking the spatial derivative of this last equation with respect to the i-th coordinate and using what we have found in 3.72, we get the equation of motion for the density contrast, which reads in the Fourier space as

$$\delta'' + \mathcal{H}\delta' - \frac{a^2\bar{\rho}_m}{2M_p^2}\delta + \frac{\beta}{M_p}k^2\delta\phi = 0, \tag{3.83}$$

where we have used

$$\nabla^2_{\mathbf{x}}\Psi_N = \frac{a^2}{2M_p^2}\left(\delta\rho_m + \delta\rho_\phi\right) \simeq \frac{a^2\bar{\rho}_m}{2M_p^2}\delta, \tag{3.84}$$

since, along the minimum trajectory, the variation of energy density of the scalar remains small compared to the Planck mass, as shown earlier in this chapter. Using the analytic solution we found in 3.66, we are able to obtain the final form of the density contrast equation, which is given by

$$\delta'' + \mathcal{H}\delta' - \frac{a^2\bar{\rho}_m}{2M_p^2}\delta\left[1 + \frac{2\beta^2}{1+\frac{a^2m^2}{k^2}}\right] = 0. \tag{3.85}$$

This is a remarkable result since it shows that, just knowing the time evolution of the mass and the coupling to matter function, it is possible to completely reconstruct the linear dynamics. We can also identify the influence regime of the fifth force, in fact, on scales larger than the Compton wavelength of the scalar field, where $k \ll am(a)$, the second term in square brackets is highly suppressed and we recover the same equation of the Λ-CDM model; while for $k \geq am(a)$ we have an anomalous

growth. As we have explained in the previous section, in order to describe the behaviour of MG models, we have to deal with four or five new parameters: in general, increasing the strenght of β, properly changing either the coupling factor $\beta,\ \beta_\star,\ \beta_0$, the exponents $q,\ s$ or the time $a_\star$ where modifications arise, will result in a stronger matter clustering; conversely increasing value of m, via the prefactor $m_0,\ m_\star$, the exponents $r,\ p$ or the starting time $a_\star$, will reduce the range of gravity modification, weakening the matter clustering.
The advantages of this parametrization do not stop here, in fact, as we will explain in the next chapter, it can be used also to describe the non-linear dynamics of the scalar field, even allowing us to specify its spatial configuration: this will help us, since our goal is to investigate non-linear phenomena, as the gravitational collapse, where we expect to find deviations from the cosmological standard model.

Chapter 4

Spherical Collapse

In order to investigate the structure formation, we need large N-body simulations, which are very time and resource consuming. These simulations are adapt to test physical models whose parameter space is well experimentally constrained, as the Λ-CDM model, rather than wide parameters space as in modified gravity models, where we have four or even five new parameters. In these year, step by step, through laboratory, astrophysical and cosmological tests, we are eliminating large regions of such space but this is not enough. Then an analytic or semi-analytic description of different phenomena can help us to isolate some interesting regions of the MG parameter space that will be investigated in a second step through numerical simulations.

4.1 Spherical Collapse in GR

Since we want to compare the MG collapse to the usual collapse in GR, we will introduce the latter in this section. We will analyze the simpler collapse model, where we have an initial spherical symmetry which we suppose to be maintained in time, at least until what we will define the "end"of the collapse.
We will study the collapse in the matter era, starting from recombination, at $z_i = 1100$, until matter-dark energy equality, at $z_e = 0.33$, because here we can assume that $\Omega_m = 1$ and neglect other components, i.e. we will consider an Einstein-de Sitter Universe. Actually, the matter era starts well before recombination, at $z_{eq} \sim 3 \cdot 10^3$, but until this moment baryonic matter will be in equilibrium with radiation and any gravitational collapse is avoided. After recombination baryonic matter fall in CDM potential well and they start evolving together. We choose to stop our collapse at the matter-dark energy equality instead of considering the end at $z = 0$ as done in several papers (see e.g. [4],[18]) because in the dark energy era the density perturbation growth slows down and perturbations eventually freeze out; moreover, we want to carry on all the calculations analytically as long as we can and, in the MG case, a non-zero Ω_{de} can complicate our problem.
Since in our Universe we will have just matter, we will drop the subscript $_m$ when we will talk about the density. In this framework, let's consider at z_i a spherical region with a slightly perturbed density $\bar{\rho}_i(1 + \delta_i)$, where $\delta_i \ll 1$, with respect to the background and with initial radius r_i, enclosing a mass $M = \frac{4\pi}{3}\bar{\rho}_i(1 + \delta_i)r_i^3$. A corollary of the well known Birkhoff theorem [28]

Theorem. *A spherically symmetric gravitational field in empty space must be static, with a metric given by the Schwarzschild solution.*

state that

Corollary. *The metric inside an empty spherical cavity at the center of a spherical symmetric system must be equivalent to the flat-space Minkowski metric $\eta_{\mu\nu}$,*

therefore, since our perturbation lives inside such a cavity, it decouples from the rest of the Universe and it evolves according to his properties. The spherical dynamics reduces to the usual Newtonian dynamics

$$\ddot{r} = -\frac{GM}{r^2}, \tag{4.1}$$

from which we can obtain the usual energy conservation

$$\frac{1}{2}\dot{r}^2 - \frac{MG}{r} = \frac{1}{2}\dot{r}_i^2 - \frac{MG}{r_i} = -\kappa \tag{4.2}$$

where $\kappa > 0$, since the initial total energy is negative. We can prove this last statement assuming that the perturbation initial velocity is due only to the Universe expansion i.e. $\dot{r}_i = \dot{a}_i x_i = H_i r_i$, so that the kinetic energy will read as $\frac{H_i^2 r_i^2}{2}$ while the potential energy will be given by $-\frac{GM}{r_i} = -\frac{H_i^2 r_i^2 (1+\delta_i)}{2}$, obtaining in this way $\kappa = \frac{H_i^2 r_i^2 \delta_i}{2}$; in other words, the small fluctuation δ_i will give to the system the small energy necessary to begin to collapse. Through a rescaling $r \to \sqrt{2\kappa}\tilde{r}$ we get

$$\tilde{r} = \frac{A^2}{\dot{\tilde{r}}^2 + 1}, \tag{4.3}$$

where $A^2 = \frac{MG}{\sqrt{2\kappa^3}} = \frac{1+\delta_i}{H_i \delta_i^{3/2}}$ depends from the initial conditions; then we can solve 4.3 through a parametric procedure: first we define $p = \dot{\tilde{r}}$, then we derive with respect to the time equation 4.3 obtaining

$$\tilde{r} = \frac{A^2}{p^2 + 1} \tag{4.4}$$

$$t = -2A^2 \int \frac{dp}{(p^2+1)^2} \tag{4.5}$$

and finally, using the substitution $\frac{1}{p} = \tan\frac{\theta+\theta_i}{2}$ and going back to the physical coordinate, we are able to find the parametric solution

$$t(\theta) = \frac{A^2}{2}\left[\theta + \theta_i - \sin(\theta+\theta_i)\right], \quad r(\theta) = \sqrt{2\kappa}\tilde{r}(\theta) = \sqrt{2\kappa}\frac{A^2}{2}\left[1 - \cos(\theta+\theta_i)\right]. \tag{4.6}$$

Usually in literature this θ_i parameter is not introduced, but we have put it in order to obtain non-singular quantities at the beginning of the collapse. In the end, recalling that in a matter-dominated Universe $H = \frac{2}{3t}$, we obtain

$$t(\theta) = t_i \frac{3(1+\delta_i)}{4\delta_i^{3/2}}\left[\theta + \theta_i - \sin(\theta+\theta_i)\right], \quad r(\theta) = r_i \frac{(1+\delta_i)}{2\delta_i}\left[1 - \cos(\theta+\theta_i)\right]. \tag{4.7}$$

Requiring that $r(\theta = 0) = r_i$ we are able to fix the θ_i parameter as

$$\theta_i = \arccos\frac{1-\delta_i}{1+\delta_i} \simeq 2\sqrt{\delta_i} \tag{4.8}$$

since the initial overdensity is small, therefore also the θ_i parameter will be small. Finally, we can compute the cosmological scale factor for the flat, matter-dominated Universe, finding

$$a(t) = a_{e.m.e.} t_{e.m.e.}^{-\frac{2}{3}} t^{\frac{2}{3}} = \frac{a_i}{\delta_i}\left[\frac{3}{4}(1+\delta_i)\left[\theta + \theta_i - \sin(\theta+\theta_i)\right]\right]^{\frac{2}{3}}, \tag{4.9}$$

where $a_{e.m.e.}$ and $t_{e.m.e.}$ are associated to the end of the matter-dominated era.
Since our goal is to study the overdensity evolution, let's introduce a new quantity directly relate to such variable: first of all let's define the comoving Lagrangian coordinate $q = \left(\frac{3M}{4\pi\bar{\rho}_0}\right)^{1/3}$ of a shell that include the same mass M of our perturbation in an uniform Universe; then, requiring that the mass is conserved during the collapse, we have that

$$M = \frac{4\pi}{3}\rho r^3 = \frac{4\pi}{3}\bar{\rho}(1+\delta)r^3 = \frac{4\pi}{3}\bar{\rho}a^3q^3, \tag{4.10}$$

therefore we can introduce the normalized radius $y = (1+\delta)^{-\frac{1}{3}} = \frac{r}{aq}$, which explicitly reads in our Universe as

$$y_0(\theta) = \frac{r(\theta)}{a(\theta)q} = \sqrt[3]{\frac{2}{9}}\frac{1-\cos(\theta+\theta_i)}{[\theta+\theta_i-\sin(\theta+\theta_i)]^{\frac{2}{3}}} \tag{4.11}$$

and where, by construction, $y(0) = (1+\delta_i)^{-\frac{1}{3}} \simeq 1$, hence its name.
According to our parametrization the collapse will start at some $t_i > 0$, then the physical radius will increase due to the expansion of the Universe until the turn around moment at $t_{ta} = t(\pi - \theta_i) = \frac{3\pi t_i(1+\delta_i)}{4\delta_i^{3/2}}$, where the body reaches its maximum size r_{ta} and the physical radius begins to decrease (the comoving size will always decrease), completely collapsing to a point at $\theta = 2\pi - \theta_i$.
We can extract some useful information about the collapse studying the linear regime: for small values of $\theta + \theta_i$ we can expand both quantities in 4.7 up to the second order as

$$\frac{r(\theta)}{r_{ta}} = \frac{1}{2}[1-\cos(\theta+\theta_i)] \simeq \frac{(\theta+\theta_i)^2}{4}\left[1-\frac{(\theta+\theta_i)^2}{12}\right] \tag{4.12}$$

$$\frac{t(\theta)}{t_{ta}} = \frac{1}{\pi}[\theta+\theta_i-\sin(\theta+\theta_i)] \simeq \frac{(\theta+\theta_i)^3}{6\pi}\left[1-\frac{(\theta+\theta_i)^2}{20}\right]. \tag{4.13}$$

Keeping only the leading order in both expressions we find the background expansion in a matter dominated universe

$$\frac{r_{bg}(\theta)}{r_{ta}} = \frac{1}{4}\left(\frac{6\pi t}{t_{ta}}\right)^{\frac{2}{3}}, \tag{4.14}$$

while condidering both terms in 4.13 can compute the linear growth

$$\frac{r_{lin}(\theta)}{r_{ta}} = \frac{1}{4}\left(\frac{6\pi t}{t_{ta}}\right)^{\frac{2}{3}}\left[1-\frac{1}{20}\left(\frac{6\pi t}{t_{ta}}\right)^{\frac{2}{3}}\right], \tag{4.15}$$

thus the linear density contrast will evolve with respect to the background according to

$$1+\delta_{lin} = \frac{\rho_{lin}}{\rho_{bg}} = \frac{r_{bg}^3}{r_{lin}^3} \simeq 1+\frac{3}{20}\left(\frac{6\pi t}{t_{ta}}\right)^{\frac{2}{3}}. \tag{4.16}$$

The body will eventually collapses to a point in a finite time $t_c = t(2\pi - \theta_i) = 2t_{ta}$, where the linear density contrast, extrapolated at this moment, reads as

$$\delta_c = \delta_{lin}(t_c) = \frac{3}{20}(12\pi)^{\frac{2}{3}} \simeq 1.686, \tag{4.17}$$

independently from initial conditions of the collapsing body, in particular from the mass of the object. This feature is mantained also in an Universe where there is also

a cosmological constant, but in this case the critical value will slightly depend the matter density fraction Ω_m at the redshift of interest (see e.g. [25]) and the critical value will be a bit smaller. Using the explicit expression for t_{ta}, we can see that the linear density contrast evolves in time as

$$\delta \simeq \frac{3}{5}\delta_i \left(\frac{t}{t_i}\right)^{\frac{2}{3}} = \frac{3}{5}\delta_i \frac{a}{a_i} = \frac{3}{5}\delta_i \frac{1+z_i}{1+z}, \tag{4.18}$$

therefore if the initial overdensity value, extrapolated at some later time (redshift) t (z), reaches or exceeds the critical value given in 4.17, then the perturbation collapses or has already collapsed by that time: this will be an useful criterion to determine the future of perturbations we will consider. Physically speaking, the collapsing body will not reach point-size dimensions, in fact when densities are high, even a tiny departure from the spherical symmetry can create shocks, whose dissipation will convert the kinetic energy of collapsing shells into thermal random motion, heating the material and producing an equilibrium state with a finite size R_{vir}. A complete reconstruction of the dynamics of the collapse, even in such regions, can be found in [24]. We can derive when the virialization happens, in fact, at such moment, the Virial Theorem states that $E_{tot} = \frac{E_G}{2}$. Considering an uniform density perturbation, whose enclosed mass scales from $r = 0$ to $r = R$ as $m = \frac{4\pi}{3}\rho r^3$, its gravitational energy reads as

$$E_G = -\int_0^M dm \frac{Gm}{r(m)} = -\frac{3}{5}\frac{GM^2}{R}; \tag{4.19}$$

moreover, assuming that the mass and the energy are conserved during the collapse, we can easily calculate the total energy at the turn around, where the only contribution is the gravitational one. In the end we find that at virialization $-\frac{3}{5}\frac{GM^2}{r_{ta}} = -\frac{3}{5}\frac{GM^2}{2R_{vir}}$, therefore the virialized radius will be half of the maximum radius, fixing $\theta_{vir} = \frac{3}{2}\pi - \theta_i$. At such time, the density contrast will be given by

$$\delta_{vir} = y^{-3}(\theta_{vir}) - 1 \simeq 147 \tag{4.20}$$

and also numerical simulations proved that gravitationally bound structure arise when the objects become 150-200 times denser than the background. From now on when we will speak of "the end of the collapse"we will mean the virialization moment. To characterize this moment we will choose the value $\delta_{vir} = 200$, in order to be consistent to what has done in [4], which will be our comparison reference for the following sections. Requiring that virialization happens at the end of matter era, we can find the unknowns quantities δ_i and θ_c numerically solving the equations

$$\frac{1}{1+z_{e.m.e.}} = a(\theta_c) = \frac{a_i}{\delta_i}\left(\frac{3}{4}(1+\delta_i)\left[\theta_c + \theta_i - \sin(\theta_c+\theta_i)\right]\right)^{\frac{2}{3}} \tag{4.21}$$

$$y_0(\theta_c) = \sqrt[3]{\frac{2}{9}}\frac{1-\cos(\theta_c+\theta_i)}{\left[\theta_c+\theta_i-\sin(\theta_c+\theta_i)\right]^{\frac{2}{3}}} = (201)^{-\frac{1}{3}}, \tag{4.22}$$

obtaining $\delta_i \simeq 3.2 \cdot 10^{-3}$ (therefore $\theta_i \simeq 0.113$) and $\theta_c = 4.69$ (from now on the collapsing time will be $t_c = t(\theta_c)$). This will fix the height of the critical barrier to $\delta_c = 1.589$.

In the following sections we will introduce the MG scenario, where the physical radius r, therefore the normalized radius $y(\theta)$, will evolve in a different way; on the other hand, since we want to compare the collapses in these two cases, we choose to mantain the same "clock"given in 4.7, which in principle was defined along with the physical radius of this scenario.

4.2 Spherical Collapse in MG

In this case, always assuming spherical symmetry, the physical radius will increase also due to the fifth force, in fact a shell of radius $r(t)$ will evolve according to

$$\ddot{r} = -\frac{\partial \Psi_N}{\partial r} - \frac{\partial \Psi_\phi}{\partial r}. \tag{4.23}$$

While before we could find an analytic expression for the normalized radius $y = \frac{r}{aq}$, now we have to properly derive its equation of motion. The LHS of 4.23 explicitly reads as

$$\frac{\ddot{r}}{aq} = \ddot{y} + 2H\dot{y} + \frac{\ddot{a}}{a}y \tag{4.24}$$

and considering the normalized radius as a function of the new time variable $\eta = \log a(t)$, instead of the usual cosmic time, we obtain that $\dot{y} = \frac{dy}{dt} = H\frac{dy}{d\eta} = Hy'$ and that the RHS of the last equation is given by

$$H^2\left[y'' + \left(2 + \frac{\dot{H}}{H^2}\right)y' + \frac{\ddot{a}}{aH^2}y\right]. \tag{4.25}$$

Using the overbar to indicate background quantities, in an Universe where both matter and dark energy are present, the first and the second Friedman equations read as

$$\frac{\ddot{a}}{a} = -\frac{\bar{\rho}_m + (1+3w_{de})\bar{\rho}_{de}}{6M_p^2} = H^2\left[1 + \frac{\dot{H}}{H^2}\right], \quad H^2 = \frac{\bar{\rho}_m + \bar{\rho}_{de}}{3M_p^2}, \tag{4.26}$$

so that we can calculate

$$\frac{\ddot{a}}{aH^2} = -\frac{\Omega_m}{2}\left[1 + (1+3w_{de})\frac{\Omega_{de}}{\Omega_m}\right]. \tag{4.27}$$

On the other hand, the gravitational potential evolves due to the complete matter density, according to the modified Poisson equation

$$\nabla^2\Psi_N = 4\pi G\left[\rho_m(r) + (1+3w_{de})\bar{\rho}_{de}\right], \tag{4.28}$$

therefore, integrating once this equation, since dark-energy energy is spatially uniform, we find

$$\begin{aligned}\frac{\partial \Psi_N}{\partial r} &= \frac{4\pi G}{r^2}\int_0^r d\tilde{r}\tilde{r}^2\left[\rho_m(\tilde{r}) + (1+3w_{de})\bar{\rho}_{de}\right] = \frac{4\pi G r}{3}\left[\frac{3M}{4\pi r^3} + (1+3w_{de})\bar{\rho}_{de}\right] = \\ &= \frac{4\pi G r}{3}\left[\bar{\rho}_{m0}a^{-3}y^{-3} + (1+3w_{de})\bar{\rho}_{de}\right] = \frac{\bar{\rho}_m r}{6M_p^2}\left[y^{-3} + (1+3w_{de})\frac{\Omega_{de}}{\Omega_m}\right],\end{aligned} \tag{4.29}$$

obtaining in the end

$$\frac{1}{aqH^2}\frac{\partial \Psi_N}{\partial r} = \frac{y}{rH^2}\frac{\partial \Psi_N}{\partial r} = \frac{y\Omega_m}{2}\left[y^{-3} + (1+3w_{de})\frac{\Omega_{de}}{\Omega_m}\right]. \tag{4.30}$$

Gathering together all the pieces from 4.25, 4.27 and 4.30, we find

$$y'' + \frac{1}{2}\left(1 - 3w_{de}\Omega_{de}\right)y' + \frac{\Omega_m}{2}\left[y^{-3} - 1\right]y = -\frac{3M_p^2\Omega_m y}{\bar{\rho}_m r}\frac{\partial \Psi_A}{\partial r} = -\frac{3\beta M_p\Omega_m y}{\bar{\rho}_m a r}\frac{\partial \phi}{\partial x}, \tag{4.31}$$

where in the LHS we have the usual result we would find in the Λ-CDM cosmological model while in RHS we have the fifth force contribution, a peculiar characteristic of our MG models.
It is clear that we need to understand how the scalar field evolves both temporally and spatially: in order to do so we will use again the $\beta(a) - m(a)$ parametrization, showing that it is an effective framework also in the study of the non-linear dynamics. The spatial profile of the field is given by the quasi-static KG equation

$$\frac{1}{a^2}\nabla^2\phi = \frac{\partial V}{\partial \phi} + \rho_m \frac{\partial \log A}{\partial \phi}, \tag{4.32}$$

where $\rho_m = \bar{\rho}_m(1+\delta) = \bar{\rho}_{m0}a^{-3}(1+\delta)$ is the complete, position-dependent density of our body. In the previous chapter we have reconstructed background field values starting from the background density, i.e. we have found $\bar{\phi}(a)$, while now we have to deal with the local value $\phi(x)$ associated to the complete density. Let's define the function $\alpha = a(\bar{\phi})$, which associate to a given value of the background field the corresponding scale factor, i.e. $a(\bar{\phi})$ is the inverse function of $\bar{\phi}(a)$: this function allow us define the field $\alpha(\mathbf{x})$ as the scale factor observed when the background field value is equal to the local field value or, in a mathematical fashion, $\bar{\phi}[\alpha(\mathbf{x})] = \phi(\mathbf{x})$. From the minimum equation 3.9 evaluated at the local value of the field we obtain as before

$$\frac{d\phi}{d\alpha} = \frac{3\bar{\rho}_\alpha \beta_\alpha}{\alpha M_p m_\alpha^2}. \tag{4.33}$$

where $\bar{\rho}_\alpha = \bar{\rho}_{m0}\alpha^{-3}$, $\beta_\alpha = \beta(\bar{\phi}(\alpha)) = \beta(\phi(\mathbf{x}))$ and $m_\alpha^2 = m^2(\bar{\phi}(\alpha)) = m^2(\phi(\mathbf{x}))$. Thanks to this new quantity and to the spherical symmetry, we can now rewrite the quasi-static KG equation 4.32 as follows: the LHS reads as

$$\frac{d\phi}{d\alpha}\left[\frac{d^2\alpha}{dx^2} + \frac{2}{x}\frac{d\alpha}{dx}\right] + \frac{d^2\phi}{d\alpha^2}\left(\frac{d\alpha}{dx}\right)^2, \tag{4.34}$$

where

$$\frac{d^2\phi}{d\alpha^2} = \frac{3\bar{\rho}_0}{M_p}\frac{d}{d\alpha}\left(\frac{\beta_\alpha}{m_\alpha^2\alpha^4}\right) = \frac{d\phi}{d\alpha}\frac{d}{d\alpha}\log\frac{\beta_\alpha}{m_\alpha^2\alpha^4}, \tag{4.35}$$

while terms in the RHS, using the minimum equation, will read as

$$\frac{\rho_m\beta}{M_p} = \frac{\bar{\rho}_{m0}(1+\delta)a^{-3}\beta_\alpha}{M_p}, \tag{4.36}$$

$$\frac{dV}{d\phi} = -\frac{\bar{\rho}_\alpha\beta_\alpha}{M_p} = -\frac{\bar{\rho}_{m0}\alpha^{-3}\beta_\alpha}{M_p}. \tag{4.37}$$

Gathering all these terms, equation 4.32 has become

$$\frac{1}{x^2}\frac{d}{dx}\left[x^2\frac{d\alpha}{dx}\right] + \log\frac{\beta_\alpha}{m_\alpha^2\alpha^4}\left(\frac{d\alpha}{dx}\right)^2 = \frac{m_\alpha^2\alpha^4}{3a}\left[1+\delta-\frac{a^3}{\alpha^3}\right]. \tag{4.38}$$

Finally, using this new quantity, we can modify equation 4.31 in order to obtain the complete normalized radius equation

$$y'' + \frac{1}{2}\left(1 - 3w_{de}\Omega_{de}\right)y' + \frac{\Omega_m}{2}\left[y^{-3}-1\right]y = -\frac{9\Omega_m\beta_\alpha^2 a y}{m_\alpha^2\alpha^4 x}\frac{\partial\alpha}{\partial x}. \tag{4.39}$$

The first difference that arises in the MG scenario is that now there is not anymore scale indipendence, in fact we have a set of two coupled equation, where the field evolves in time and space according to the density profile $\delta(t,x)$ and the density

evolves also due to the additional fifth force profile. Because of this coupled behaviour, a complete and rigorous study of the spherical collapse can be done only following the dynamics of all shells. Since this can be done just numerically, we follow [3] and adopt another approach: we will focus our attention just on the shell which enclose the mass M we are interested in and we will use an ansatz for density profile. This is enough in order to have manageable numerical simulation, in fact at each step we can calculate the density profile shape, the field profile and how the radius changes, but it is still too much complicated if we want to find a semi-analytic description, as we can see from the specific shape chose in [4], and it is also meaningless since the density profile choice is arbitrary, therefore in the next section we will try to find a way to overcome this problem.

4.3 Field Profile

The first idea that can be considered is to choose, as in GR, a spatially uniform top-hat perturbation which encloses a mass M and has the general profile

$$\delta(t,x) = \begin{cases} \delta(t) & x \leq x_M \\ 0 & x > x_M \end{cases}, \tag{4.40}$$

where x_M is the comoving coordinate of the outer shell, which we will follow during the collapse, of our perturbation. Even without drawing the profile or launching some numerical simulation, we can immediately guess what could be the problem in this approach: the critical point is that the field has to evolve from its background value to its internal value all at once in a not so extended region, instead of exploiting the rising density profile to slowly evolve over larger distances from the exterior to the interior value. This would imply that the gradient of the field, evaluated at our reference shell, which contributes to determine the fifth force strenght, will be excessively large, overestimating the fifth force strength; moreover, since the field can't properly follow the density profile, it will hardly reach its potential minimum inside the collapsing body and this will result in a lack of screening, as we have explained in the second chapter.
On the base of these considerations, we can conclude that we definitively need some intermediate or transition region between the body and the cosmological background, where the density profile can smoothly vary, in order to achieve sensible results. This fact introduces a substantial problem, since equation 4.38 is highly non-linear, therefore even some trivial profile will produce an analytically unsolvable equation. To overcome this issue, we decide to start from a different point, i.e. from the profile of α, for which we have numerical simulations that can guide our choices (see [4] or bottom-right panels of Figure 4.1 and 4.4). Since deeply inside and outside the object we have that field profile is almost constant, we decide to take in these regions a spatially uniform density profile as we have done before, while in the transition region $[x_M, x_\epsilon]$, where $x_\epsilon = x_M(1+\epsilon)$ and ϵ will be properly chosen on the base of the cited numerical simulations, the density is an unknown (for now) quantity. In physical coordinates, the complete matter density profile will now read as

$$\rho(r) = \begin{cases} \bar{\rho}[1+\delta(t)] & r \leq r_M \\ \bar{\rho}[1+\delta(t,r)] & r_M < r < r_\epsilon \\ \bar{\rho} & r \geq r_\epsilon \end{cases}. \tag{4.41}$$

Then, since we expect that the first derivative will assume small values, we further simplify the LHS of equation 4.38 assuming that the second term, in which appears

the squared first derivative, is negligible with respect to the first one. Introducing the rescaled variable $\tilde{\alpha} = \frac{\alpha}{a}$, the α profile equation 4.38 reads as

$$\frac{1}{x^2}\frac{d}{dx}\left[x^2\frac{d\tilde{\alpha}}{dx}\right] = \frac{m_{a\tilde{\alpha}}^2 a^2 \tilde{\alpha}}{3}\left[\tilde{\alpha}^3(1+\delta) - 1\right]. \tag{4.42}$$

In the inner and outer region, according to density profile shape 4.41, we can expand $\tilde{\alpha}$ as $\tilde{\alpha}_0(t) + \delta\tilde{\alpha}(t,x)$, where $\delta\tilde{\alpha} \ll \tilde{\alpha}$ is a small perturbation with respect to the background value, and find the perturbed equation

$$\begin{aligned}\frac{1}{x^2}\frac{d}{dx}\left[x^2\frac{d\delta\tilde{\alpha}}{dx}\right] &= \frac{m_{a\tilde{\alpha}_0}^2 a^2 \tilde{\alpha}_0}{3}\left[\tilde{\alpha}_0^3(1+\delta) - 1\right] + \\ &+ \frac{m_{a\tilde{\alpha}_0}^2 a^2}{3}\left[3\tilde{\alpha}_0^3(1+\delta) + \left(\tilde{\alpha}_0^3[1+\delta] - 1\right)\left(1 + \frac{\tilde{\alpha}_0}{m_{a\tilde{\alpha}_0}^2}\left.\frac{dm_{a\tilde{\alpha}}^2}{d\tilde{\alpha}}\right|_{a\tilde{\alpha}_0}\right)\right]\delta\tilde{\alpha} = \\ &= S + k^2\delta\tilde{\alpha},\end{aligned} \tag{4.43}$$

where in the last line we have defined the two quantities k^2 and S, for now assumed both as positives, even if we have still to prove it.
Deeply outside the body, for $x > x_\epsilon$, where $\delta = 0$, we can grasp how the screening mechanism works: looking to equation 4.38 we can see that in this case the disappearance of the fifth force ($\frac{d\alpha}{dx} = 0$) can be obtained if $\alpha \to a$, i.e. in the weak field regime, as confirmed also by numerical simulations. Therefore it is reasonable to choose $\tilde{\alpha}_0 = 1$, so that

$$S = 0, \quad k^2 \equiv k_o^2 = m_a^2 a^2 \tag{4.44}$$

and equation 4.43 is given by

$$\frac{1}{x^2}\frac{d}{dx}\left[x^2\frac{d\delta\tilde{\alpha}}{dx}\right] - k_o^2\delta\tilde{\alpha} = 0. \tag{4.45}$$

Asking that the perturbation vanishes at spatial infinity, i.e. $\delta\tilde{\alpha}(x \to \infty) \to 0$, only the decreasing exponential solution survives and the complete profile in this region reads as

$$\tilde{\alpha}(x) = 1 - D\frac{e^{-k_o x}}{x}, \tag{4.46}$$

where D is a constant.
Inside the collapsing object, for $x \leq x_M$, where the density is spatially uniform, $S \neq 0$ and $k^2 \equiv k_i^2$, equation 4.43 reads as

$$\frac{1}{x^2}\frac{d}{dx}\left[x^2\frac{d\delta\tilde{\alpha}}{dx}\right] - k_i^2\delta\tilde{\alpha} = S. \tag{4.47}$$

Requiring that the solution is non-singular at the origin, i.e. $\left.\frac{d\delta\tilde{\alpha}}{dx}\right|_{x\to 0} \to 0$, the complete profile reads as

$$\tilde{\alpha}(x) = \tilde{\alpha}_0 - \frac{S}{k_i^2} + A\frac{\sinh(k_i x)}{k_i x}, \tag{4.48}$$

where $\tilde{\alpha}_0$ and A are constant we have to determine. Since we want our expansion around $\tilde{\alpha}_0$ to be faithful, i.e. that our expansion is effectively done around the background value, we have to require that $\delta\tilde{\alpha}(x \to 0) \to 0$, which implies that

$$A - \frac{S}{k_i^2} = 0. \tag{4.49}$$

Finally, because of difficulties we have already mentioned, in the intermediate region we will interpolate the field profile between the interior solution 4.48 and the exterior one 4.46 with the simplest profile choice, i.e. the linear one: here we will assume that the complete (background plus perturbation) α profile will have the convenient form

$$\tilde{\alpha}(x) = B + \frac{C-B}{\epsilon x_M}(x - x_M), \tag{4.50}$$

where B and C are constants. Such field profile will indirectly define, through equation 4.42, the density profile

$$1 + \delta(x) = \frac{1}{\tilde{\alpha}^3} + \frac{3}{m^2_{a\tilde{\alpha}} a^2 x^2 \tilde{\alpha}^4} \frac{d}{dx}\left(x^2 \frac{d\tilde{\alpha}}{dx}\right), \tag{4.51}$$

so that we are able to check if the density profile shape, associated to our linear approximation, is reasonable. Of course this method creates some issues, for example nothing assures us that the density profile will be continuous passing from inside the body to the transition region and from the latter to the outer one.
Imposing continuity of $\tilde{\alpha}$ and $\frac{d\tilde{\alpha}}{dx}$ both at $x = x_M$ and $x = x_\epsilon$ we can determine the four coefficients $A,\ B,\ C,\ D$, therefore the complete profile will be given by

$$\tilde{\alpha}(x) = \begin{cases} \tilde{\alpha}_0 - \frac{S}{k_i^2} + \left(1 - \tilde{\alpha}_0 + \frac{S}{k_i^2}\right) \frac{k_i x_M (k_o x_\epsilon + 1)}{\cosh(k_i x_M)[k_i x_M + k_o x_\epsilon \tanh(k_i x_M) + f(\epsilon)]} \frac{\sinh(k_i x)}{k_i x} & x \leq x_M \\ 1 - \left(1 - \tilde{\alpha}_0 + \frac{S}{k_i^2}\right) \frac{k_i x_M - \tanh(k_i x_M)}{k_i x_M + k_o x_\epsilon \tanh(k_i x_M) + f(\epsilon)} [1 + \epsilon(k_o x_\epsilon + 2)] + & \\ \quad + \frac{k_o x_\epsilon + 1}{x_M} \left(1 - \tilde{\alpha}_0 + \frac{S}{k_i^2}\right) \frac{k_i x_M - \tanh(k_i x_M)}{k_i x_M + k_o x_\epsilon \tanh(k_i x_M) + f(\epsilon)} (x - x_M) & x_M < x < x_\epsilon \\ 1 - \left(1 - \tilde{\alpha}_0 + \frac{S}{k_i^2}\right) \frac{k_i x_M - \tanh(k_i x_M)}{k_i x_M + k_o x_\epsilon \tanh(k_i x_M) + f(\epsilon)} \frac{x_\epsilon^2}{x_M} \frac{e^{k_o(x_\epsilon - x)}}{x} & x \geq x_\epsilon \end{cases} \tag{4.52}$$

where we have defined

$$f(\epsilon) = \epsilon \left[k_o x_\epsilon + 2\right] \left[k_i x_M - \tanh(k_i x_M)\right] \tag{4.53}$$

and, as expected, we find that $\tilde{\alpha}$ is bound to be lesser than one.
In this way we can find the explicit form of equation 4.49, which now reads as

$$\frac{\tilde{\alpha}_0}{1 - \tilde{\alpha}_0} \frac{[\tilde{\alpha}_0^3(1+\delta) - 1]\left[\frac{\cosh(k_i x_M)(k_i x_M + k_o x_\epsilon \tanh(k_i x_M) + f(\epsilon))}{k_i x_M (1 + k_o x_\epsilon)} - 1\right]}{[\tilde{\alpha}_0^3(1+\delta) - 1]\left[1 + \frac{\tilde{\alpha}_0}{m^2_{a\tilde{\alpha}_0}} \left.\frac{dm^2_\alpha}{d\tilde{\alpha}}\right|_{a\tilde{\alpha}_0}\right] + 3\tilde{\alpha}_0^3(1+\delta)} = 1 \tag{4.54}$$

and gives the evolution of α_0 in time: even without solving numerically this equation, we can roughly predict the behaviour of the scalar field inside the body, in particular in the two extreme regimes, when $k_i x_M \to 0$ and when $k_i x_M \gg 1$. In the first regime, where the outer shell is well inside the Compton wavelength of the scalar field and will fully feel the fifth force, the second square bracket in the numerator will tend to zero, so, in order to balance this contribution to obtain a finite value of the LHS of 4.54, we will have that $\tilde{\alpha}_0 \to 1$, i.e. the field will not evolve from its background value, as expected from the lack of screening. In the second regime, the outer shell will be outside the Compton wavelenght and the same square bracket will be dominate by the exponential term $e^{k_i x_M}$ so, in order to achieve some compensation, $\tilde{\alpha}_0$ will tend to the value $(1+\delta)^{-\frac{1}{3}}$ which is associated to the screening condition, as we could have eventually seen also in the complete α equation 4.38. Moreover, we can see that the evolution of $\tilde{\alpha}_0$ is ϵ-dependent, stressing again the importance of the transition region.

Now that we have fully derived the field profile behaviour we have to check that our assumption about neglecting the square derivative term was consistent, i.e. that the the ratio between the second term in the LHS of equation 4.38 and the first one, which reads as

$$R_{der} = \left| \frac{d}{d\alpha} \log\left(\frac{\beta_\alpha}{m_\alpha^2 \alpha^4}\right) \left(\frac{d\alpha}{dx}\right)^2 \Big/ \frac{1}{x^2}\frac{d}{dx}\left(x^2 \frac{d\alpha}{dx}\right) \right|, \tag{4.55}$$

is much less than one all along the collapse.
Then, in order to study the fifth force behaviour and to compare it to the Newtonian one, we will calculate their ratio and we will analyze its dependence from the collapsing object mass, as well as its spatial and temporal evolution. Given the density profile 4.41, the mass enclosed in a shell with physical size r reads as

$$M(r) = \begin{cases} \frac{4\pi}{3}\bar{\rho}(1+\delta)r^3 & r \leq r_M \\ M_{body} + \frac{4\pi}{3}\bar{\rho}[r^3 - r_M^3 + 3\int_{r_M}^{r} dr'(r')^2\delta(r')] & r_M < r < r_\epsilon \\ M_{body} + M_{tr} + \frac{4\pi\bar{\rho}}{3}(r^3 - r_\epsilon^3) & r \geq r_\epsilon \end{cases}, \tag{4.56}$$

where we have defined the mass enclosed in the transition region as $M_{tr} = M(r_\epsilon) - M_{body}$. Switching to the comoving radial coordinate, the mass profile reads as

$$M(x) = \begin{cases} \frac{4\pi}{3}\bar{\rho}_0(1+\delta)x^3 & x \leq x_M \\ \frac{4\pi}{3}\bar{\rho}_0[x^3 + \delta x_M^3 + 3\int_{x_M}^{x} dx'(x')^2\delta(x')] & x_M < x < x_\epsilon \\ \frac{4\pi}{3}\bar{\rho}_0[x^3 + \delta x_M^3 + 3\int_{x_M}^{x_\epsilon} dx'(x')^2\delta(x')] & x \geq x_\epsilon \end{cases}, \tag{4.57}$$

so the Newtonian force that such shell will feel is given by

$$F_N(x) = -\frac{GM(x)}{a^2x^2} = \begin{cases} -\frac{\bar{\rho}_0 x}{6M_p^2a^2}[1+\delta] & x \leq x_M \\ -\frac{\bar{\rho}_0 x}{6M_p^2a^2}[1 + \delta\frac{x_M^3}{x^3} + \frac{3}{x^3}\int_{x_M}^{x} dx'(x')^2\delta(x')] & x_M < x < x_\epsilon \\ -\frac{\bar{\rho}_0 x}{6M_p^2a^2}[1 + \delta\frac{x_M^3}{x^3} + \frac{3}{x^3}\int_{x_M}^{x_\epsilon} dx'(x')^2\delta(x')] & x \geq x_\epsilon \end{cases}. \tag{4.58}$$

On the other hand the fifth force profile is given by

$$F_\phi(x) = -\frac{1}{a}\frac{\partial \Psi_A}{\partial x} = -\frac{1}{a}\frac{\beta}{M_p}\frac{\partial\phi}{\partial\alpha}\frac{\partial\alpha}{\partial x} = -\frac{3\bar{\rho}_0\beta_\alpha^2}{aM_p^2\alpha^4 m_\alpha^2}\frac{\partial\alpha}{\partial x} \tag{4.59}$$

where, from 4.52, the first derivative of the field profile reads as

$$\frac{d\tilde{\alpha}(x)}{dx} = \begin{cases} \left(1 - \tilde{\alpha}_0 + \frac{S}{k_i^2}\right)\frac{k_i x_M(k_o x_\epsilon + 1)}{\cosh(k_i x_M)[k_i x_M + k_o x_\epsilon \tanh(k_i x_M) + f(\epsilon)]}\frac{k_i x\cosh(k_i x) - \sinh(k_i x)}{k_i x^2} & x \leq x_M \\ \left(1 - \tilde{\alpha}_0 + \frac{S}{k_i^2}\right)\frac{k_i x_M - \tanh(k_i x_M)}{k_i x_M + k_o x_\epsilon \tanh(k_i x_M) + f(\epsilon)}\frac{k_o x_\epsilon + 1}{x_M} & x_M < x < x_\epsilon \\ \left(1 - \tilde{\alpha}_0 + \frac{S}{k_i^2}\right)\frac{k_i x_M - \tanh(k_i x_M)}{k_i x_M + k_o x_\epsilon \tanh(k_i x_M) + f(\epsilon)}\frac{x_\epsilon^2}{x_M}\frac{k_o x + 1}{x^2}e^{k_o(x_\epsilon - x)} & x \geq x_\epsilon \end{cases}. \tag{4.60}$$

The ratio between them, calculated on the outer shell x_M, will reads as

$$R_F(x_M) = \frac{F_\phi(x_M)}{F_N(x_M)} = \frac{18 a y_0^2 \beta_{\alpha_M}^2}{q\alpha_M^4 m_{\alpha_M}^2}\left.\frac{\partial\alpha}{\partial x}\right|_{x_M} \tag{4.61}$$

and it will play a crucial role in the study of the collapse, as we will explain later.

h	0.67
ρ_{0c}	$1.88h^2 \cdot 10^{-29}$ g/cm^3
Ω_{m0}	0.31
$M_\odot$	$1.99 \cdot 10^{33}$ g
Mpc	$3.09 \cdot 10^{24}$ cm

Table 4.1: List of cosmological parameters used in numerical simulations.

m_0	0.334 h Mpc^{-1}
r	1
β_0	0.5
s	0.12

(a) Dilaton

m_0	0.017 h Mpc^{-1}
m	0.5
β_0	1
n	0.25
$z_\star$	1

(b) Symmetron

Table 4.2: List of dilaton and symmetron model parameters used in numerical simulations.

4.4 Numerical Simulations: Field Profile

In order to verify that our result are sensible, we will choose a dilaton and a symmetron model, we will calculate all the previously introduced quantities and then we will compare them to numerical simulations in [4], which will be our comparison reference all along this chapter: we do so not to check that we have obtained the same numerical values, since in the cited paper the body virializes at $z = 0$ and the collapse continues also during the dark-energy era, but to see if we can obtain values and behaviours that are plausible. The natural extension of this work is to properly numerically simulate the collapse in our conditions and then to compare the values, but this will not be done in this thesis. In our simulations we will consider the cosmological parameter given in Table 4.1, while the dilaton and symmetron parameters are presented in Table 4.2 and correspond to the A3 models in [4].
The lagrangian coordinate q will read as

$$q = \frac{y_M}{x_M} = \left(\frac{3M}{4\pi\bar{\rho}_{m0}}\right)^{\frac{1}{3}} = 0.39h^{\frac{2}{3}}M^{\frac{1}{3}}, \tag{4.62}$$

where lenghts are expressed in $h^{-1}Mpc$ and masses in $10^{10}h^{-1}M_\odot$.
We will assume that the density inside the halo will evolve as in GR; strictly speaking, this is false but since we expect to find in MG just little deviations from GR, as approximation it is valid. Moreover, as we said, the overdensity evolution is coupled to the field evolution and we would like to decouple these equations: this will be our density ansatz inside the body.
Then, in order to calculate the field profile, we need to define how much large is the transition region: looking to the cited reference, we see that in both cases the density profile reaches the background value around 50 $h^{-1}Mpc$, therefore we will define ϵ in such a way that $x_\epsilon = 50\ h^{-1}Mpc$.
Finally, we will study the mass range $[10^{10}\ h^{-1}M_\odot, 10^{15}\ h^{-1}M_\odot]$, which spans from small galaxies to large clusters of galaxies.

4.4.1 Dilaton

In this case we have

$$m_\alpha = m_0 \alpha^{-r}, \quad \beta_\alpha = \beta_0 e^{\frac{s}{2r-3}\left(\alpha^{2r-3}-1\right)}, \tag{4.63}$$

therefore, specifying the relevant quantities previously introduced, we have

$$k_i^2 = \frac{m_0^2 \tilde{\alpha}_0^{-2r} a^{2-2r}}{3}\left[2r-1+(4-2r)\tilde{\alpha}_0^3(1+\delta)\right], \tag{4.64}$$

$$S = \frac{m_0^2 a^{2-2r}\tilde{\alpha}_0^{1-2r}}{3}\left[\tilde{\alpha}_0^3(1+\delta)-1\right] \tag{4.65}$$

and the derivatives ratio we will use to evaluate the goodness of our approximation reads as

$$\begin{aligned} R_{der} &= \left| \frac{2r-4+s\alpha^{2r-3}}{\alpha}\left(\frac{d\alpha}{dx}\right)^2 \Big/ \frac{1}{x^2}\frac{d}{dx}\left(x^2\frac{d\alpha}{dx}\right)\right| = \\ &= \left| \frac{2r-4+s(a\tilde{\alpha})^{2r-3}}{\tilde{\alpha}}\left(\frac{d\tilde{\alpha}}{dx}\right)^2 \Big/ \frac{1}{x^2}\frac{d}{dx}\left(x^2\frac{d\tilde{\alpha}}{dx}\right)\right|. \end{aligned} \tag{4.66}$$

In Figure 4.1 we can compare which are the resulting profiles produced by our model to the ones given by the numerical procedure: in our case we can see that we obtained reasonable shapes both of the α and the density contrast profile. Concerning the field profile, we can notice that at the end of the transition region it tends to be too much flattened towards the background value, while in exact case the growth is less steep. In our model, bodies with mass larger than $10^{13}\ h^{-1}M_\odot$ are almost screened at virialization, as in their. We can also notice that the density profile obtained, even if it isn't continuous and shows a significant jump in the lower mass case, reminds the shape of a possible real profile, underlining that our transition region ansatz points in the right direction. Clearly the presense of such discontinuity at the outer shell position will produce an overestimated field gradient, therefore a bigger fifth force.

In the left panel of Figure 4.2 we can check that in our model the term we have neglected is always smaller than the first one we kept, showing that our approach is consistent. Moreover, from the right panel, we can see what we would have obtained if we had taken the bare top-hat approach we have discarded, where we had not considered the existence of a transition region: in general the ratio is larger, but starting from $M = 10^{13}\ h^{-1}M_\odot$ the neglected term would have been comparable to the other one during the collapse and, in clusters of galaxies, it even exceeds it, making the approximated field profile unreliable.

In the end we analyze the fifth force: as it is shown in top-left panel of Figure 4.3, at the end of the collapse, on the outer shell, the fifth force is highly suppressed for highly massive objects, while for smaller objects we approach to the characteristic value $2\beta^2$ that correspond to the thick-shell regime. From the top-right panel we can see that in the early phases of the collapse the fifth force on the outer shell was considerably suppressed, then it quickly rose to set on an almost constant value; in the end, the fact that the ratio shows a small decline signals the appearance of the screening mechanism. Finally, we can compare the spatial profile produced by our model to the numerical solution, finding out that our result can catch the general behaviour, in fact we can recognize the "plateau"inside the object, that sort of cusp around the shell position and the common decay outside the transition region, which is more abrupt in our model because of the exponential suppression on the background value we discussed earlier.

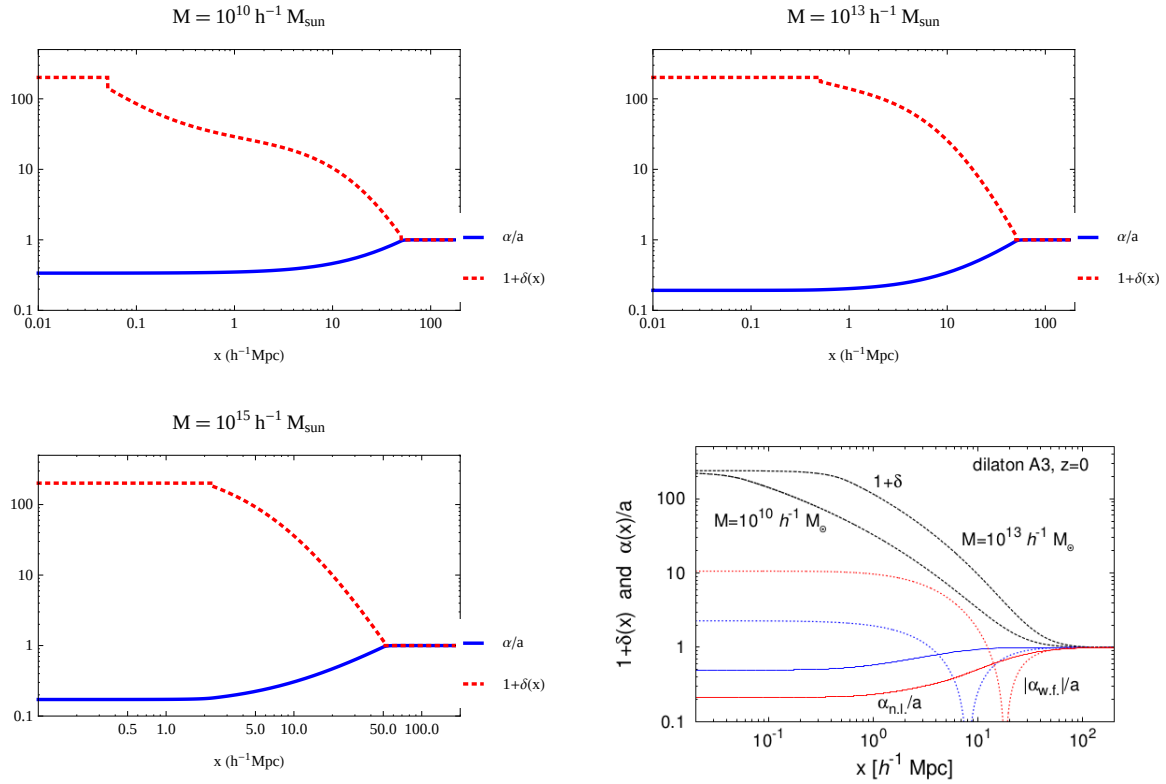

Figure 4.1: $\tilde{\alpha}$ and density contrast profiles from our modelization (top-left/right and bottom-left panels) and from full numerical simulations (bottom-right panel). In the latter one, the blue (red) curve represents the $\tilde{\alpha}$ profile for an object with mass 10^{10} $h^{-1}M_{\odot}$ (10^{13} $h^{-1}M_{\odot}$).

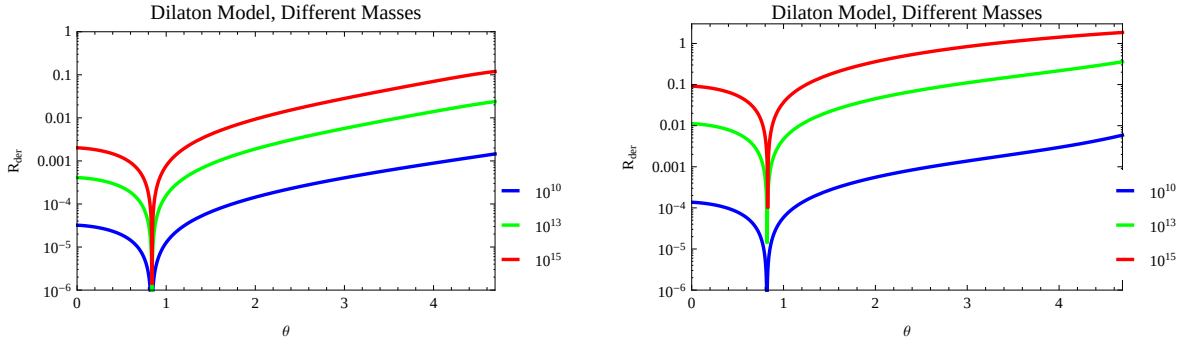

Figure 4.2: Derivatives ratio, for different masses of the collapsing body, in presence (on the left) and in absence (on the right) of the transition region. Masses unit is $h^{-1}M_{\odot}$.

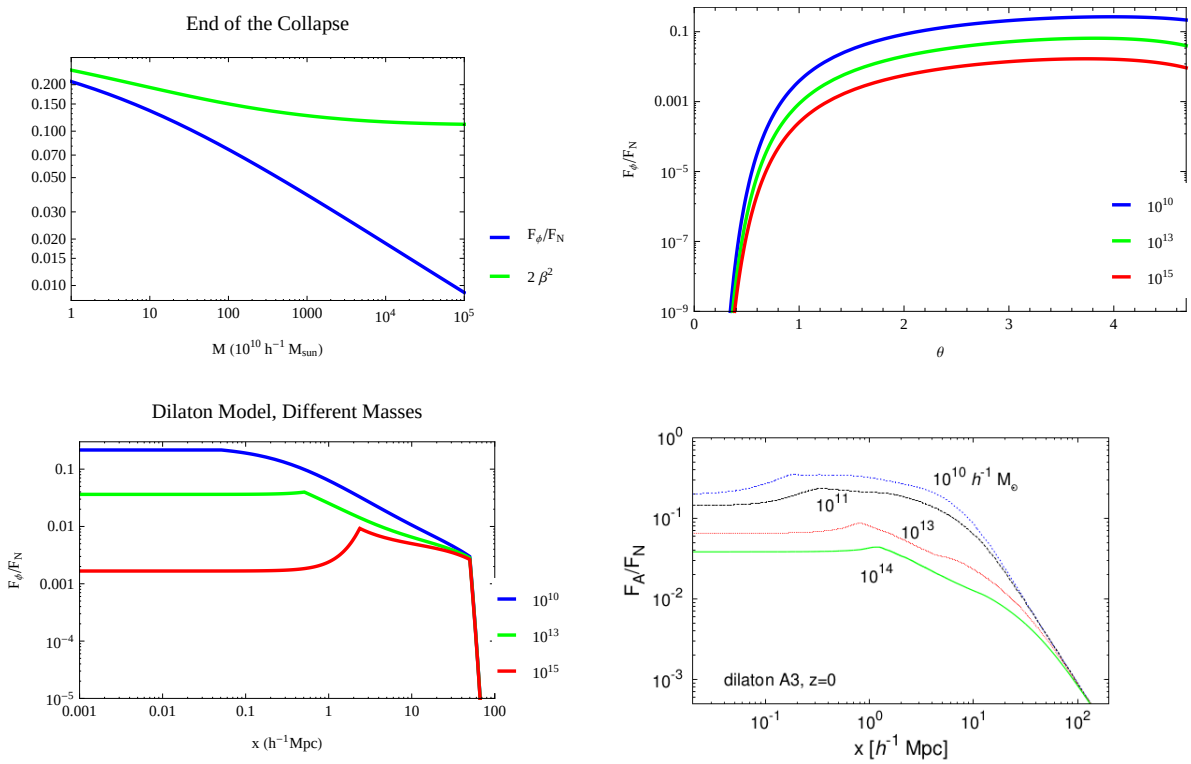

Figure 4.3: On upper panels we have the mass (left) and time (right), parametrized by the θ variable, dependence of the forces ratio on the outer shell. On lower panels we have the approximated (left) and numerical (right) spatial profile, where masses units are $h^{-1}M_\odot$.

4.4.2 Symmetron

In this case we have

$$m_\alpha = m_\star \left[1 - \left(\frac{a_\star}{a}\right)^3\right]^m, \quad \beta_\alpha = \beta_\star \left[1 - \left(\frac{a_\star}{a}\right)^3\right]^n \tag{4.67}$$

therefore, as done before, we can explicitly write

$$k_i^2 = \frac{m_\star^2 a^2}{3}\left[3\tilde{\alpha}_0^3(1+\delta)\left(1 - \frac{a_\star^3}{a^3\tilde{\alpha}_0^3}\right) + \left(\tilde{\alpha}_0^3(1+\delta) - 1\right)\left(1 + (6m-1)\frac{a_\star^3}{a^3\tilde{\alpha}_0^3}\right)\right]\left[1 - \frac{a_\star^3}{a^3\tilde{\alpha}_0^3}\right]^{2m-1} \tag{4.68}$$

$$S = \frac{m_\star^2 a^2 \tilde{\alpha}_0}{3}\left[\tilde{\alpha}_0^3(1+\delta) - 1\right]\left[1 - \frac{a_\star^3}{a^3\tilde{\alpha}_0^3}\right]^{2m} \tag{4.69}$$

and the derivatives ratio will read as

$$\begin{aligned} R_{der} &= \left| \frac{(4+3n-6m)a_\star^3 - 4\alpha^3}{\alpha\left(\alpha^3 - a_\star^3\right)}\left(\frac{d\alpha}{dx}\right)^2 \Bigg/ \frac{1}{x^2}\frac{d}{dx}\left(x^2\frac{d\alpha}{dx}\right)\right| = \\ &= \left| \frac{(4+3n-6m)a_\star^3 - 4(a\tilde{\alpha})^3}{\tilde{\alpha}\left[(a\tilde{\alpha})^3 - a_\star^3\right]}\left(\frac{d\tilde{\alpha}}{dx}\right)^2 \Bigg/ \frac{1}{x^2}\frac{d}{dx}\left(x^2\frac{d\tilde{\alpha}}{dx}\right)\right|. \end{aligned} \tag{4.70}$$

In Figure 4.4 we can see that in this case differences between our profile and the reference one is stronger, in fact, for low mass objects, the field profile barely moves away from the background value. Probably this is due to the fact that in our case, since virialization happens earlier than in their case, the field has less time to evolve and drift away from the background value. Moreover, since the coupling to matter appears in late times, the field cannot smoothly evolve along with the density and, as we have pointed out, large gradients do not allow a proper screening. This happened despite the fact that symmetron has a more efficient screening mechanism, since in our case a body will be screened if in the inner region $\alpha \to a_\star = \frac{1}{2}$ or, equivalently, $\tilde{\alpha} \to \frac{a_\star}{a}$, because for such value the scalar field mass becomes zero, therefore the RHS of 4.38 becomes zero too, forcing $\frac{d\alpha}{dx} \to 0$.

In Figure 4.5 we can see that also in this case our solution is consistent with approximations we made and that the existence of a transition region helps, although in this case the smallness of these value is also due to the little gradient values in our α profile.

Because of the heavy lack of screening, as we can see from the top-left panel in Figure 4.6, it is clear that in the whole range of masses we are really close to the thick-shell regime and that the fifth force will become even greater than the Newtonian one, even if this happens after $\theta_\star$, defined by $a_\star = a(\theta_\star)$. Moreover, the absence of screening allows the field to propagate further its fifth force, which will not decay as fast as in the dilaton case, and the difference in the relative strength between large and small mass objects is tiny. On the bottom-right panel we can see what we should expect from a proper simulation, where indeed the fifth force on the outer shell can be comparable to the Newtonian one for small objects, but it does not become dominant during all the collapse; moreover we can see that from medium to large object, the fifth force inside the body is highy suppressed.

4.5 Numerical Simulations: Collapse

Finally, now that we have analyzed our profile behaviour, we are ready to deal with the collapse dynamics of the outer shell, given by equation 4.39. Since we work in

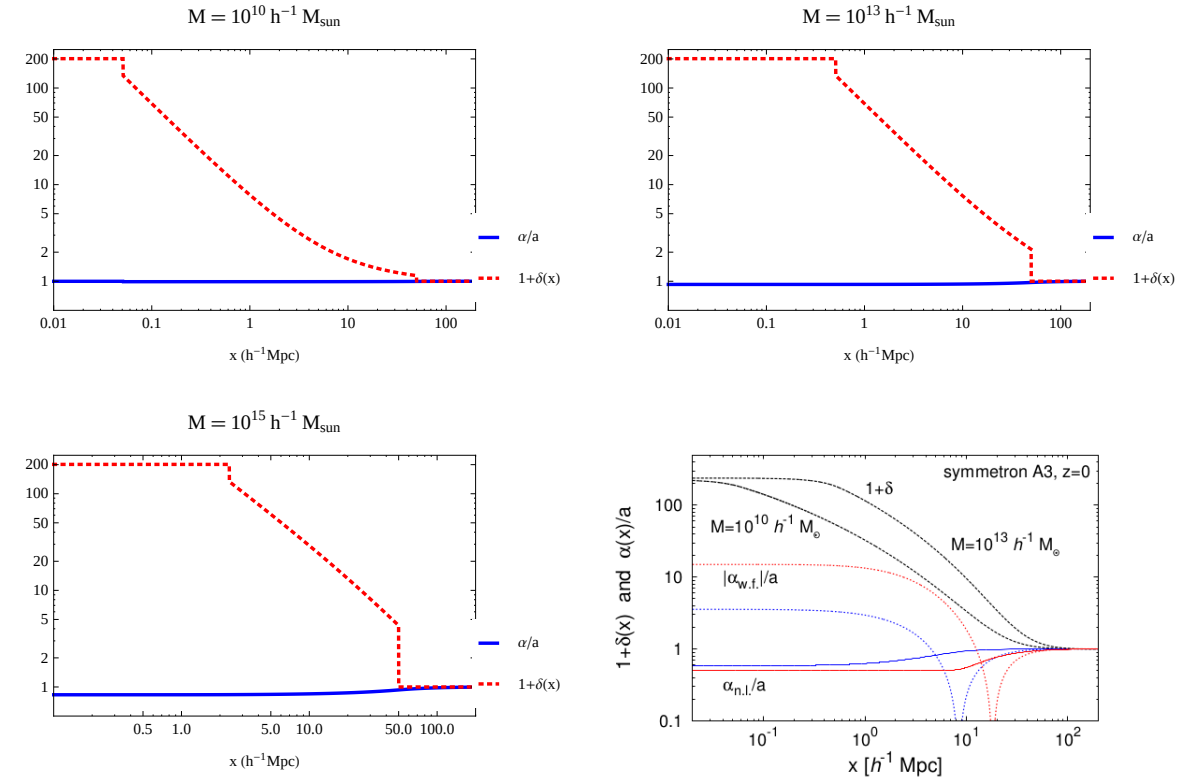

Figure 4.4: $\tilde{\alpha}$ and density contrast profiles from our modelization (top-left/right and bottom-left panels) and from full numerical simulations (bottom-right panel). In the latter one, the blue (red) curve represents the $\tilde{\alpha}$ profile for an object with mass 10^{10} $h^{-1}M_{\odot}$ (10^{13} $h^{-1}M_{\odot}$).

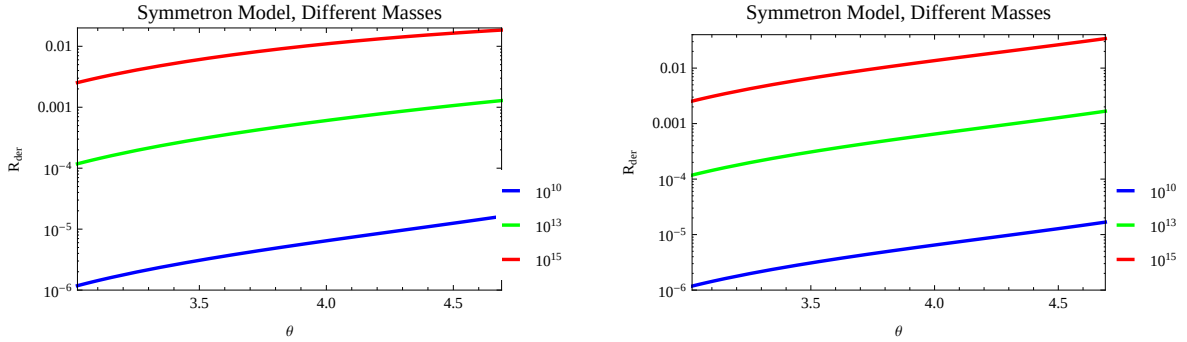

Figure 4.5: Derivatives ratio, for different masses of the collapsing body, in presence (on the left) and in absence (on the right) of the transition region. Masses unit is $h^{-1}M_{\odot}$.

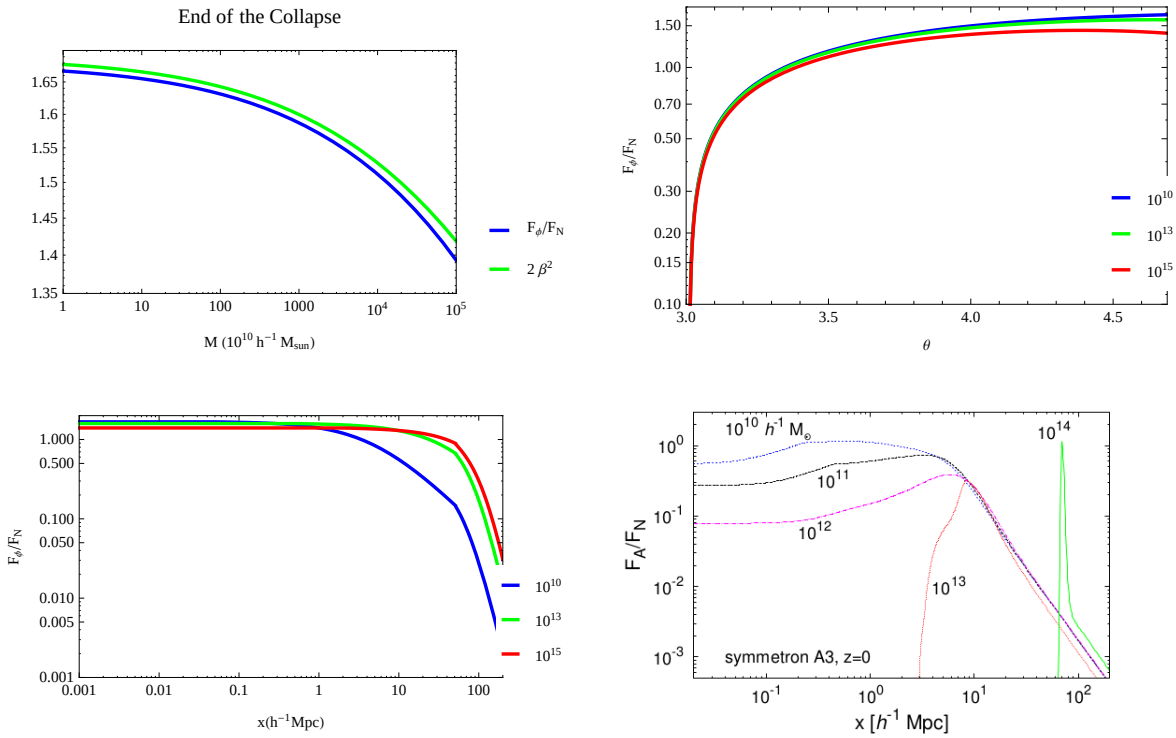

Figure 4.6: On upper panels we have the mass (left) and time (right), parametrized by the θ variable, dependence of the forces ratio on the outer shell. On lower panels we have the approximated (left) and numerical (right) spatial profile, where masses units are $h^{-1}M_\odot$.

the matter dominated era, we can assume that $\Omega_m = 1 - \Omega_{de} = 1$, therefore the normalized radius equation will read as

$$y'' + \frac{1}{2}y' + \frac{1}{2}\left[y^{-3} - 1\right] y = -\frac{9\beta_\alpha^2 a y}{m_\alpha^2 \alpha^4 x}\frac{\partial \alpha}{\partial x}. \tag{4.71}$$

Since we have fixed our clock as in the GR framework, we want to rewrite this last equation in such a way that the time variable is θ: we know that

$$\eta = \log a(\theta) = \log\left[\frac{a_i}{\delta_i}\left[\frac{3(1+\delta_i)}{4}\right]^{\frac{2}{3}}\left[\theta + \theta_i - \sin(\theta+\theta_i)\right]^{\frac{2}{3}}\right], \tag{4.72}$$

therefore we can use

$$\frac{d\eta}{d\theta} = \frac{2}{3}\frac{1-\cos(\theta+\theta_i)}{\theta+\theta_i-\sin(\theta+\theta_i)} \tag{4.73}$$

to rewrite time derivatives with respect to η as

$$y' = \frac{d\theta}{d\eta}\frac{dy}{d\theta} = \left(\frac{d\eta}{d\theta}\right)^{-1}\dot{y}, \tag{4.74}$$

$$y'' = \frac{d\theta}{d\eta}\frac{d}{d\theta}\left[\left(\frac{d\eta}{d\theta}\right)^{-1}\dot{y}\right] = \left(\frac{d\eta}{d\theta}\right)^{-2}\left[\ddot{y} - \left(\frac{d\eta}{d\theta}\right)^{-1}\frac{d^2\eta}{d\theta^2}\dot{y}\right], \tag{4.75}$$

where

$$\frac{d^2\eta}{d\theta^2} = \frac{2}{3}\frac{\left[\theta+\theta_i-\sin(\theta+\theta_i)\right]\sin(\theta+\theta_i) - \left[1-\cos(\theta+\theta_i)\right]^2}{\left[\theta+\theta_i-\sin(\theta+\theta_i)\right]^2}. \tag{4.76}$$

Using the explicit expression of y_0 we found in GR, we can rearrange our equation as

$$\begin{aligned}[1-\cos(\theta+\theta_i)]\ddot{y} + \left[\frac{4}{3}\frac{[1-\cos(\theta+\theta_i)]^2}{\theta+\theta_i-\sin(\theta+\theta_i)} - \sin(\theta+\theta_i)\right]\dot{y} + \\ + y_0^3\left(y^{-3}-1\right)y = -\frac{18 a y_0^3 \beta_\alpha^2}{q\alpha^4 m_\alpha^2}\frac{\partial\alpha}{\partial x}.\end{aligned} \tag{4.77}$$

Now, in order to explicitly see modifications from GR, we decide to write y as $y_0 Y$, where y_0 will represent the bare GR contribution, while Y is purely due to MG. Since y_0 satifies equation 4.77 when the RHS is put to zero, then Y will satisfy

$$\begin{aligned}[1-\cos(\theta+\theta_i)]\ddot{Y} + \left[\frac{4}{3}\frac{[1-\cos(\theta+\theta_i)]^2}{\theta+\theta_i-\sin(\theta+\theta_i)} - \sin(\theta+\theta_i) + 2[1-\cos(\theta+\theta_i)]\frac{\dot{y}_0}{y_0}\right]\dot{Y} + \\ + \left(Y^{-3}-1\right)Y = -\frac{18 a y_0^2 \beta_\alpha^2}{q\alpha^4 m_\alpha^2}\frac{\partial\alpha}{\partial x},\end{aligned} \tag{4.78}$$

where we can immediately see that the RHS modulus is nothing else than the ratio between the fifth force and Newtonian gravity, evaluated on the edge shell, we found in 4.61. A small consistency check shows that, if the fifth force is turned off, this equation admits as solution $Y = 1$, obtaining in such a way $y = y_0$ and recovering GR. Of course, a smaller ratio will produce fewer deviations from GR. Assuming that we have the same initial conditions of the GR collapse, in general in these models the collapse will be shorter since we have an additional force, but there is also another way to see this fact: we can fix the duration of the collapse to the GR one, in order to last for the whole matter era, and we can change the initial overdensity value,

showing in this way that a smaller overdensity is required to collapse.
In order to fix initial conditions in the dilaton case, let's notice that in this framework Y is nothing less than the ratio of the overdensities in GR and MG, therefore, from the definition of y, $Y(0) = \frac{y_{MG}(0)}{y_0(0)} = \left(\frac{1+\delta_{i,GR}}{1+\delta_{i,MG}}\right)^{1/3}$. Then, since at the beginning of the collapse $\frac{F_\phi(x_M)}{F_N(x_M)} \ll 1$ as we showed in Figure 4.3, we want to impose that the evolution of y in MG is the same of GR, therefore

$$\dot{y}_{MG}(0) = \dot{y}_0(0)Y(0) + y_0(0)\dot{Y}(0) \simeq \dot{y}_0(0) \Longrightarrow \dot{Y}(0) = [1 - Y(0)]\,\frac{\dot{y}_0(0)}{y_0(0)}, \tag{4.79}$$

where $Y(0)$ will be chosen in such a way that the body collapses at the end of the matter era. From the value of $Y(0)$ we can derive the initial overdensity

$$\delta_{i,MG} = \frac{1 + \delta_{i,GR}}{Y^3(0)} - 1 \tag{4.80}$$

and we can extrapolate it at the virialization time, finding

$$\delta_{c,MG} = \frac{3}{5}\frac{1+z_i}{1+z_e}\delta_{i,MG}. \tag{4.81}$$

In Figure 4.7 we can see the solution of equation 4.78 for objects with different masses: as expected, for larger objects we find smaller deviations from GR, resulting in a necessary overdensity closer to the pure GR value. From the top-right panel, we can observe the important effect of the MG model: the critical overdensity is not anymore scale indipendent as in a Einstein-de Sitter or in a Λ-CDM Universe, but it depends from the mass of the considered body. This mass-dependent critical threshold curve tells us that for smaller bodies is easier to collapse and it can be used, as we will show in the next chapter, to determine how the number of virialized structure changes. Further, through a comparison with the reference paper result, we can notice that our range of values is plausible, even if our curve does not turn up towards the barrier at low masses, probably because we overestimate the size of the fifth force, as explained in the field profile section, resulting in a smaller initial overdensity. According to what we have shown for the dilaton case, we can deduce that our semi-analytical approximation for the field and the collapsing body produced sensible results and it is worthy of deeper numerical investigations.

For the symmetron the procedure is different, in fact until $\theta_\star$ the fifth force is zero because so it is the coupling to matter. After that it starts increasing from zero, therefore at $\theta_\star$ we have $Y(\theta_\star) = 1$ and $\dot{Y}(\theta_\star) = 0$. After this moment Y begins to drift away from 1, ending up at some $Y(\theta_c) < 1$. We can derive the new overdensity requiring that

$$y(\delta_{i,MG}, \theta_c) = y_0(\delta_{i,MG}, \theta_c)Y(\theta_c) = y_0(\delta_{i,GR}, \theta_c) \tag{4.82}$$

and solving this equation for $\delta_{i,MG}$, after that we can extrapolate its value to the virialization time as in 4.81. From what we have seen in Figure 4.6, in this case the fifth force is too intense to obtain meaningful results, therefore we will minimally modify the parameters of the model in order to show how the procedure works, in particular we will choose a new coupling to matter $\beta'_\star$ in such a way that the forces ratio, evaluated at the end of the collapse for the largest objects with mass $10^{15}h^{-1}M_\odot$, is equal in the symmetron and in the dilaton case. Since this is just a constant rescaling, it will reduce the fifth force in the same way in all the range mass but it will not affect the field profile, therefore the relative diffence between that ratio evaluated at the upper and at the lower bound in the mass range will

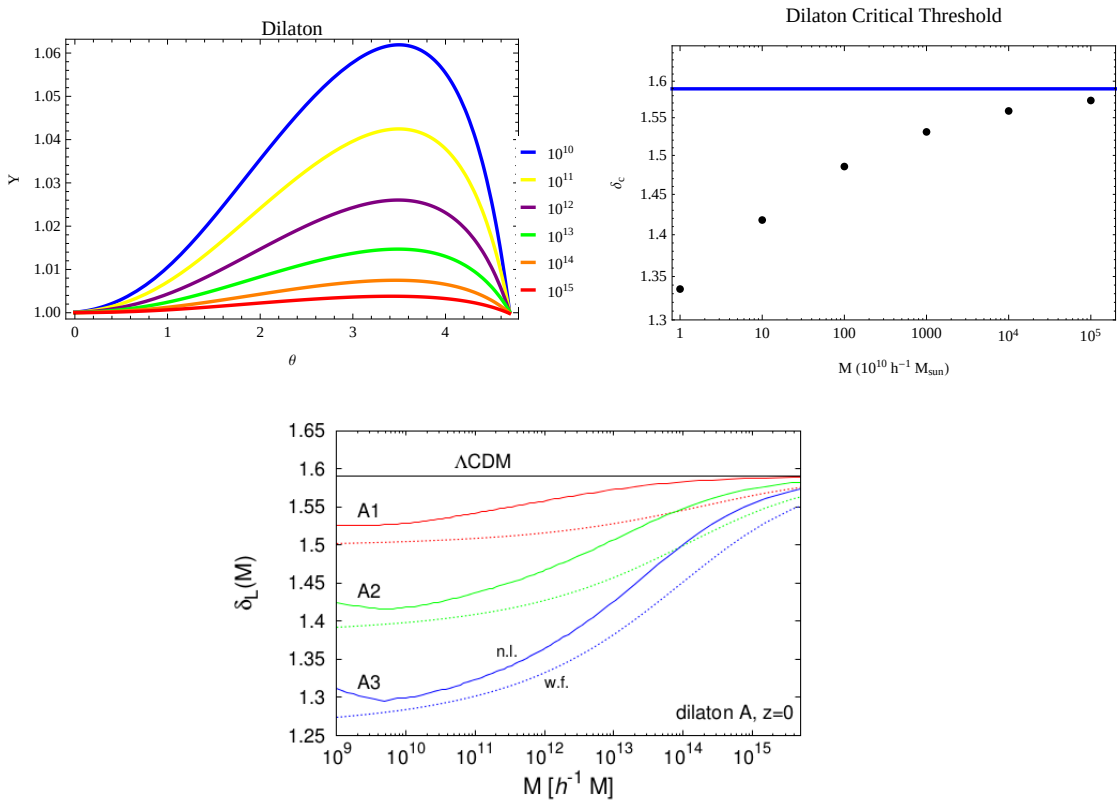

Figure 4.7: On the upper panel, sizes of modifications on overdensity evolution (top-left panel) and on critical threshold (top-right) from GR in the dilaton model. On the lower panel, the critical threshold obtained from numerical simulations. Our model parameters are the same of $A3$.

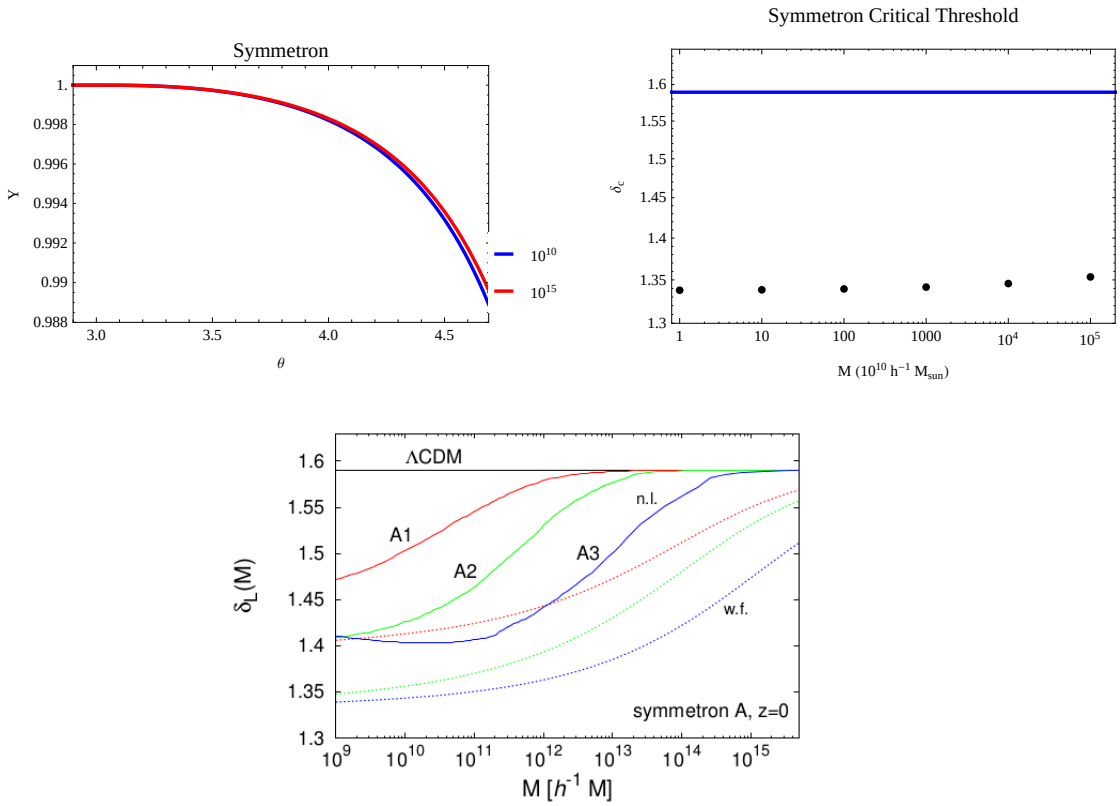

Figure 4.8: On the upper panel, sizes of modifications on overdensity evolution (top-left panel) and on critical threshold (top-right) from GR in the dilaton model. On the lower panel, the critical threshold obtained from numerical simulations. Our model parameters are the same of $A3$.

shrink, obtaining in such a way an almost constant (in the mass range) fifth force. This procedure wiil not alter the screening property and the forces ratio will remain close to the $2\beta^2$ curve. That's the reason for which we have such a tiny difference between high and low mass objects in Figure 4.8, while in numerical simulations we can see that their behaviour isn't similar. Nevertheless, also in this case we observe that the required overdensity has diminished, as in the dilaton case. In this case our approximation, which was potentially good as shown from the derivatives ratio, displays some limit: surely the substantially different collapsing time has produced remarkable effects and performing some complete numerical simulations in the same conditions should clarify where problems arise and, maybe, how we can fix them.

Chapter 5

Excursion Set Theory

The aim of this chapter is to investigate the influence of the additional fifth force (which affects, as we saw in the previous chapter, the initial overdensity necessary to collapse) on the formation of gravitationaly bound structures, called haloes; we will focus in particular on their abundance, although the method we will introduce can be used also to estimate other haloes properties, such as the accretion rate, the survival time or the merger history. We know that these haloes are composed mainly by DM, but since we considered an identical coupling between DE and every kind of matter (dark or not), we do not have to worry about doing any distinction; in fact, from a gravitational point of view, they will show the same behaviour.
In order to do so, we will use the Excursion Set Theory (EST), an analytical framework relating the statistics of haloes to fluctuations of the density field in primordial times, which is based on the assumptions that these objects grew from small amplitude fluctuations because of gravitational instability and that their sites correspond to regions, called excursion sets, where the density field, smoothed on a suitable scale, exceeds some critical value, called threshold or barrier.
Since a rigorous study of large scale structures formation can be performed only through N-body simulations, which are computationally expensive even in the Λ-CDM model, this method can provide some insight on this topic because it produces results which we can directy compare to experimental data, despite all the approximation we have to make. This will result in a great advantage in the study of MG effects, in fact, through such comparison, we will eventually be able in the future to constrain the parameter space of MG models, which is bigger and less known than the standard cosmological model one.

5.1 Notation

First of all, we have to introduce some fundamental quantities of the theory, such as the background density $\bar{\rho}$ and the density contrast

$$\delta(\mathbf{x}) = \frac{\rho(\mathbf{x})}{\bar{\rho}} - 1, \tag{5.1}$$

which will allow us to study fluctuations in the density field $\rho = \bar{\rho}(1+\delta)$. Its Fourier transform is given by

$$\delta(\mathbf{x}) = \int \frac{d^3k}{(2\pi)^3} \hat{\delta}(\mathbf{k}) e^{-i\mathbf{k}\cdot\mathbf{x}}. \tag{5.2}$$

and since it is a real field, Fourier coefficients obey $\hat{\delta}^*(\mathbf{k}) = \hat{\delta}(-\mathbf{k})$. In the standard framework, this field is set during the inflationary era and is assumed to be

a statistically homogeneous and isotropic Gaussian random field. Because of this assumption, the power spectrum, which is nothing else than the Fourier transform of the two-point function and tells us which are the relevant modes, is given by

$$\langle\hat{\delta}(\mathbf{k})\hat{\delta}^*(\mathbf{p})\rangle = \langle\hat{\delta}(\mathbf{k})\hat{\delta}(-\mathbf{p})\rangle = (2\pi)^3 P(\mathbf{k})\delta^{(3)}(\mathbf{k}-\mathbf{p}), \tag{5.3}$$

where $P(\mathbf{k}) = P(k)$ because of isotropy. Now, using 5.3, we can prove the previous statement, in fact

$$\begin{aligned}\xi(\mathbf{r}) &= \langle\delta(\mathbf{x})\delta(\mathbf{x}+\mathbf{r})\rangle = \\ &= \int \frac{d^3k}{(2\pi)^3}\frac{d^3p}{(2\pi)^3} e^{-i\mathbf{k}\cdot\mathbf{x}} e^{-i\mathbf{p}\cdot(\mathbf{x}+\mathbf{r})}\langle\hat{\delta}(\mathbf{k})\hat{\delta}(\mathbf{p})\rangle = \\ &= \int \frac{d^3k}{(2\pi)^3} P(k) e^{i\mathbf{k}\cdot\mathbf{r}} = \\ &= \int \frac{d^3k}{(2\pi)^3} P(k) e^{-i\mathbf{k}\cdot\mathbf{r}},\end{aligned} \tag{5.4}$$

where in the last passage we sent $\mathbf{k} \to -\mathbf{k}$.
Since LSS evolved hierarchically, i.e. small haloes formed earlier than bigger ones and in a second step they merged together in order to form larger structures, and present structures on all scales we would like to analyze in detail different ranges of masses. In order to do so, it is quite natural to pass from the raw density field we defined in 5.1 to a smoothed one through a convolution with some window (or filter) function W, which weights the density field inside some region with characteristic scale R. In practice, from now on, we will consider the smoothed density contrast field

$$\delta(\mathbf{x}, R) = \int d^3y \delta(\mathbf{y}) W(\mathbf{x}-\mathbf{y}, R) = \int \frac{d^3k}{(2\pi)^3}\hat{\delta}(\mathbf{k})\hat{W}(\mathbf{k}, R)e^{-i\mathbf{k}\cdot\mathbf{x}}. \tag{5.5}$$

This window function is usually normalized to 1, therefore we can rewrite it as

$$1 = \int d^3y W(\mathbf{x}-\mathbf{y}, R) = \frac{1}{V_W}\int d^3y W'(\mathbf{x}-\mathbf{y}, R), \tag{5.6}$$

where W' is the dimensionless window function and V_W is the window volume with whom we can associate to the smoothed region the mass $M = \bar{\rho}(1+\delta)V_W$. The root mean-squared fluctuation of the density (and therefore of the mass) in the window reads as

$$S(R) = \sigma^2(R) = \langle\delta^2(\mathbf{x}, R)\rangle = \int \frac{d^3k}{(2\pi)^3} P(k)\hat{W}^2(\mathbf{k}, R). \tag{5.7}$$

Let's notice that the mass M, the smoothing scale R and the variance S can be used equivalently to measure the same perturbation, in fact $M(R)$ monotonically increases with R (obvious: bigger regions will be more massive) and, under quite general conditions, for example that $\hat{W}$ is a monotonically decreasing function of R, $S(R)$ monotonically decreases with R. In hierachical models, S increases starting at very large scale from 0 because of our assumption on the statistics of the initial density field; as soon as scale starts decreasing, we begin to observe bigger fluctuations in the density: this will imply, as we will see in the next section, that it will be easier for small haloes to collapse. Then, these small structures will accrete material and merge together in order to form bigger haloes.
Finally, let's remark that the window function is not given *a priori*, but depends on choices we make.

5.2 Haloes Number in GR

The first attempt to find some relation for the number of virialized structure was made by Press and Schechter [20]. In their article, they developed a model where the collapse of an overdense region of size R, which encloses a mass M determined by the smoothing window choice, occurs when the smoothed density reaches some critical threshold δ_c at some redshift z: in the previous chapter the value for δ_c was given by the extrapolation of initial overdensity to the moment of virialization, but other choices can be made, for example a common choice is to pick the redshift value when the physical radius of our object completely collapses to zero; moreover we saw that this quantity was constant in GR while it is an increasing function of the mass in MG. Clearly, if that value is exceeded, the object collapses earlier. They also assumed that objects collapse on small scale without that non-linearities influence the collapse of larger scale objects: this fact holds when the additional large scale power generated by those non-linearities are small compared to primordial fluctuation in the power spectrum; this assumption simplifies the problem, allowing us to consider different scales behaviour as indipendent from larger or smaller scales.
Since the smoothed field $\delta(\mathbf{x}, R)$ is a Gaussian random variable due to the previous assumptions, its probability distribution reads as

$$P(\delta; R) = \frac{1}{\sqrt{2\pi S(R)}} e^{-\frac{\delta^2}{2S(R)}} \tag{5.8}$$

and the cumulative probability $F(M)$ for a region to have a smoothed density above the threshold reads as

$$F(M) = 1 - C(M) = 1 - \int_{-\infty}^{\delta_c} d\delta P(\delta; R) = \frac{1}{2}\text{erfc}\left[\frac{\nu}{\sqrt{2}}\right], \tag{5.9}$$

where $C(M)$ it's the complementary probability to not reach the barrier and $\nu = \frac{\delta_c}{\sigma(M)}$ is the height of the threshold in standard deviation units. This cumulative probability physically represents the probability that the volume associated to the mass M is already gravitationally bound or, equivalently, the fraction of gravitationally bound volumes, so the number of virialized haloes with mass between M and $M + dM$ will read as

$$\frac{dn}{dM} dM = \frac{\bar{\rho}}{M} \left|\frac{dF}{dM}\right| dM. \tag{5.10}$$

In hierarchical models, where $\sigma(R) \to \infty$ when $R \to 0$, we would expect that all the mass stays in some collapsed object, i.e. $F(R = 0) = 1$: here arises the problem in this approch, because, as we can read from equation 5.9, $F(0) = \frac{1}{2}$. Press and Schechter were conscious about this problem and identified its origin in a counting problem of underdense regions: these patches were not counted even if they are inside some bigger overdense region, which surely would have collapsed.
The solution of this "cloud-in-cloud"problem was found by Bond, Cole, Efstathiou and Kaiser [1]: in their approach they fixed the spatial position $\mathbf{x}$ (which won't appear anymore in the argument of the smoothed density field) and varied the smoothing scale, starting from very large values of R, analyzing how the field $\delta(R)$ behaves and searching for the biggest scale such that the critical threshold is reached. In this approach, instead of considering spatial averages of one realization of the initial density field, they consider averages over different realizations at a fixed position. Keeping the same assumptions on the primordial density field, when $R \to \infty$, $\delta(R) \to 0$ and $\sigma(R) \ll \delta_c$, therefore the probability that such large region collapses

is absolutely negligible; however, once R decreases, $\sigma(R)$ will increase, as well as the probability to reach the critical value, until when it becomes significant: due to this reason, in the following part we will try to determine the probability to have a first upcrossing at some scale S.
Let's imagine to start at some small S_0, corresponding to some big R_0, when the overdensity value is δ_0; once we slightly change the smoothing scale into $R_0 - \Delta R$, the variance increases to $S_0 + \Delta S$ and the overdensity changes in $\delta_0 + \Delta\delta$, where $\Delta\delta$ is given by a distribution probability that in general may depend from the starting point (S_0, δ_0) and from the size of ΔS. If we choose a k-space top-hat filter $\hat{W}(\mathbf{k}, R) = \Theta(1 - kR)$ (where Θ is the Heaviside function) the change in the smoothing scale corresponds to the inclusion of a set indipendent modes, uncorrelated from those previously included, therefore, for a fixed ΔS, the probability distribution of $\Delta\delta$ is Gaussian and reads as

$$\Psi(\Delta\delta; \Delta S) = \frac{1}{\sqrt{2\pi\Delta S}} e^{-\frac{(\Delta\delta)^2}{2\Delta S}}, \tag{5.11}$$

such that the mean and the variance are given by

$$\langle \Delta\delta \rangle = \int d(\Delta\delta)\Psi(\Delta\delta; \Delta S)(\Delta\delta) = 0 \tag{5.12}$$

$$\left\langle (\Delta\delta)^2 \right\rangle = \int d(\Delta\delta)\Psi(\Delta\delta; \Delta S)(\Delta\delta)^2 = \Delta S, \tag{5.13}$$

indipendently from the starting point. Because of this Markov property, considering a whole series of ΔS consecutive increments, the value of $\delta(S)$ executes a Brownian motion and the probability to reach some value δ when the scale changes from S to $S + \Delta S$ evolves according to the Chapmann-Kolmogorov (CK) equation

$$P(\delta, S + \Delta S) = \int d(\Delta\delta)\Psi(\Delta\delta; \Delta S)P(\delta - \Delta\delta, S). \tag{5.14}$$

Without the Markov property guaranteed by our filter choice, we could not have written this last equation, because we should have considered the whole history of our trajectory: the choice of this filter is due to the fact that it allows us to carry on analytically the calculation, despite the fact that it has not a well defined associated volume V_W. Expanding 5.14 around $P(\delta, S)$ and taking the limit $\Delta S \to 0$, we find that $P(\delta, S)$ evolves according to the diffusion equation

$$\frac{\partial P}{\partial S} = \frac{1}{2}\frac{\partial^2 P}{\partial \delta^2}. \tag{5.15}$$

This result is exact because every odd moment $\left\langle (\Delta\delta)^{2n+1} \right\rangle$ is zero while every even moment $\left\langle (\Delta\delta)^{2n} \right\rangle$ is proportional to some positive, integer power of ΔS. We want to find a solution to 5.15 (the general form of the solution is well known) such that it satisfies the general initial condition

$$P(\delta, S_0) = \delta^{(1)}(\delta - \delta_0) \tag{5.16}$$

and two specific boundary condition: the first one is that P has to be finite when $\delta \to -\infty$ (rigourously speaking, we should have $\delta > -1$, otherwise the density would be negative, but neglecting this fact we can carry on calculations and still obtain meaningful results); the second one is $P(\delta_c, S) = 0$: since we are interested only in the first upcrossing of the barrier, we have to remove from our counting each trajectory that has already reached the critical threshold. This can be done by

putting an absorbing barrier at $\delta = \delta_c$ and Chandrasekhar [11] noticed that, since every path that reaches δ_c has the same probability to go upward or downward due to the $\Delta\delta$ distribution, our condition could be imposed through the images method, subtracting the contribution of another source put at $2\delta_c - \delta_0$. The complete solution reads as

$$P(\delta, S; \delta_0, S_0) = \frac{1}{\sqrt{2\pi(S - S_0)}} \left[e^{-\frac{(\delta-\delta_0)^2}{2(S-S_0)}} - e^{-\frac{(2\delta_c-\delta_0-\delta)^2}{2(S-S_0)}} \right], \tag{5.17}$$

therefore $F(M)$ reads as

$$F(M) = 1 - \int_{-\infty}^{\delta_c} d\delta P(\delta, S; \delta_0, S_0) = \text{erfc}\left[\frac{\delta - \delta_0}{2(S - S_0)} \right], \tag{5.18}$$

without the prefactor $\frac{1}{2}$, solving the Press-Schechter problem. Now we are able to calculate the first upcrossing probability

$$\begin{aligned} \mathcal{F}(S)dS = \frac{dF}{dS}dS = -\left(\int_{-\infty}^{\delta_c} d\delta \frac{dP}{dS} \right) dS = \\ = -\frac{1}{2}\left(\int_{-\infty}^{\delta_c} d\delta \frac{d^2P}{d\delta^2} \right) dS = -\frac{1}{2}\left. \frac{dP}{d\delta} \right|_{\delta_c} dS = \\ = \frac{\delta_c - \delta_0}{\sqrt{2\pi(S - S_0)^3}} e^{-\frac{(\delta_c-\delta_0)^2}{2(S-S_0)}}, \end{aligned} \tag{5.19}$$

so, setting the starting point to $(S_0, \delta_0) = (0, 0)$, the number of virialized haloes will read as

$$\frac{dn}{dM}dM = \frac{\bar{\rho}}{M}\frac{dF}{dS}\left|\frac{dS}{dM}\right| dM = \sqrt{\frac{2}{\pi}}\frac{\bar{\rho}}{M^2}\left|\frac{d\log\sigma}{d\log M}\right| \nu e^{-\frac{\nu^2}{2}} dM = \frac{\bar{\rho}}{M^2}\left|\frac{d\log\sigma}{d\log M}\right| \nu f(\nu) dM. \tag{5.20}$$

Comparing this result to full N-body simulations (see e.g. Figure 3 in [29]), we can see that we have obtained a surprisingly good approximation, although this formula overestimates the number of small haloes and underestimates the number of big haloes. In this framework, several authors have analytically modified the $\nu f(\nu)$ expression in order to obtain even a better accuracy (see e.g. [23],[16]).

5.3 Haloes Number in MG

We are now ready to discuss how the smoothing scale dependent threshold $\delta_c(S)$, which we will call moving barrier, influences the number of virialized objects in a MG scenario. This section is organized as follows: first of all we will completely state the problem and, since it is too difficult to solve it directly, we will transform it into an equivalent one; then we will solve this new problem with the standard Quantum Mechanics path integral formalism and finally we will discuss about how to impose the boundary conditions, which will give us the correct solution from which we would be able to calculate the number of haloes.

5.3.1 Statement of the Problem

In order to carry on the calculations analytically, we choose a top-hat filter in the momenta space, so that we will have uncorrelated steps and the transition probability, for a fixed variation in the smoothing scale ΔS, has the zero mean gaussian distribution

$$\Psi_1(\Delta\delta'; \Delta S) = \frac{1}{\sqrt{2\pi\Delta S}} e^{-\frac{(\Delta\delta')^2}{2\Delta S}}. \tag{5.21}$$

The CK equation tells us that the probability to reach a certain height δ, once the smoothing scale has changed by ΔS, is given by

$$P_1(\delta, S + \Delta S) = \int d(\Delta\delta')\Psi_1(\Delta\delta'; \Delta S)P_1(\delta - \Delta\delta', S) \tag{5.22}$$

As before, we expand both member of this last equation around $P_1(\delta, S)$ and we take the $\Delta S \to 0$ limit, obtaining that the probability P_1 has to satisfy the diffusion equation

$$\frac{\partial P_1}{\partial S} = \frac{1}{2}\frac{\partial^2 P_1}{\partial \delta^2} \tag{5.23}$$

with the same initial condition decided before

$$P_1(\delta, S_0) = \delta^{(1)}(\delta - \delta_0) \tag{5.24}$$

but also with the different boundary condition

$$P_1(\delta_c(S), S) = 0, \ \forall S. \tag{5.25}$$

Since the shape of the barrier is not given *a priori* but it depends from specific model parameters, imposing this condition will be the main problem to overcome.
To solve this issue we have to notice (and we will prove it in a second moment) that our problem is equivalent to the one where the barrier is fixed at the GR value $\delta_c(S = 0) = \delta_c$, which we have to recover at large scales, and steps are still uncorrelated but their distribution has a smoothing scale dependent mean $-\Delta\delta_c(S) \equiv -\Delta\delta_c$. Physically speaking, we can justify this idea in the following way: a moving barrier introduces some preferred direction, in fact it will be easier (harder) to cross it if it's a decreasing (increasing) function of S; so, in order to replicate this kind of behaviour when the barrier is constant, we have to set the mean to $-\Delta\delta_c$. This idea arises from some sort of equivalence principle: since the step size does not depend from the height (i.e. the density contrast δ) because of our filter choice, we cannot decide if the barrier is coming towards us at a given rate or we are going towards the barrier with the opposite rate. Said in a different way, the behaviour of the relative distance between us and the barrier is the same in both cases.
In this new second case, the transition probability will be

$$\Psi_2(\Delta\delta; S, \Delta S) = \frac{1}{\sqrt{2\pi\Delta S}} e^{-\frac{(\Delta\delta + \Delta\delta_c)^2}{2\Delta S}} \tag{5.26}$$

and the new CK equation will read as

$$P_2(\delta, S + \Delta S) = \int d(\Delta\delta)\Psi_2(\Delta\delta; S, \Delta S)P_2(\delta - \Delta\delta, S). \tag{5.27}$$

Following the same procedure, we find out that P_2 has to obey the modified diffusion equation

$$\frac{\partial P_2}{\partial S} = h(S)\frac{\partial P_2}{\partial \delta} + \frac{1}{2}\frac{\partial^2 P_2}{\partial \delta^2}, \qquad h(S) = \frac{d\delta_c(S)}{dS}, \tag{5.28}$$

where a new drift term appeared, and has to satisty the new and easier boundary condition

$$P_2(\delta_c, S) = 0, \ \forall S. \tag{5.29}$$

Finally we show that, only on the base of the relative distance $\gamma = \delta - \delta_c(S)$ between a point and the barrier, we can not say in which case we are. Let's consider the case in which the barrier is constant ($\delta_c(S) = \delta_c(S + \Delta S) = \delta_c$) and the transition

probability is given by a gaussian distribution with a $g(S, \Delta S) \neq 0$ mean and ΔS variance. The CK equation reads as

$$\begin{aligned} P(\gamma, S + \Delta S) &= P(\delta - \delta_c(S + \Delta S), S + \Delta S) = \\ &= \int d(\Delta\delta)\Psi(\Delta\delta; S, \Delta S)P(\delta - \delta_c(S + \Delta S) - \Delta\delta, S) = \\ &= \int d(\Delta\delta)\frac{e^{-\frac{[\Delta\delta - g(S,\Delta S)]^2}{2\Delta S}}}{\sqrt{2\pi\Delta S}}P(\delta - \delta_c(S + \Delta S) - \Delta\delta, S). \end{aligned} \tag{5.30}$$

Changing variable to $\Delta\delta' = \Delta\delta - g(S, \Delta S)$ equation 5.30 becomes

$$\begin{aligned} &\int d(\Delta\delta')\frac{e^{-\frac{(\Delta\delta')^2}{2\Delta S}}}{\sqrt{2\pi\Delta S}}P(\delta - \delta_c(S + \Delta S) - g(S, \Delta S) - \Delta\delta', S) = \\ &= \int d(\Delta\delta')\frac{e^{-\frac{(\Delta\delta')^2}{2\Delta S}}}{\sqrt{2\pi\Delta S}}P(\delta - \delta_c(S) - \Delta\delta', S) = \\ &= \int d(\Delta\delta')\Psi'(\Delta\delta'; \Delta S)P(\delta - \delta_c(S) - \Delta\delta', S) \end{aligned} \tag{5.31}$$

where we have defined $\delta_c(S) = \delta_c(S + \Delta S) + g(S, \Delta S) \neq \delta_c(S + \Delta S)$. If we indicate with $\langle\rangle$ ($\langle\rangle'$) averages with respect to the Ψ (Ψ') probability density function, then we have passed from a situation in which

$$\langle\Delta\delta\rangle = g(S, \Delta S); \quad \left\langle(\Delta\delta)^2\right\rangle = \Delta S \tag{5.32}$$

to a situation in which

$$\left\langle\Delta\delta'\right\rangle' = 0; \quad \left\langle(\Delta\delta')^2\right\rangle' = \Delta S \tag{5.33}$$

as we wanted to. Since the two situations are identical ($P(\gamma, S + \Delta S)$ is the same!) we can choose to work in the case we prefer.

5.3.2 Path Integral Formalism

Because of our last consideration, we choose to search for a solution of equation 5.28 using the path integral formalism in QM.
First of all we have to transform our diffusion equation in a Schrödinger equation, where the smoothing scale S will play the role of time and the overdensity δ will be the spatial position, so, from now on, we will use the change of variable $S = t$ and $\delta = x$; moreover we will set $\hbar = 1$ and use the standard definition of the momentum operator $\hat{P} = -i\partial_x$. Then we have to introduce states and wavefunctions: the probability to be in a position x at time t will be given by

$$P(x, t) = \psi(x, t) = \langle x|\psi(t)\rangle \tag{5.34}$$

so, according to our initial condition 5.24,

$$P(x, t_0) = \langle x|\psi(t_0)\rangle = \langle x|x_0\rangle = \delta^{(1)}(x - x_0). \tag{5.35}$$

Equation 5.28 (up to a contraction with the bra $\langle x|$) now becomes

$$\frac{\partial\left|\psi(t)\right\rangle}{\partial t} = \left[-\frac{\hat{P}^2}{2} + ih(t)\hat{P}\right]\left|\psi(t)\right\rangle. \tag{5.36}$$

In the end, we introduce the Euclidean time $\tau = -it$ and in this way we are able to recover the proper Schrödinger equation

$$i\frac{\partial |\psi(\tau)\rangle}{\partial \tau} = \left[\frac{\hat{P}^2}{2} - h(\tau)\hat{P}\right]|\psi(\tau)\rangle = H(\hat{P},\tau)\,|\psi(\tau)\rangle\,, \tag{5.37}$$

where $H(\hat{P},\tau)$ is a time dependent hamiltonian and $h(\tau) = \frac{\partial \delta_c(\tau)}{\partial \tau}$. Starting from 5.37 we can construct the time evolution operator

$$U(\tau,\tau_0) = \exp\left[-i\int_{\tau_0}^{\tau} d\tau' H(\hat{P},\tau')\right] = e^{-i\left[\frac{\hat{P}^2}{2}(\tau-\tau_0)-\hat{P}((\delta_c(\tau)-\delta_c(\tau_0))\right]}, \tag{5.38}$$

where we did not need to consider any kind of chronological product because the operator $\hat{P}$ does not act on the function $h'(\tau)$, making the commutator $[h'(\tau_1)\hat{P}, h'(\tau_2)\hat{P}]$ identically zero. Let's also remind the important property of the time evolution operator

$$U(\tau,\tau_0) = U(\tau,\tau_1)U(\tau_1,\tau_0) \tag{5.39}$$

which will be useful in the following part.
Finally, we are ready to build the probability to be at (x,t) given that we started at (x_0,t_0): considering a generic state $|\psi'\rangle$ and the evolution of the initial state $|\psi\rangle = U(\tau,\tau_0)\,|\psi_0\rangle$, their transition amplitude reads as

$$\begin{aligned}&\left\langle\psi'\right| U(\tau,\tau_0)\,|\psi_0\rangle = \int dx d\tilde{x}\,\langle\psi'|x\rangle\,\langle x|\,U(\tau,\tau_0)\,|\tilde{x}\rangle\,\langle\tilde{x}|\psi_0\rangle = \\ &= \int dx d\tilde{x}\psi'^*(x,\tau)\psi_0(\tilde{x},\tau_0)K(x,\tau,\tilde{x},\tau_0) = \int dx\psi'^*(x,\tau)K(x,\tau,x_0,\tau_0),\end{aligned} \tag{5.40}$$

where we have introduced two completeness relations in the position and K is the kernel, i.e. the matrix element of U in the position representation. From the last member we can identify

$$K(x,t;x_0,t) = P(x,t;x_0,t_0) = P(\delta,S;\delta_0,S_0) \tag{5.41}$$

and it immediately follows from 5.39 that $\forall\tau_1 : \tau_0 < \tau_1 < \tau$

$$K(x,\tau;x_0,\tau_0) = \int dx_1 K(x,\tau;x_1,\tau_1)K(x_1,\tau_1;x_0,\tau_0). \tag{5.42}$$

On the base of this last property, we can divide our time interval in N smaller intervals where

$$\tau_0 < \tau_1 < ... < \tau_{N-1} < \tau_N = \tau, \quad \tau_{j+1} - \tau_j = \frac{\tau-\tau_0}{N} = \epsilon, \tag{5.43}$$

in order to rewrite

$$K(x,\tau;x_0,\tau_0) = \int dx_1...dx_{N-1}\prod_{j=0}^{N-1} K(x_{j+1},\tau_{j+1};x_j,\tau_j) \tag{5.44}$$

Then we can evaluate, using a completeness relation in the momenta and the integral representation of the Dirac delta,

$$\begin{aligned}
K(x_{j+1},\tau_{j+1};x_j,\tau_j) &= \langle x_{j+1}|\, U(\tau_{j+1},\tau_j)\,|x_j\rangle = \\
&= \langle x_{j+1}|\, e^{-i\left[\frac{\hat{P}^2}{2}(\tau_{j+1}-\tau_j)-\hat{P}((\delta_c(\tau_{j+1})-\delta_c(\tau_j))\right]}\,|x_j\rangle = \\
&= \int dp_j\, \langle x_{j+1}|\, e^{-i\left[\frac{\hat{P}^2}{2}(\tau_{j+1}-\tau_j)-\hat{P}((\delta_c(\tau_{j+1})-\delta_c(\tau_j))\right]}\,|p_j\rangle\,\langle p_j|x_j\rangle = \\
&= \int \frac{dp_j}{2\pi} e^{-i\left[\frac{p_j^2}{2}(\tau_{j+1}-\tau_j)-p_j((\delta_c(\tau_{j+1})-\delta_c(\tau_j))\right]} e^{ip_j(x_{j+1}-x_j)} = \\
&= \frac{1}{\sqrt{2\pi i\epsilon}} \exp\left[\frac{i\epsilon}{2}\left(\frac{x_{j+1}-x_j}{\epsilon}+\frac{\delta_c(\tau_j+\epsilon)-\delta_c(\tau_j)}{\epsilon}\right)^2\right]
\end{aligned} \tag{5.45}$$

In the $\epsilon \to 0$ (or equivalently $N \to \infty$) limit, the last terms reduces to

$$\frac{1}{\sqrt{2\pi i\epsilon}} \exp\left[\frac{i\epsilon}{2}\left(x'_j+h(\tau_j)\right)^2\right] = \frac{1}{\sqrt{2\pi i\epsilon}} \exp\left[i\epsilon L(x'_j,\tau_j)\right] \tag{5.46}$$

so that we can calculate

$$\begin{aligned}
K(x,\tau;x_0,\tau_0) &= \lim_{N\to\infty}\left(\frac{1}{2\pi i\epsilon}\right)^{\frac{N}{2}} \int dx_1 ... dx_{N-1} \prod_{j=0}^{N-1} e^{i\epsilon L(x'_j,\tau_j)} = \\
&= \lim_{N\to\infty}\left(\frac{1}{2\pi i\epsilon}\right)^{\frac{N}{2}} \int dx_1 ... dx_{N-1} e^{i\epsilon\sum_{j=0}^{N-1} L(x'_j,\tau_j)} = \\
&= \int_{x(\tau_0)=x_0}^{x(\tau)=x} Dx(\tau^*) e^{i\int_{\tau_0}^{\tau} d\tau^* L(x'(\tau^*),\tau^*)},
\end{aligned} \tag{5.47}$$

where the lagrangian reads as

$$L(x'(\tau^*),\tau^*) = \frac{1}{2}\left[x'(\tau^*)+h(\tau^*)\right]^2. \tag{5.48}$$

Since our action is quadratic, we can exactly expand it around the "classical" path $x_c(\tau)$ given by Eulero-Lagrange equation

$$0 = \frac{d}{d\tau^*}\frac{\partial L}{\partial x'(\tau^*)} = \frac{d}{d\tau^*}\left(x'(\tau^*)+h(\tau^*)\right) \tag{5.49}$$

which has solution

$$x'_c(\tau^*)+h(\tau^*) = c, \tag{5.50}$$

where c is a constant. Imposing that $x_c(\tau_0) = x_0$ we find

$$x_c(\tau^*) - x_0 = c(\tau^*-\tau_0) + \delta_c(\tau_0) - \delta_c(\tau^*) \tag{5.51}$$

and imposing $x_c(\tau) = x$ we are able to fix

$$c = \frac{x-x_0}{\tau-\tau_0} + \frac{\delta_c(\tau)-\delta_c(\tau_0)}{\tau-\tau_0}. \tag{5.52}$$

Taking a small variation around the classical path $x(\tau^*) = x_c(\tau^*) + \delta x(\tau^*)$ which vanishes at borders, i.e. $\delta x(\tau_0) = \delta x(\tau) = 0$, our Lagrangian becomes

$$L(x'(\tau^*),\tau^*) = \frac{1}{2}c^2 + c\delta x'(\tau^*) + \frac{1}{2}(\delta x'(\tau^*))^2 \tag{5.53}$$

and the kernel reads as

$$K(x,\tau;x_0,\tau_0) = e^{\frac{ic^2(\tau-\tau_0)}{2}} \int_{\delta x(\tau_0)=0}^{\delta x(\tau)=0} D\delta x(\tau^*) e^{\frac{i}{2}\int_{\tau_0}^{\tau} d\tau^*(\delta x')^2} = \frac{1}{\sqrt{2\pi i(\tau-\tau_0)}} e^{\frac{ic^2(\tau-\tau_0)}{2}} \tag{5.54}$$

5.3.3 Complete Solution

Now we can go back to old variables and obtain

$$P_2(\delta, S; \delta_0, S_0) = \frac{1}{\sqrt{2\pi(S - S_0)}} \exp\left[-\frac{[\delta - \delta_0 + \delta_c(S) - \delta_c(S_0)]^2}{2(S - S_0)}\right]. \tag{5.55}$$

As for the constant barrier case, we want to obtain the complete solution

$$P_2(\delta, S; \delta_0, S_0) - P_2'(\delta, S; \delta_0', S_0), \tag{5.56}$$

which obeys to equation 5.28 and has the right boundary condition given by 5.29, adapting the images method we have already seen. While in the previous case this could be easily done because the probability to go upward or downward, once the barrier was reached, was the same, this time the situation isn't anymore symmetric due to the scale-dependent non-zero mean (or, in the alternative picture, because of the moving barrier).
Starting from numerical simulations (which use the first picture, see e.g. [18],[4]), we have noticed that barriers of physical interest do not diverge, i.e.

$$\delta_c(S = 0) - \delta_c(\bar{S}), \tag{5.57}$$

where $\bar{S}$ is the variance associated to the lower bound in the mass range we considered in the previous chapter, is some finite and actually not too big quantity: we can extend this result to the $\bar{S} \to \infty$ limit because, even considering the worst scenario, the barrier has a lower bound, 0, which can not be reached. In fact, if at some scale the overdensity required for the collapse would be zero, then we would be in a situation where arbitrary patches of the homogeneous and isotropic background decide to collapse on their own! Our situation is similar to a Brownian motion in one dimension with an absorbing barrier, therefore we can state that every path, sooner or later, will hit the barrier: due to this reason we can divide the set of all path according to the first crossing time T, being certain to do not forget any path. Considering one of such families, i.e. fixing T, and arbitrary choosing that the "image"path will start at $\delta_0' = 2\delta_c - \delta_0$ as in the constant barrier case, we find that

$$P_T(\delta, S; \delta_0, S_0) = \frac{1}{\sqrt{2\pi(S - S_0)}} \left[e^{-\frac{[\delta - \delta_0 + \delta_c(S) - \delta_c(S_0)]^2}{2(S - S_0)}} - e^{-\frac{[\delta + \delta_0 - 2\delta_c + \delta_c(S) - \delta_c(S_0)]^2}{2(S - S_0)}} f(T)\right], \tag{5.58}$$

where we have defined

$$f(T) = e^{-2(\delta_c - \delta_0)\frac{\delta_c(T) - \delta_c(S_0)}{T - S_0}} \tag{5.59}$$

in such a way that $P_T(\delta_c, T; \delta_0, S_0) = 0$. Let's remark that 5.58 satisfies our differential equation and both our boundary and initial condition. Then, in order to find the complete probability, we need some "weight"function $\mu(T)$ which gives the probability of each crossing time and such that $\int_{S_0}^{+\infty} dT\mu(T) = 1$ because, as already explained, each path hits the barrier. In the end, we obtain

$$\begin{aligned} P(\delta, S; \delta_0, S_0) &= \int_{S_0}^{+\infty} dT\mu(T) P_T(\delta, S; \delta_0, S_0) = \\ &= \frac{1}{\sqrt{2\pi(S - S_0)}} \left[e^{-\frac{[\delta - \delta_0 + \delta_c(S) - \delta_c(S_0)]^2}{2(S - S_0)}} - e^{-\frac{[\delta + \delta_0 - 2\delta_c + \delta_c(S) - \delta_c(S_0)]^2}{2(S - S_0)}} \int_{S_0}^{+\infty} dT\mu(T) f(T)\right]. \end{aligned} \tag{5.60}$$

Moreover (this will be crucial in the following calculation), because of our crossing time division and since we can say that every path that crosses the barrier "disappears"because of the subtraction, by definition we have

$$P(\delta, S)|_{\delta_c} := P_S(\delta_c, S)|_{\delta_c} = 0; \quad \left.\frac{d^n P}{d\delta^n}\right|_{\delta_c} := \left.\frac{d^n P_S}{d\delta^n}\right|_{\delta_c}, \tag{5.61}$$

in fact every time we decide to evaluate P at the threshold value we are implicitly selecting a specific crossing time. Now let's check that we can recover, at least, the two known analytic result.

Example (Constant Barrier Case)**.** In this case $\delta_c(S) = \delta_c \ \forall S$, so $f(T) = 1$ and we have

$$P(\delta, S; \delta_0, S_0) = \frac{1}{\sqrt{2\pi(S - S_0)}} \left[e^{-\frac{(\delta-\delta_0)^2}{2(S-S_0)}} - e^{-\frac{(\delta+\delta_0-2\delta_c)^2}{2(S-S_0)}} \right] \tag{5.62}$$

as we know. The rest follows automatically as explained in the previous section.

Example (Linear Barrier Case)**.** This is the only other case analitically solved for the first time in [22]. Here $\delta_c(S) = \delta_c + \beta S$, therefore $f(T) = e^{-2\beta(\delta_c-\delta_0)}$ doesn't depend on T and factorizes out of the integral. Setting $S_0 = \delta_0 = 0$ we can compare

$$P(\delta, S; 0, 0) = \frac{1}{\sqrt{2\pi S}} \left[e^{-\frac{(\delta+\beta S)^2}{2S}} - e^{-\frac{(\delta-2\delta_c+\beta S)^2}{2S}} e^{-2\beta\delta_c} \right] \tag{5.63}$$

to the result in [29], finding that they are identical. The case in which $\beta > 0$ does not really fit in our description because not all the paths will cross the barrier; nevertheless we can extend our formalism noticing that if a path does not hit the barrier, it does not need an image path, i.e. we do not need to subtract anything. Therefore the result is still valid.

The fraction of trajectories which has crossed the barrier is given by

$$F(S) = 1 - C(S) = 1 - \int_{-\infty}^{\delta_c} d\delta P(\delta, S; \delta_0, S_0) \tag{5.64}$$

where $C(S)$ has been already defined before. The first upcrossing rate will be given by

$$\begin{aligned} \mathcal{F}(S) &= -\int_{-\infty}^{\delta_c} d\delta \frac{dP}{dS} = \\ &= -\int_{-\infty}^{\delta_c} d\delta \left[h(S)\frac{dP}{d\delta} + \frac{1}{2}\frac{d^2P}{d\delta^2} \right] \\ &= -\left[h(S)P(\delta, S; \delta_0, S_0) + \frac{1}{2}\frac{dP}{d\delta}(\delta, S; \delta_0, S_0) \right]_{-\infty}^{\delta_c}. \end{aligned} \tag{5.65}$$

Using definitions in 5.61, the last member of the previous equation reads as

$$\begin{aligned} &- h(S)P_S(\delta, S; \delta_0, S_0)|_{\delta_c} - \left.\frac{1}{2}\frac{dP_S}{d\delta}(\delta, S; \delta_0, S_0)\right|_{\delta_c} = -\left.\frac{1}{2}\frac{dP_S}{d\delta}\right|_{\delta_c} = \\ &= -\left[-\frac{\delta - \delta_0 + \delta_c(S) - \delta_c(S_0)}{2(S - S_0)\sqrt{2\pi(S - S_0)}} e^{-\frac{[\delta-\delta_0+\delta_c(S)-\delta_c(S_0)]^2}{2(S-S_0)}} + \right. \\ &\quad \left. + \frac{\delta + \delta_0 - 2\delta_c + \delta_c(S) - \delta_c(S_0)}{2(S - S_0)\sqrt{2\pi(S - S_0)}} e^{-\frac{[\delta+\delta_0-2\delta_c+\delta_c(S)-\delta_c(S_0)]^2}{2(S-S_0)}} f(S) \right]_{\delta_c} = \\ &= \frac{\delta_c - \delta_0}{\sqrt{2\pi(S - S_0)^3}} e^{-\frac{[\delta_c-\delta_0+\delta_c(S)-\delta_c(S_0)]^2}{2(S-S_0)}}. \end{aligned} \tag{5.66}$$

Before going on, let's analyze these two quantities to get a deeper understanding of what our function $\mu(T)$ really represents: keeping the crossing time division, we have that $F_T(S) = \Theta(S - T)$ since all paths of a given family have or have not crossed the barrier, therefore we can rewrite $F(S)$ as

$$F(S) = \int_{S_0}^{+\infty} dT\mu'(T)F_T(S) = \int_{S_0}^{S} dT\mu'(T), \tag{5.67}$$

where $dT\mu'(T)$ is the probability to cross the barrier in the interval $[T, T + dT]$. In principle, nothing assures us that every path will cross a generic barrier, so we can also define the total probability to cross the barrier as

$$F(\infty) := \lim_{S\to+\infty} F(S) = \int_{S_0}^{+\infty} dT\mu'(T) \leq 1. \tag{5.68}$$

Using this last relation, we can see that

$$1 = \int_{S_0}^{+\infty} dT \frac{\mu'(T)}{F(\infty)} = \int_{S_0}^{+\infty} dT\mu(T), \tag{5.69}$$

clarifying the fact that $dT\mu(T)$ is nothing else than the conditional probability to cross in the infinitesimal interval $[T, T + dT]$ given the fact that our path actually hits the barrier (in other words, we recover the joint probability law). Finally from equation 5.67 we can derive immediately that $\mathcal{F}(S) = \mu'(S)$.
Using the first upcrossing rate we see how the number of haloes changes, in fact, setting $S_0 = \delta_0 = 0$, we have

$$\begin{aligned} \left.\frac{dn}{dM}\right|_{MG} &= \sqrt{\frac{2}{\pi}} \frac{\bar{\rho}}{M^2} \left|\frac{d\log\sigma}{d\log M}\right| \nu \exp\left[-\frac{1}{2}\left(\nu + \frac{\delta_c(\sigma^2) - \delta_c(0)}{\sigma}\right)^2\right] = \\ &= \sqrt{\frac{2}{\pi}} \frac{\bar{\rho}}{M^2} \left|\frac{d\log\sigma}{d\log M}\right| \nu \exp\left[-\frac{1}{2}\left(\frac{\delta_c(\sigma^2)}{\sigma}\right)^2\right]. \end{aligned} \tag{5.70}$$

First of all, let's notice that the moving barrier gives corrections only to the exponent argument: for large haloes, when $\delta_c(\sigma^2) \to \delta_c$, we recover exactly the GR result while we expect to find a bigger number of small haloes, since for small masses $\delta_c(\sigma^2) < \delta_c$, because small objects are less screened. Then we can see that in the whole mass range $\left.\frac{dn}{dM}\right|_{MG} \geq \left.\frac{dn}{dM}\right|_{GR}$ and also this result is expected since we have an additional force acting during the collapse. Finally, let's remark that something similar to this result was already used in published articles (see e.g. [4]), even if it was not formally proven.

Chapter 6

Conclusions

In this thesis we have tried to treat the structure formation problem in modified gravity using semi-analytical method. After having quickly motivated the introduction of particular scalar fields models which have screening mechanisms that hide the field presence in high density environments, we exposed how they evolved along the Universe history and which theoretical constrains they must satisfy, in order to be compatible with observations. Due to the fact that their temporal evolution is tightly bound, we have introduced a way to parametrize them only according to their time-dependent mass and coupling-to-matter functions, which allow us to reconstruct both the temporal and the spatial dynamics. Since this class of models introduces a scale dependent fifth force which act along with Einstein gravity, we have investigated the gravitational collapse of matter perturbations, which leads to the formation of the first virialized structures. After having pointed out differences with respect to the Newtonian collapse, we have analyzed the MG collapse in an original way, using both analytic and numerical techniques. For models that has a slow evolution all along the collapse, such as the dilaton, we succeed in finding a good modelization that allowed us to obtain sensible field profiles, force profiles and the so called moving barrier, typical of these scenarios. On the other hand, our approach has shown some criticality in models which have a quick evolution, as the symmetron. Finally, in order to appreciate observational differences from GR, we used the Excursion Set Theory to determine the number of virialized structures, in particular we find an analytic extension of such theory to the moving barrier case.
The natural continuation of this work points in three different directions.
Since during the collapse asphericities grow and become significant, the general structure that it forms are pancakes. In order to treat analytically or semi-analytically the ellispoidal collapse we need to state also the angular dynamics of both the perturbation and the scalar field.
Then we can properly numerical simulate the spherical collapse (and eventually also the ellipsoidal one, if we have accomplished the first point) in the same conditions we have derived our profile, in order to understand where the critical points are and how to obtain a more reliable semi-analytic approximation. This will be very useful in the symmetron case, where, due to the singularity of the coupling function, our approach had some problems.
Finally, we can going on deriving other halo properties, following the standard procedure that the Excursion Set Theoryprovides us.

Bibliography

[1] Bond, J. R. et al. *ApJ* **379** (1991), 440.

[2] Brax, P., Davis, A.-C., and Li, B. *Phys. Let. B* **75** (2012), 38.

[3] Brax, P. and Valageas, P. *Phys. Rev. D* **86** (2012), 063512.

[4] Brax, P. and Valageas, P. *Phys. Rev. D* **88** (2013), 023527.

[5] Brax, P. et al. *Phys. Rev. D* **70** (2004), 123518.

[6] Brax, P. et al. *Phys. Rev. D* **78** (2008), 104021.

[7] Brax, P. et al. *Phys. Rev. D* **82** (2010), 063519.

[8] Brax, P. et al. *Phys. Rev. D* **83** (2011), 104026.

[9] Brax, P. et al. *Phys. Rev. D* **86** (2012), 044015.

[10] Brax, P. et al. *JCAP* **10** (2012), 002.

[11] Chandrasekhar, S. *Rev. Mod. Phys.* **15** (1943), 2.

[12] Copeland, E. J., Sami, M., and Tsujikawa, S. *Int. J. Mod. Phys. D* **15** (2006), 1753.

[13] Damour, T. and Polyakov, A. M. *Nucl. Phys. B* **423** (1994), 532.

[14] Hinterbichler, K. and Khoury, J. *Phys. Rev. Lett.* **104** (2010), 231301.

[15] Hinterbichler, K. et al. *Phys. Rev. D* **84** (2011), 103521.

[16] Jenkins, A. et al. *MNRAS* **321** (2001), 372.

[17] Khoury, J. and Weltman, A. *Phys. Rev. D* **69** (2004), 044026.

[18] Li, B. and Efstathiou, G. *MNRAS* **421** (2012), 1431.

[19] Perlmutter, S. et al. *Astrophys. J.* **517** (1999), 565.

[20] Press, W. H. and Schechter, P. *ApJ* **187** (1974), 425.

[21] Riess, A. G. et al. *Astron. J.* **116** (1998), 1009.

[22] Sheth, R. K. *MNRAS* **300** (1998), 1057.

[23] Sheth, R. K. and Tormen, G. *MNRAS* **308** (1999), 119.

[24] Valageas, P. *A. & A.* **382** (2002), 450.

[25] Valageas, P. *A. & A.* **508** (2009), 93.

[26] Weinberg, S. *Rev. Mod. Phys.* **61** (1989), 1.

[27] Weinberg, S. *Cosmology*. 2008.

[28] Weinberg, S. *Gravitation and Cosmology: Principles and Applications of the General Theory of Relativity*. 1972.

[29] Zentner, A. R. *Int. J. Mod. Phys. D* **16** (2007), 763.

Acknowledgements

This thesis represents in many ways the end of a path that I started five years ago and the beginning of a new one that starts now, therefore here I would like to thank all the people that I think that have played an important role during these years.

For what concerns Physics, I would like to deeply thank my supervisor Philippe Brax for the great willingness he showed, for his guide during these month but also for the bunch of recommendation letters that he wrote. Working with you was indeed inspiring and I hope you are proud of results that I achieved. Of course meeting you would not be possible if my other supervisor, Sabino Matarrese, did not put us in touch, therefore I would like to thank him too, even for the help he gave me in finding a PhD. Finally I would like to thank the person who inspired me to choose Physics, my third year high school Physics professor, Silvia Losso, one of the best teacher that I had.

After that, I would like to thank all my huge family, in particular my mother Cinzia and my father Alberto, for having given me the possibility to follow my dreams and ambitions.

During these years I met a lot of people, but certainly they would not been the same without my dearest friends Monica, Marco and Nicolò, which I woud like to thank for all the time we spent together, the fun we had and for being so close to me even during the last year.

Finally, I thank all my friends from the Shu Ren Kan for all the nice experiences I had and the warm welcome that I received every time, even if after my last year I spent abroad.